TAMPEREEN TEKNILLINEN YLIOPISTO
TAMPERE UNIVERSITY OF TECHNOLOGY

VILLE RINTA-HIIRO

BUFFER AND BACKFILL INTERACTION IN KBS-3V DISPOSAL CONCEPT FOR SPENT NUCLEAR FUEL – 1/6 SCALE EXPERIMENT

Master of Science Thesis

Examiner: Professor Pauli Kolisoja
Examiner and topic approved in the Faculty of Business and Built Environment on 9 September 2015

ABSTRACT

TAMPERE UNIVERSITY OF TECHNOLOGY
Master's Degree Program in Civil Engineering
VILLE RINTA-HIIRO: Buffer and Backfill Interaction in KBS-3V Disposal Concept for Spent Nuclear Fuel – 1/6 Scale Experiment
Master of Science Thesis, 86 pages, 16 Appendix pages
January 2016
Major: Infrastructures
Examiner: Professor Pauli Kolisoja
Keywords: KBS-3V, buffer, backfill, bentonite

Final disposal of spent nuclear fuel is planned to start at 2020s in Olkiluoto, Finland. The reference disposal concept in Finland is KBS-3V in which copper-iron canisters containing the spent fuel are placed into vertical deposition holes and surrounded by a buffer which refers to bentonite clay, a material which starts to swell when it is exposed to water. Bentonite will also be used to backfill deposition tunnels where the deposition holes will be drilled. The final disposal requires long-term safety plans due to a long time span of spent nuclear fuel decay. Groundwater flow, rock movements and changes in environmental conditions might jeopardize the long-term safety. This thesis covered a mock-up experiment where test equipment was built in cooperation with VTT and Posiva. Purpose of the thesis was to study interaction between the buffer and the backfill.

The 1/6 scale test equipment consisted of a tube and a tunnel which simulated the deposition hole and the deposition tunnel of the KBS-3V concept. The tube and the tunnel were filled with bentonite blocks and pellets, and water with a salinity of 1 % was supplied into the tube at a rate of 0.1 l/min. In the tunnel there were eight open outlets for the water to flow out. Water distribution, bentonite swelling, formation of water channels, bentonite erosion, and water outflow rate were investigated during the 62 day test. After the test, samples from the bentonite blocks and pellets were taken for water content and density analyses, and a possible vertical displacement of the buffer was examined.

Water started to flow out from the tunnel after two days. The water flowed out from the same outlet during the first 59 days after which the water supply was stopped for about an hour due to adding of a tracer. After this, the water distributed towards dry areas in the tunnel and started to flow out from the other end of the tunnel. During the first days of the test, higher erosion rates occurred occasionally after which the erosion rate settled to an almost constant level. A vertical displacement of about 40 mm of the center of the uppermost buffer block was found after the test. The tunnel pellet layer above the buffer was compressed from 130 mm to approximately 100 mm.

The main findings in this study included: (1) water used same flow paths with the continuous inflow from the same location, (2) the one hour pause in the water inflow sealed some of the water channels and after the restart of the water inflow the water flowed towards dry areas in the tunnel, (3) the vertical displacement of approximately 40 mm of the top surface of the uppermost buffer block occurred and it was probably mainly a result from swelling of the uppermost buffer block, (4) almost fully saturated tunnel pellets with high densities were found from above the buffer after the test.

TIIVISTELMÄ

TAMPEREEN TEKNILLINEN YLIOPISTO
Rakennustekniikan koulutusohjelma
VILLE RINTA-HIIRO: Puskurin ja tunnelitäytön vuorovaikutus käytetyn ydinpolttoaineen KBS-3V-loppusijoituskonseptissa – 1/6 koe
Diplomityö, 86 sivua, 16 liitesivua
Tammikuu 2016
Pääaine: Infrarakenteet
Tarkastaja: professori Pauli Kolisoja
Avainsanat: KBS-3V, puskuri, tunnelitäyttö, bentoniitti

Käytetyn ydinpolttoaineen loppusijoitus Olkiluodossa on suunniteltu aloitettavan 2020-luvulla. Loppusijoituksen konsepti Suomessa on KBS-3V, jossa käytetty polttoaine asennetaan kuparista ja raudasta valmistettuihin kanistereihin, jotka sijoitetaan pystysuuntaisiin loppusijoitusreikiin. Kanisterit ympäröidään veden vaikutuksesta paisuvalla puskurimateriaalilla, joka on bentoniittisavea. Bentoniittia käytetään myös täyttämään loppusijoitustunnelit, joiden lattioihin loppusijoitusreiät porataan. Loppusijoitus vaatii pitkän aikavälin turvallisuussuunnittelua johtuen ydinpolttoaineen radioaktiivisesta hajoamisesta. Pitkäaikaisturvallisuutta vaarantavia tekijöitä voivat olla pohjaveden virtaus, kallion liikahdukset sekä ympäristöolosuhteiden muutokset. Tässä opinnäytteessä käsiteltiin mallikoetta, jota varten oli rakennettu koelaitteisto VTT:n ja Posivan toimesta. Tarkoituksena oli tutkia puskurimateriaalin ja tunnelitäyttömateriaalin vuorovaikutusta.

Mittakaavaltaan 1/6 oleva testilaitteisto koostui loppusijoitusreikää simuloivasta putkesta ja loppusijoitustunnelia simuloivasta tunnelista, jotka täytettiin bentoniittiblokeilla ja -pelleteillä. Suolapitoisuudeltaan 1 % olevaa vettä syötettiin putkeen virtausnopeudella 0,1 l/min. Tunnelissa oli kahdeksan ulostuloreikää vedelle. Testin kesto oli 62 päivää, jonka aikana tutkittiin veden leviämistä laitteistossa, bentoniitin paisumista, vesikanavien muodostumista, bentoniittimateriaalien eroosiota sekä veden ulosvirtauksen määrää. Testin jälkeen otettiin bentoniittilohkoista ja -pelleteistä näytteitä vesipitoisuuden ja tiheyden määrityksiä varten sekä tutkittiin mahdollista puskurimateriaalin ylösnousua.

Vesi virtasi ulos tunnelista ensimmäisen kerran kahden päivän jälkeen. Vesi virtasi samasta ulostuloreiästä ensimmäisen 59 päivän ajan, jonka jälkeen veden virtaus testilaitteeseen katkaistiin noin tunnin ajaksi väriaineen lisäyksen takia. Tämän jälkeen veden virtaussuunta tunnelissa muuttui kohti aluetta, joka oli pysynyt kuivana tähän asti. Myös veden ulostuloreitti vaihtui tunnelin toiseen päätyyn. Runsasta eroosiota havaittiin ajoittain ensimmäisten testipäivien aikana, jonka jälkeen eroosio asettui lähes vakiotasolle. Ylimmän puskurilohkon yläosan havaittiin nousseen noin 40 mm testin aikana. Puskurin yläpuolella oleva pellettikerros oli paksuudeltaan ennen testiä 130 mm ja testin jälkeen kerroksen paksuudeksi mitattiin noin 100 mm.

Tämän tutkimuksen päätuloksia olivat: (1) samasta kohdasta tulevalla vedensyötöllä vesi käytti samoja virtausreittejä, (2) yhden tunnin kestänyt vedensyötön tauko sulki veden virtausreittejä ja vedensyötön alettua uudelleen vesi virtasi tunnelissa kohti siihen asti kuivana pysyneitä alueita, (3) ylimmän puskurilohkon noin 40 mm nousu johtui todennäköisesti pääasiassa ylimmän puskurilohkon paisumisesta, (4) puskurin yläpuolella olleesta tunnelin pellettikerroksesta otetut näytteet olivat lähes täysin saturoituneita ja suuren tiheyden omaavia.

PREFACE

This thesis was carried out at the Technical Research Centre of Finland (VTT) in Espoo, Finland, during a research trainee period from June 2015 to December 2015. The thesis was related to nuclear waste disposal technology and was done within the team of Infrastructure Health in cooperation with Posiva Oy, the company responsible for nuclear waste management in Finland. The thesis covered a laboratory experiment which was funded by Posiva.

I would like to thank VTT, Posiva and Tampere University of Technology (TUT) for the opportunity to carry out my thesis and especially VTT for the possibility to work in such an encouraging environment. My warm thanks for the guidance go to my supervisors Mrs. Jutta Peura from VTT and Mr. Pauli Kolisoja from TUT. I also want to express my gratitude to my co-workers at VTT for the assistance and support which I truly appreciate.

In Helsinki, Finland, on 27 December 2015

Ville Rinta-Hiiro

CONTENTS

LIST OF ABBREVIATIONS AND TERMS

Backfill	Bentonite blocks and pellets used to fill the deposition tunnels.
Buffer	Bentonite blocks and pellets surrounding the canister in the deposition holes.
Canister	Spent nuclear fuel will be placed into canisters that consist of iron inserts and copper shells.
Cebogel QSE	Type of bentonite pellets potentially used for backfilling the deposition tunnels, originated from Milos, Greece.
Closure	Structures for closing the underground openings in the final disposal facility.
EBS	Engineered Barrier System which includes: closure, backfill, buffer and canister as components of the KBS-3V concept.
EMDD	Effective Montmorillonite Dry Density.
Ibeco RWC BF	Type of bentonite blocks potentially used for backfilling the deposition tunnels, originated from Milos, Greece.
KBS-3V	The reference concept for the final disposal in Finland.
LO1, LO2	Loviisa power plant reactors 1 and 2.
MX-80	Reference type of bentonite blocks and pellets used for filling the deposition holes, originated from Wyoming, USA.
OL1, OL2, OL3	Olkiluoto power plant reactors 1, 2 and 3.
ONKALO	Underground Rock Characterization Facility.
Plug	Concrete barrier installed to the ends of the deposition tunnels after backfilling.
Posiva	The company responsible for the nuclear waste management in Finland.
TDS	Total Dissolved Solids.
Tube	In this experiment, a plastic tube simulated the deposition hole rock wall and it was filled with buffer blocks and pellets.
Tunnel	In this experiment, a steel frame tunnel simulated the deposition tunnel rock wall and it was filled with backfill blocks and pellets.
TURVA-2012	Posiva's design basis for the KBS-3V concept in safety point of view.
VAHA	Posiva's requirement management system with five levels.

1. INTRODUCTION

Nuclear waste disposal technology has been researched in Finland since 1970s. According to plans, the disposal will start in Finland in the near future. Olkiluoto has been chosen as the disposal site where spent nuclear fuel will be disposed of at a depth of over 400 m in bedrock. In Finland, the nuclear waste disposal technology is based on a KBS-3V concept where vertical boreholes are drilled in floors of deposition tunnels. In the concept, spent nuclear fuel is inserted inside copper-iron canisters which are placed into boreholes. Bentonite blocks and pellets are used for filling the boreholes as buffer material and the deposition tunnels as backfill material. The bentonite will start to swell and seal the holes and the tunnels after it is exposed to water.

This thesis is a part of a project at the Technical Research Centre of Finland (VTT) where test equipment was built at about 1/6 scale in the laboratory, simulating the deposition hole and the tunnel of the KBS-3V concept. The hole and the tunnel will both be filled with bentonite blocks and pellets. Water simulating Olkiluoto's groundwater flows through the system. Stresses of the hole and the tunnel are monitored and the pressure inside the tunnel as well. During the test, samples are taken from the outflowing water to define erosion of the bentonite material. During dismantling, bentonite samples are taken for water content and density analyses. Also, possible water flow paths and vertical displacement of the buffer will be investigated.

The thesis studied interaction between the buffer and the backfill. So far, very few experimental studies including both the buffer and the backfill have been done in Finland. Knowledge of the buffer and backfill interaction is based on small-scale buffer or backfill studies, bentonite material studies and modelling studies. It is assumed that swelling of the buffer due to water causes heaving of the high density buffer to the lower density backfill. Due to the swelling, the density of the buffer decreases which can lead to an increase of permeability and decrease of mechanical strength of the buffer. Consequences might include canister movements, corrosion, failure and also migration of radionuclides through the buffer, thus jeopardizing the long-term safety. (Keto et al. 2009)

With this study of the early age performance of the bentonite there is a possibility to understand better the buffer and backfill interaction and to compare the results to previous studies and their hypotheses. The results are used to support the buffer and backfill design, material specifications and monitoring program of the engineered barrier system (EBS). The results of the thesis also give useful data for the first full-scale construction demonstration of buffer and backfill together in Finland that is planned to start at Olkiluoto's disposal site in 2017.

2. BACKGROUND

2.1 Nuclear waste disposal at Olkiluoto site

In 2001, a decision-in-principle was made in the Finnish Government regarding disposal of spent nuclear fuel produced by the Olkiluoto and Loviisa nuclear power plants. Power plants already in operation were included in the decision-in-principle. These power plants are Olkiluoto 1 (OL1), Olkiluoto 2 (OL2), Loviisa 1 (LO1) and Loviisa 2 (LO2). It was decided that the spent nuclear fuel shall be disposed of at Olkiluoto which is located in Eurajoki, on the coast in the south-western part of Finland. According to another decision-in-principle made in 2002, spent nuclear fuel from the Olkiluoto 3 (OL3), the new power plant currently under construction, will also be disposed of at Olkiluoto. Possible new power plants might change the current plans. (Posiva 2015)

Preparations for the final disposal began already in the late 1970s, at the same time as the commissioning of the nuclear power plants started. The final disposal has been researched ever since. In 2012, the construction license application for the spent nuclear fuel repository was submitted. The license application concerned a complex of two interconnected nuclear facilities, an above-ground encapsulation plant and an underground final repository. In November 2015, the construction license was granted by the Finnish Government. The operating license is planned to be applied in 2020. The final disposal is scheduled to start in the 2020s and according to the current plans, it will continue almost a hundred years. (Posiva 2015) The overall schedule for the nuclear waste management implementation of the Loviisa and Olkiluoto reactors until 2020 is shown in Figure 1.

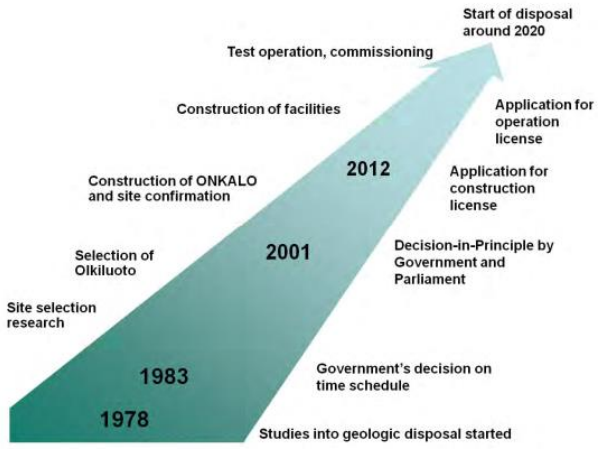

Figure 1. *Overall schedule for the nuclear waste management in Finland (Posiva 2012b).*

2.1.1 Nuclear waste

Nuclear waste is produced in nuclear power plants as a result of electricity production. Because of its radioactivity, nuclear waste needs special treatment. Nuclear waste produced in the nuclear power plants can be divided into low-, intermediate- and high-level waste. The low-level and the intermediate-level waste are generated during the operation and maintenance of the nuclear power plant and they are also known as the reactor waste. Decommissioning waste is generated during closing down of the plant and it derives from some nuclear power plant structures that become radioactive during the operation. The nuclear power companies in Finland, TVO at Olkiluoto and Fortum at Loviisa, take care of their own reactor waste and decommissioning waste which are disposed of in a reactor waste repository. (Posiva 2015)

Nuclear power plants use uranium as their fuel in electricity production. After the operation, spent nuclear fuel is high-level waste which has to be disposed of so it does not harm the biosphere. The reference time period for safety analyses is about 250,000 years so it includes at least one ice age cycle. After this the activity of the fuel is at the same level as that of a large uranium deposit. Spent nuclear fuel is stored in interim storage facilities before the final disposal. As the reactor waste repositories, also the interim storage facilities are located in the nuclear power plants. (Posiva 2015) The disposal sites of the radioactive waste are presented in Figure 2.

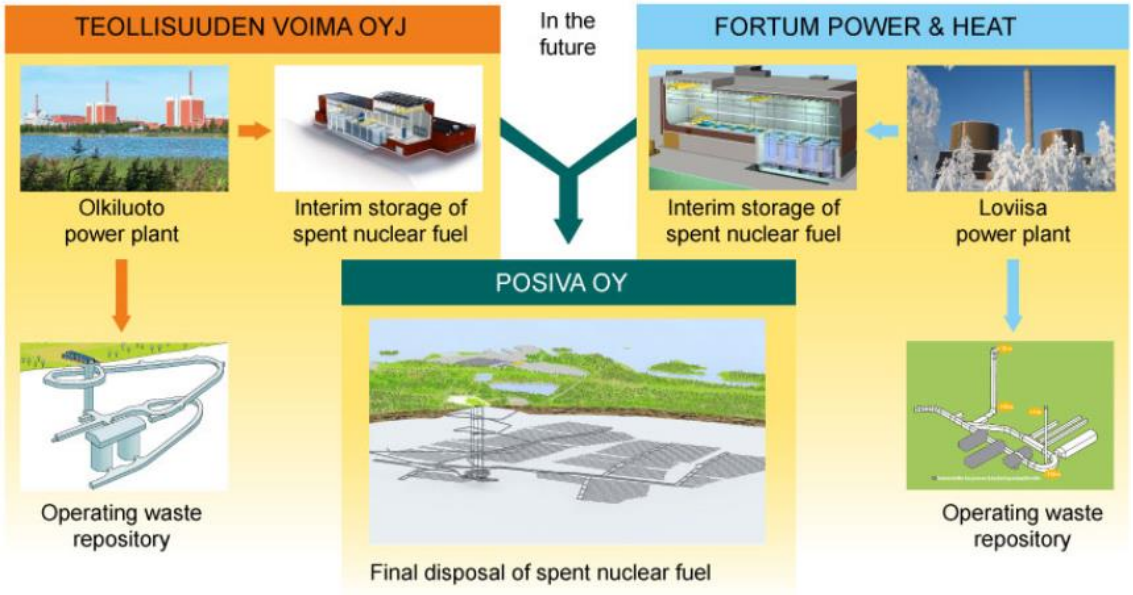

Figure 2. *Disposal sites (Posiva 2015).*

Before the spent nuclear fuel is transferred to the interim storage it is cooled down for a few years in water basins inside a reactor building. In the interim storage the fuel is stored under water for dozens of years until the radiation intensity and decay heat decrease sufficiently for transport, encapsulation and disposal. The fuel used in OL1, OL2, LO1 and LO2 requires a cooling down period of about 40 years before the final disposal whereas the fuel used in OL3 requires a cooling down period of about 60 years. From

the interim storage the fuel will be transported to the final disposal facility in special-purpose casks as special transport. (Posiva 2012a; Posiva 2015)

2.1.2 ONKALO

ONKALO is a research facility and the future spent nuclear fuel repository in Olkiluoto where excavations started in 2004. Design of ONKALO is presented in *Design of the Disposal Facility 2012* by Saanio et al. (2013). The repository facilities are located at an approximate depth of 400-450 m while the spiral-shaped access tunnel reaches the depth of 455 m. ONKALO contains also shafts including a personnel shaft, an inlet air shaft and an exhaust air shaft. The ONKALO design is developed to accommodate at maximum 9,000 tons of uranium of high-level nuclear waste. (Saanio et al. 2013) A conceptual image showing ONKALO and its location at the central part of the Olkiluoto Island is presented in Figure 3.

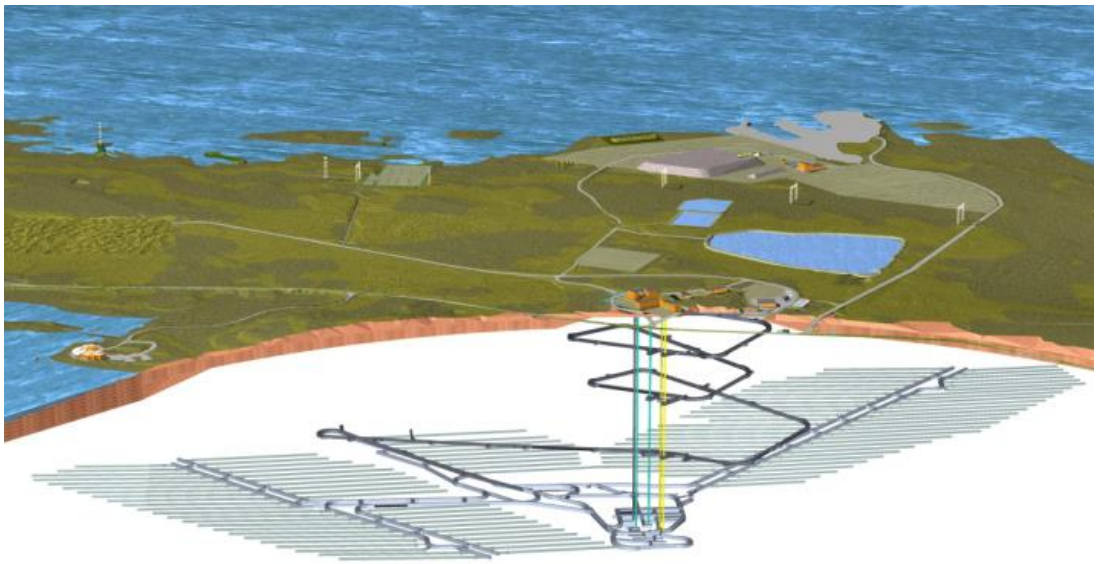

Figure 3. *ONKALO is located in the Olkiluoto bedrock (Posiva 2010).*

The facility complex at Olkiluoto comprises of two nuclear waste facilities which are the encapsulation plant and the disposal facility. In the above-ground encapsulation plant spent nuclear fuel from Loviisa and Olkiluoto is received and packed into final disposal canisters. In the disposal facility the encapsulated fuel is disposed of. (Saanio et al. 2013)

According to the current design of the disposal facility, the disposal facility will be built in a so-called parallel tunnels principle where deposition tunnels are connected by two parallel tunnels (Figure 4). Safety and flexibility during the operational phase are some of the main advantages of this principle. In the design work the aim is to maintain maximum flexibility to allow changes in the design solutions as technologies develop. (Saanio et al. 2013) The objective of the final disposal is the permanent disposal of the waste. However, it is technically possible to return the disposed of final disposal canisters from the repository at any phase. (Posiva 2010)

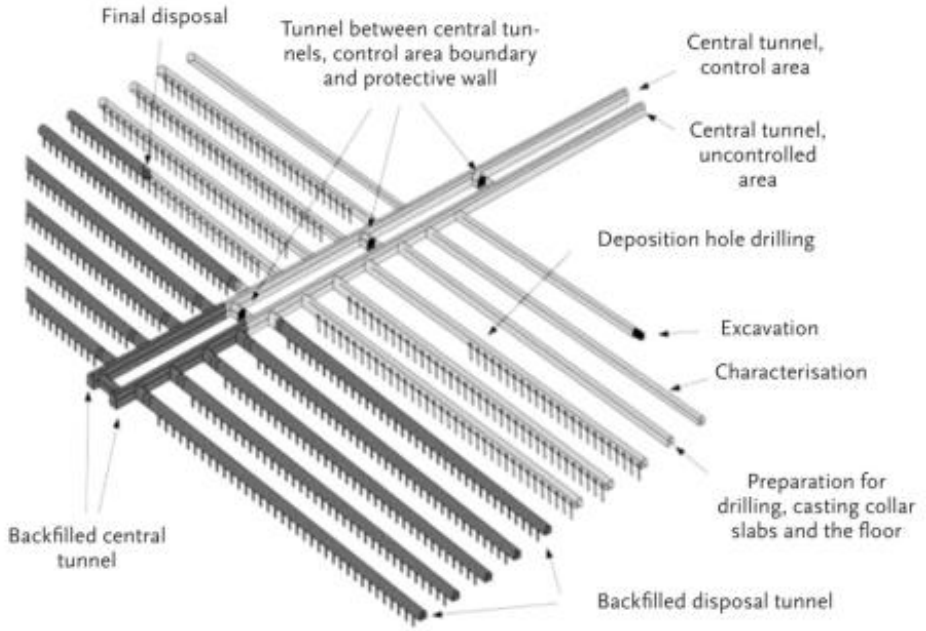

Figure 4. *The parallel tunnels principle (Posiva 2010).*

2.1.3 Bedrock properties

Site-characterization investigations in Olkiluoto have been carried out since 1980s. First the investigations focused on aboveground conditions but they have proceeded to underground research since the start of the ONKALO construction. The research gives further information of the bedrock and groundwater conditions on the final disposal site and helps to ensure the suitability of the Olkiluoto bedrock for the final disposal. Research also gives information of the impact of the construction on the bedrock conditions as well as helps to identify the most cost-effective sites for the construction. The bedrock is studied with methods from geology, hydrology and geochemistry. Photos related to core sample drilling are presented in Figure 5. Based on the research, models of the final disposal site have been made and they include geological, geochemical, hydro-geological and rock-mechanical models. The models can be used to assess the performance of the final disposal and the effects it has on the rock environment in terms of long-term safety. (Posiva 2015)

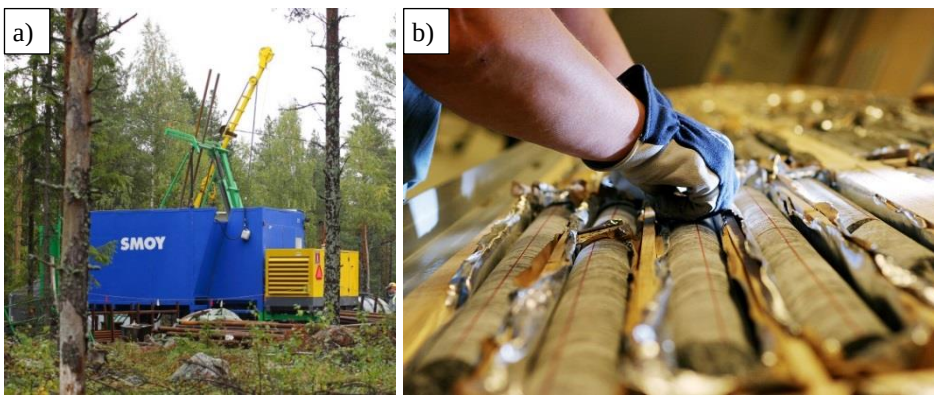

Figure 5. *a) Drilling equipment and b) drill core samples to reveal the structures and rock types of the bedrock (Posiva 2015).*

A description of the Olkiluoto site is presented in *Olkiluoto Site Description 2011* by Posiva (2012c) where bedrock geology, rock mechanics, hydrogeology and hydrogeochemistry of Olkiluoto are described. In *Site Engineering Report* by Posiva (2013), an overall framework of bedrock conditions, especially from geotechnical design and rock construction point of view is presented.

The bedrock at Olkiluoto is mainly composed of various high-grade metamorphic and migmatitic rocks of supracrustal origin. Based on the mineral composition, texture and migmatitic structure, the rocks of Olkiluoto can be divided into four major classes: 1) gneisses, 2) migmatitic gneisses, 3) TGG gneisses and 4) pegmatitic granites. (Kärki & Paulamäki 2006) Due to deformation phases, the rocks in Olkiluoto are completely oriented. The strength properties of the Olkiluoto bedrock vary largely due to the heterogeneous bedrock. Thermal properties, as well as strength properties, depend on the foliation of the rock. Thermal properties play a role when determining dimensions of the repository related to the heat generating spent nuclear fuel. The temperature at a depth of 400 m is about +10.5°C while the average temperature gradient is 1.4°C/100 m. (Posiva 2012c, cited in Saanio et al. 2013)

Salinity in Olkiluoto varies significantly. Fresh water, having TDS (total dissolved solids) >1 g/l, is found in the uppermost tens of meters. Brackish groundwater, with TDS of 1-10 g/l, is found at depths between 30 m and 400 m. At depths over 400 m, saline groundwater with TDS over 10 g/l dominates. (Posiva 2012c) The salinity at the disposal depth is approximately 10-20 g/l. Design salinity value of 35 g/l set for the bedrock is similar to the salinity of the ocean water while the maximum allowed salinity is 70 g/l. However, construction or glacial periods might cause disturbances resulting in upconing of deep saline water which increases the salinity at the repository level. (Hellä et al. 2009; Posiva 2010)

During the operation of the repository the aim is to maintain the bedrock properties as close to original as possible. Impact of the excavation is kept low and water-bearing structures as well as sealing methods, for example grouting, are used for limiting water leaks. (Saanio et al. 2013)

Due to the long time span of the safety analyses, future environmental conditions need to be estimated. The estimations are based on the assumption that the development of the conditions will follow the same principles as they have in the past under the similar conditions. The most important parameter affecting the climatic scenario development concerning the repository is the temperature change. Other relevant parameters or conditions include precipitation, glaciation, permafrost, glacial erosion, postglacial earthquakes, sea level changes and shoreline displacement, vegetation, and salinity of seawater. (Pastina & Hellä 2006)

2.1.4 KBS-3V concept

In the decision-in-principles made in the early 2000s, the final disposal of spent nuclear fuel was decided to be carried out with a KBS-3 concept. The concept was developed by SKB (Swedish Nuclear Fuel and Waste Management Co), the company responsible for the nuclear waste management in Sweden. The KBS-3 concept contains two different disposal concepts, KBS-3V and KBS-3H. The main difference between these concepts is the direction of the spent nuclear fuel placement (vertical or horizontal). The horizontal concept, KBS-3H, is presented in *Nuclear Waste Management at Olkiluoto and Loviisa Power Plants* by Posiva (2010). Posiva, the nuclear waste management company in Finland, currently plans to use the KBS-3V concept. (Posiva 2015) The KBS-3V design is based on a multi-barrier principle where copper-iron canisters containing spent nuclear fuel are emplaced vertically in individual deposition holes bored in floors of deposition tunnels at a depth of 400-450 m in the Olkiluoto bedrock. The canisters are surrounded by a swelling clay buffer material that separates the canisters from the bedrock. The deposition tunnels will be backfilled with materials with low permeability. (Posiva 2012b) A schematic view of the KBS-3V concept is presented in Figure 6 and an image representing some of the release barriers is shown in Figure 7.

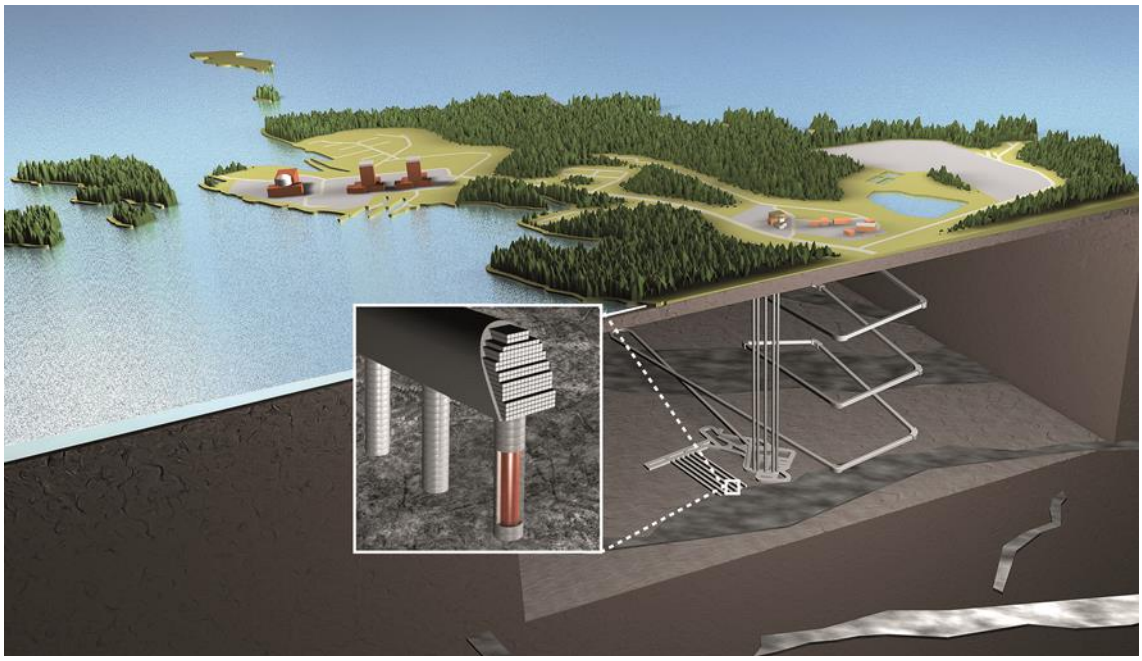

Figure 6. *KBS-3V concept (Posiva 2012b).*

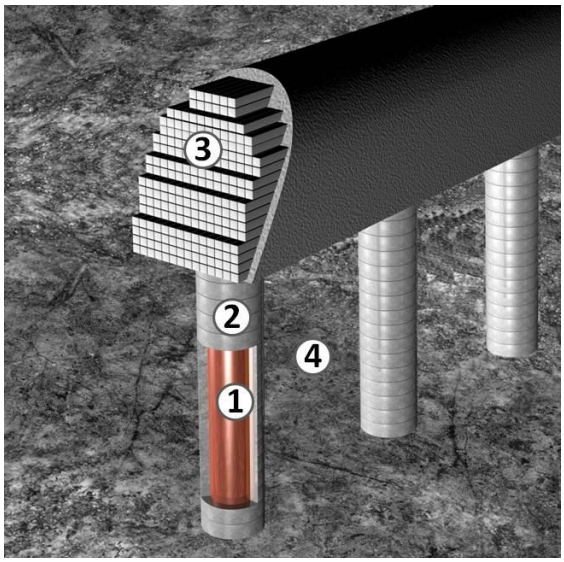

Figure 7. *Some of the release barriers of the KBS-3V concept: 1) final disposal canister, 2) bentonite buffer, 3) tunnel backfill, 4) bedrock (Posiva 2015).*

Posiva's TURVA-2012 safety case documentation presents the design basis for the KBS-3V concept from a long-term safety point of view. TURVA-2012 is based on Posiva's requirements management system (VAHA) which is an information system designed by Posiva to manage the requirements related to the geological disposal of spent nuclear fuel. The VAHA database is organized into five levels: Stakeholder requirements, System requirements, Subsystem requirements, Design requirements, and Design specifications. (Posiva 2012b) TURVA-2012 safety case portfolio and VAHA are presented in *Design Basis 2012* by Posiva (2012b).

In TURVA-2012, spent nuclear fuel, engineered barrier system (EBS) and host rock as a natural barrier form the repository system. Release of radionuclides to the living environment is prevented by this multi-barrier system of engineered barriers and host rock. With surface environment the repository system forms the disposal system which is presented in Figure 8. (Posiva 2012b)

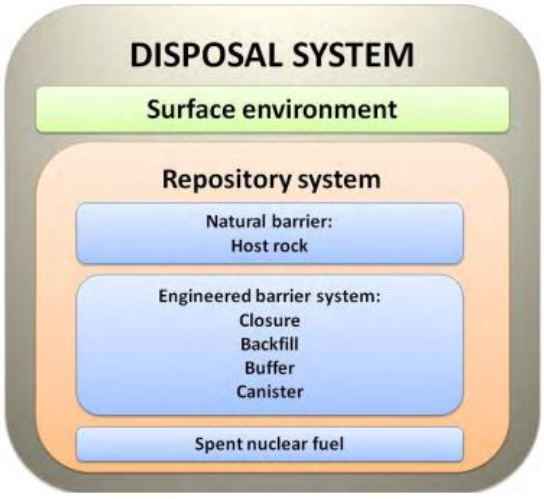

Figure 8. *Components of the disposal system (Posiva 2012b).*

All release barriers have their roles in establishing the required long-term safety of the repository system. Safety functions for the barriers have been assigned based on their role in the repository. The safety functions are presented in Table 1. In the following text some of the barriers are shortly described.

Table 1. *Safety functions of the release barriers (Posiva 2012b).*

Barrier	Safety functions
Canister	Ensure a prolonged period of containment of the spent nuclear fuel. This safety function rests first and foremost on the mechanical strength of the canister's cast iron insert and the corrosion resistance of the copper surrounding it.
Buffer	Contribute to mechanical, geochemical and hydrogeological conditions that are predictable and favourable to the canister Protect canisters from external processes that could compromise the safety function of complete containment of the spent nuclear fuel and associated radionuclides Limit and retard radionuclide releases in the event of canister failure.
Deposition tunnel backfill	Contribute to favourable and predictable mechanical, geochemical and hydrogeological conditions for the buffer and canisters Limit and retard radionuclide releases in the possible event of canister failure Contribute to the mechanical stability of the rock adjacent to the deposition tunnels.
Host rock	Isolate the spent nuclear fuel repository from the surface environment and normal habitats for humans, plants and animals and limit the possibility of human intrusion, and isolate the repository from changing conditions at the ground surface, Provide favourable and predictable mechanical, geochemical and hydrogeological conditions for the engineered barriers, Limit the transport and retard the migration of harmful substances that could be released from the repository.
Closure	Prevent the underground openings from compromising the long-term isolation of the repository from the surface environment and normal habitats for humans, plants and animals. Contribute to favourable and predictable geochemical and hydrogeological conditions for the other engineered barriers by preventing the formation of significant water conductive flow paths through the openings. Limit and retard inflow to and release of harmful substances from the repository.

Canister. The canister (Figure 9) is the first and also the most important isolator for the radionuclides in the KBS-3V concept. Canister is a container with a water- and gas-tight shell and a mechanical load-bearing insert in which the spent nuclear fuel is placed for the final disposal. The canister insert is made of cast iron which provides mechanical strength, radiation shielding and maintaining of the fuel assemblies in the required configuration. The canister shell is made of copper which has good thermal and mechanical properties and resistance to corrosion. Thickness of the current reference copper shell is 49 mm. The canisters are designed to have a lifetime of hundreds of thousands of years except in cases of manufacturing defects and operating errors that may reduce the lifetime. (Posiva 2012a; Raiko et al 2012) The canister is described in detail in *Canister Design 2012* by Raiko (2012), in *Canister Production Line 2012* by Raiko et al. (2012) and in *Description of the Disposal System 2012* by Posiva (2012b).

Figure 9. *A full-scale canister (Posiva 2015).*

Buffer. The canister is surrounded by bentonite rings, blocks and pellets. This highly compacted bentonite is referred to as buffer (Posiva 2012b). Buffer design and function are presented in more detail in chapter 2.2.1.

Backfill. The deposition tunnels leading to the deposition holes are backfilled. Thus, backfill equates materials that are used for filling the deposition tunnels. The current concept is to fill the majority of the tunnel with pre-compacted bentonite backfill blocks and the remaining volume with bentonite pellets. (Posiva 2012b) Backfill design and function are presented in more detail in chapter 2.2.2.

Closure. The closure of the disposal facility includes backfill and plugs in all manmade underground openings except deposition holes and deposition tunnels. Examples of these are the access tunnel, central tunnels, shafts, and technical rooms. After backfilling of the deposition tunnels, plugs will be installed to close the tunnels. Some sections of the plugs are part of the central tunnels so the end plugs can also be considered as closure structures. (Sievänen et al. 2012) The function of the plug is to keep the backfill in place and thus to contribute on the performance of the backfill. Depending on their location and function, the closure structures vary in their shape, dimensions and depth. (Posiva 2012b) Closure structures are described in detail in *Design, Production and Initial State of the Underground Disposal Facility Closure* by Sievänen et al. (2012), in *Description of the Disposal System 2012* by Posiva (2012a), and in *Underground Disposal Facility Closure Design 2012* by Dixon et al. (2013).

The disposed canisters produce residual heat due to radioactive decay of spent nuclear fuel inside the canisters. The temperature can be controlled by the space between the adjacent canisters and adjacent tunnels, and also by the precooling time of the spent nuclear fuel. Based on analytical and numerical heat transfer analyses performed by Ikonen & Raiko (2012), the maximum temperature of the canister is reached after about 15 years and after about 35 years the temperature begins to decrease. The maximum allowed temperature in the interface of the canister and buffer is +100°C. Thermal analyses performed by Ikonen & Raiko (2012) were used in dimensioning the distances between the canisters (canister spacing). Because of uncertainties, including variation in local rock conductivity and predicted decay power, there were safety margins for the

calculations. In addition, due to uncertainties in humidity circumstances of the environment, the dimensioning of the canister spacing was performed separately for dry and saturated case. In the dry condition the safety margin was 5°C so the maximum calculated temperature of the canister was 95°C. In the saturated condition which is more probable, the safety margin was 10°C and the maximum temperature of the canister was 90°C. With different tunnel (25-40 m) and fuel type the canister spacing in the KBS-3V repository was calculated to be between 7.2 m and 10.5 m. (Ikonen & Raiko 2012)

In *Expected Evolution of a Spent Nuclear Fuel Repository at Olkiluoto* by Pastina & Hellä (2006), expected evolution of the KBS-3V repository at Olkiluoto is described in three phases: operational phase, post-closure temperature phase, and a phase from the onset of the next glaciation until the end of the glaciation. The operational phase is the phase from the beginning of the operations until closure. Main processes in the operational phase are the thermal processes originated from the spent nuclear fuel decay heat, water uptake, swelling of the buffer and backfill bentonite, stress distribution, and rock movements due to excavation and operation (Figure 10). (Pastina & Hellä 2006)

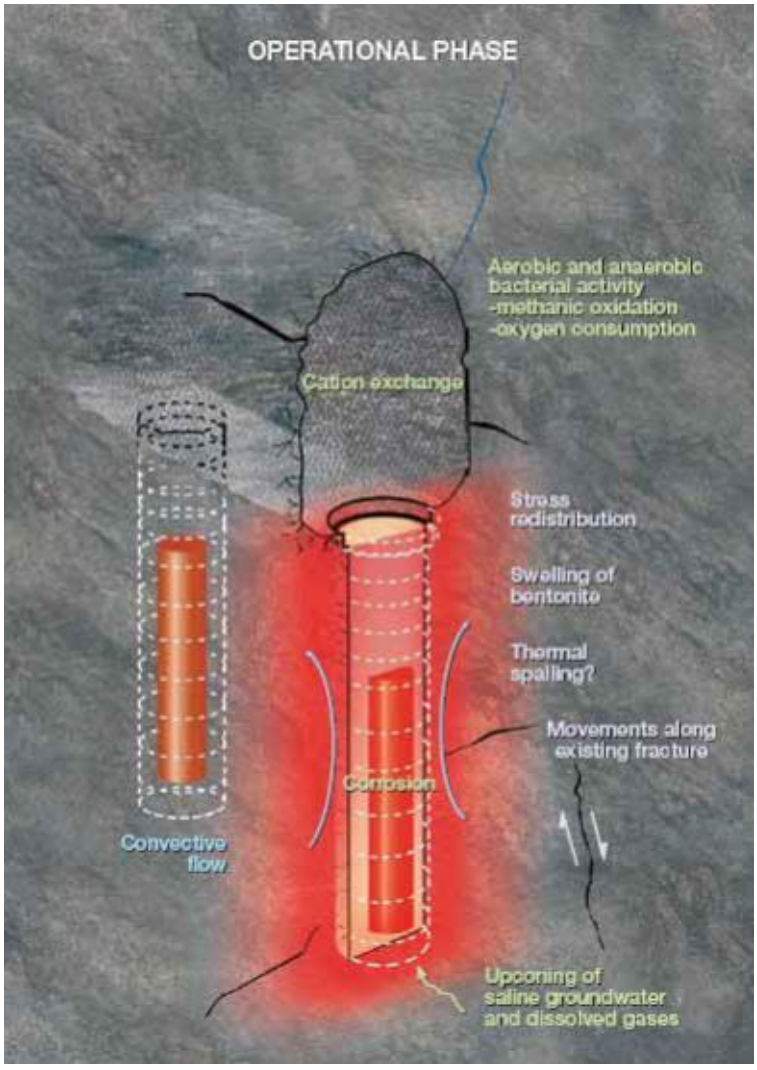

Figure 10. *Main processes in the deposition hole during the operational phase of the repository. Geologic features in the image are not in scale. (Pastina & Hellä 2006)*

2.2 Buffer and backfill in KBS-3V concept

2.2.1 Buffer design and function

Buffer is the component surrounding the canister and filling the void spaces between the canister and the rock. The buffer is described in detail in *Buffer Design 2012* by Juvankoski (2013) and in *Buffer Production Line* by Juvankoski et al. (2012). The purpose of the buffer is to protect the canister from detrimental processes (thermal, hydraulic, mechanical and chemical), maintain favorable conditions for the canister and slow down the possible transport of radionuclides. The buffer also supports the deposition hole walls and keeps the canister in the correct position. (Juvankoski 2013) Safety functions of the buffer according to *Design Basis 2012* (Posiva 2012a) are the following (listed also in Table 1):

- Contribute to mechanical, geochemical and hydrogeological conditions that are predictable and favorable to the canister.
- Protect canisters from external processes that could compromise the safety function of complete containment of the spent nuclear fuel and associated radionuclides.
- Limit and retard radionuclide releases in the event of canister failure.

Properties of the buffer enabling its capacity to maintain these safety functions include swelling pressure (density and porosity), hydraulic conductivity, stiffness and content of substances that may be harmful for the other release barriers. Design loads of the buffer include mechanical loads (own weight and pressure, and weight of the canister), thermal loads (varying temperature in time or position), chemical loads (environment around the buffer, including bacteria-induced chemical loads) and radiation load. Buffer components are also affected on handling loads during manufacturing and installation phases. (Juvankoski 2013)

The main components of the buffer are buffer blocks under and above the canister, buffer rings around the canister and pellets between the buffer blocks and the deposition hole wall. Between the canister and the buffer blocks there is a 10 mm air filled gap, and between the buffer blocks and the rock there is a 50 mm pellet-filled gap which is needed to get a contact with the rock. (Juvankoski 2013; Juvankoski et al. 2012) The 10 mm gap between the canister and the buffer is the most important thermal resistance for the canister. The thermal conduction in this gap is a result from thermal radiation and conduction in the air. This gap is assumed to stay open and dry the first decades after the canisters have been disposed. (Ikonen & Raiko 2012) The design of the buffer depends on the fuel type as is shown in Figure 11. The reference buffer design for the OL 3 fuel type is presented in Figure 12.

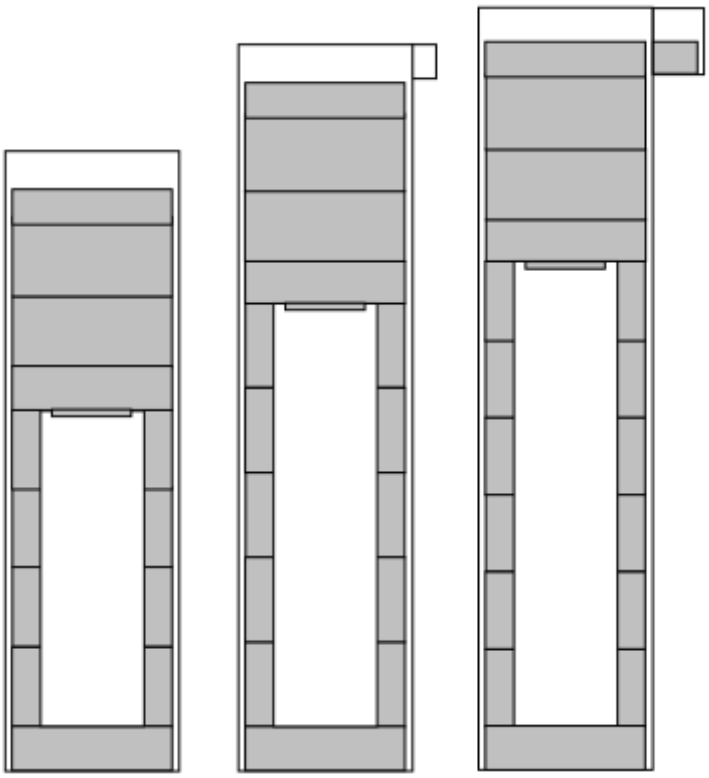

a) LO1-2 b) OL1-2 c) OL3

Block properties	LO1-2	OL1-2	OL3
Height above canister, mm	400+2*800+500=2500	400+2*800+500=2500	400+2*800+500=2500
Height around canister, mm	4*900=3600	5*960=4800	6*875=5250
Height below canister, mm	500	500	500
Total height of buffer, mm	6600	7800	8250
Block outer diameter, mm	1650	1650	1650
Block wall thickness around canister, mm	290	290	290
Canister hole diameter in ring block, m	1070	1070	1070

Figure 11. *Geometry of the installed buffer and the nominal dimensions of the buffer for the different power plant unit fuel types (Juvankoski 2013).*

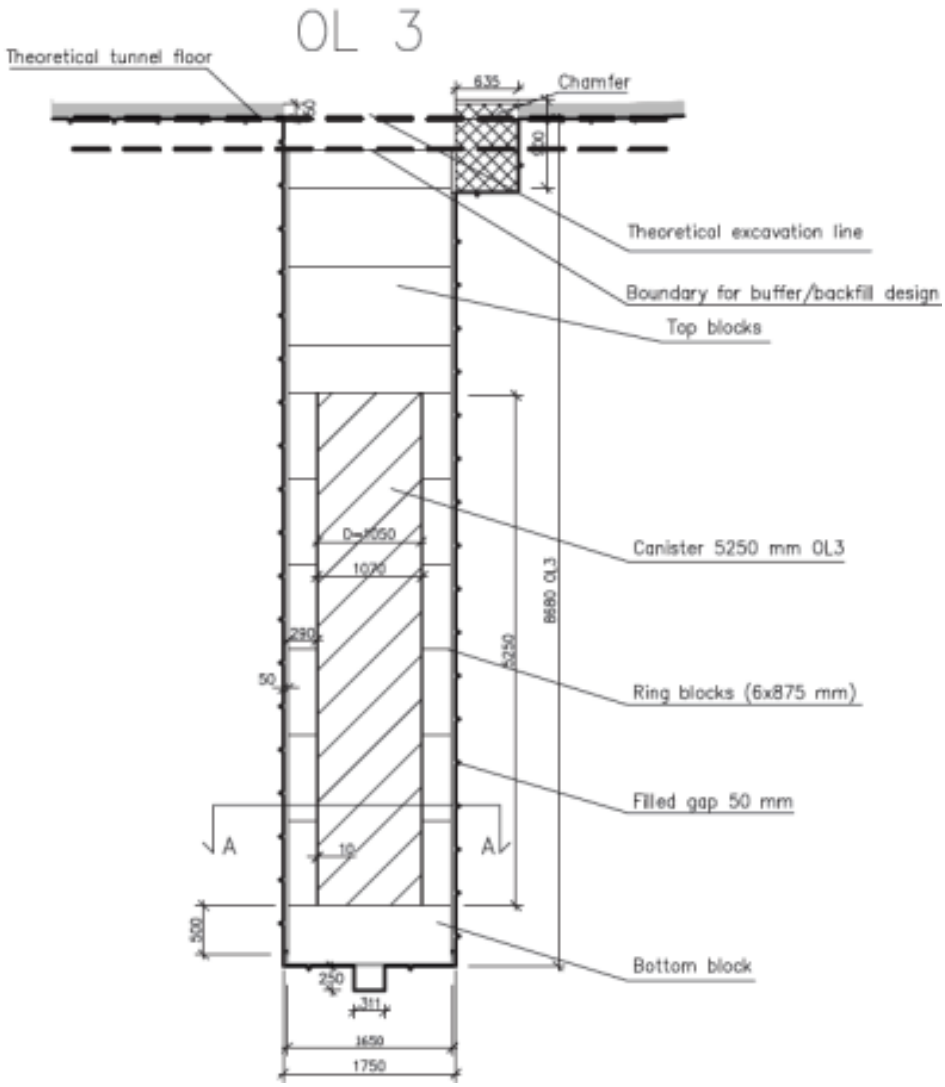

Figure 12. *The reference design of the buffer for the canister of OL3 (Juvankoski 2013).*

The reference material for both the buffer blocks (disks and rings) and the pellets is MX-80, high grade bentonite from Wyoming (USA) with montmorillonite content between 75 % and 90 %. The content of the montmorillonite, the swelling mineral, is the basis in the buffer's ability to provide required performance in the disposal system. As a design requirement, the saturated density of the buffer shall be between 1950 kg/m^3 and 2050 kg/m^3. (Juvankoski 2013) In addition to the performance targets and design requirements presented in *Design Basis 2012* (Posiva 2012a), design specifications for the buffer have been presented in VAHA Level 5 (Table 2).

Table 2. *Buffer design specifications (Juvankoski 2013).*

L5-BUF-1	**1 Definitions**
L5-BUF-2	The buffer material being considered is MX 80 type bentonite, containing mainly mineral Montmorillonite.
L5-BUF-3	The thickness of bentonite buffer from canister bottom to the bottom of deposition hole shall be at least 500 mm.
L5-BUF-4	The target thickness of bentonite buffer on top of the canister shall be 2500 mm.
L5-BUF-5	The thickness of saturated bentonite buffer between canister wall and rock shall be 350 mm ± 25 mm.
L5-BUF-6	**2 Material specifications**
L5-BUF-7	The montmorillonite content of the dry buffer material shall be 75-90% by weight
L5-BUF-8	The water content of the buffer material shall be at least 15 wt%
L5-BUF-9	The target density of buffer at saturation shall be 2000 kg/m^3 with tolerances defined in "Buffer Design 2012".*
L5-BUF-10	The total sulphur content shall be less than 1 wt%, with sulphides making, at most, half of this.
L5-BUF-11	The organics content in the bentonite shall be lower than 1 wt%
L5-BUF-12	**3 Support of other system components**
L5-BUF-13	The gap between buffer block and deposition hole shall be filled with bentonite.

*In design specification L5-BUF-9 the tolerances are: the lower boundary 1950 kg/m^3 and the upper boundary 2050 kg/m^3 for the saturated density of the buffer.

The reference method for buffer block manufacturing is isostatic compression which is described by Ritola & Pyy (2011). In this method bentonite is compressed homogeneously from all directions by hydrostatic pressure. For the buffer pellets the reference method is roller compaction (Marjavaara et al. 2013). In the roller compaction method conditioned bentonite is compacted to small briquettes or pillows with a roller compactor. (Juvankoski 2013)

Density and homogeneity of the blocks and pellets depend on the grain size distribution, water content and compression pressure. It is important that the water content stays constant during the handling, storage and transport because changes in the water content may result in cracks. High reliability with the water content and grain size distribution needs to be kept in the production. (Juvankoski 2013)

2.2.2 Backfill design and function

Backfill along with plugs is a part of the closing structures of the deposition tunnels. Backfill is the material or materials used to fill the deposition tunnels. The plugs will be placed at the mouth of the deposition tunnels. (Autio et al. 2013) A detailed backfill design is presented in *Backfill Design 2012* by Autio et al. (2013). Backfill production (excavation, processing, transport, manufacturing and installation) is presented in *Back-*

fill Production Line 2012 by Keto et al. (2013) in which also the current deposition tunnel end plug design is presented. Some of the main functions of the backfilling are limiting the hydraulic conductivity of the tunnels and preventing the loss of buffer density due to expansion of the buffer into the deposition tunnel. After the backfilling is completed, the deposition tunnels will be plugged to avoid significant water inflows and to keep the buffer and backfill in place. (Posiva 2012b) Safety functions of the deposition tunnel backfill according to *Design Basis 2012* (Posiva 2012a) are the following (listed also in Table 1):

- Contribute to favorable and predictable mechanical, geochemical, and hydrogeological conditions for the buffer and canisters
- Limit and retard radionuclide releases in the possible event of canister failure
- Contribute to the mechanical stability of the rock adjacent to the deposition tunnels

Maximum length of the deposition tunnels is 350 meters. The limitation of the tunnel length is related to excavation technology and occupational safety (Saanio et al. 2013). The theoretical volume of the deposition tunnels is roughly 874,000 m^3 (Keto et al. 2013). Cross-sectional dimensions of the deposition tunnels for the different power plant unit fuel types are presented in Figure 13.

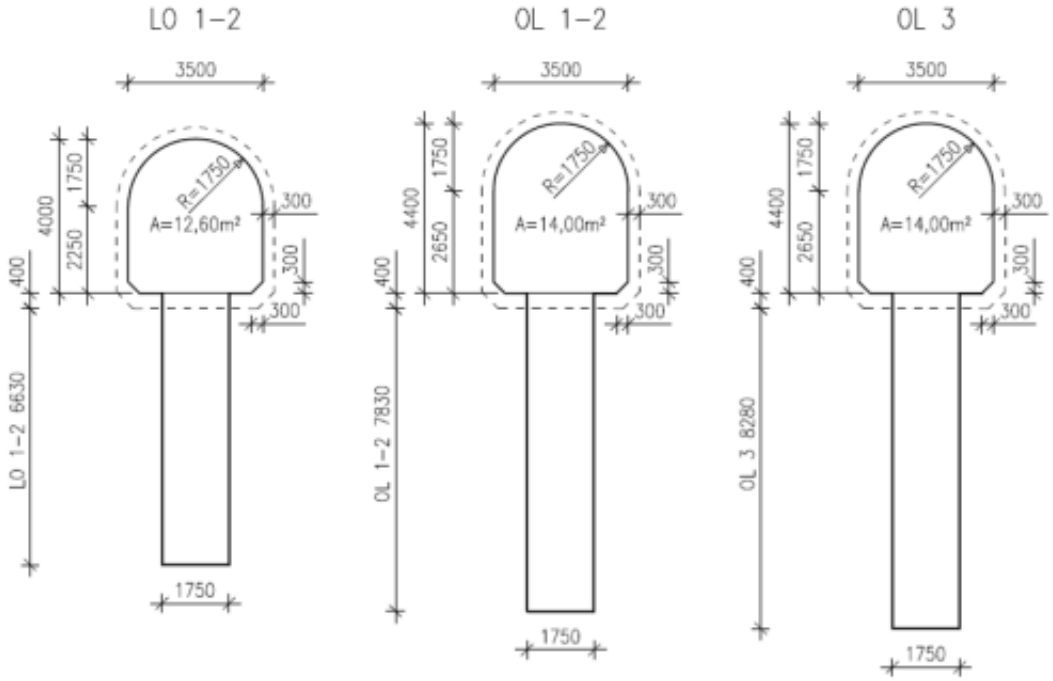

Figure 13. *Deposition tunnel dimensions (Saanio et al. 2013).*

The backfill consists of three main components: backfill blocks, foundation layer and pellets. The foundation layer is installed to provide a stable and level surface for the blocks. Spaces between the blocks and the rock will be filled with pellets. The pellets

act as water storage during the installation phase of the backfill. Water retention capacity of the pellets prevents formation of water channels and erosion of the backfill blocks.

The pellets also enable water to distribute more uniformly in the backfill. Long-term performance targets are not fulfilled until the backfill is saturated. The performance targets will be fulfilled along with the saturation when the backfill blocks compress the pellets to a higher density. (Autio et al. 2013) Schematic cross-sectional views of the deposition tunnel are shown in Figure 14.

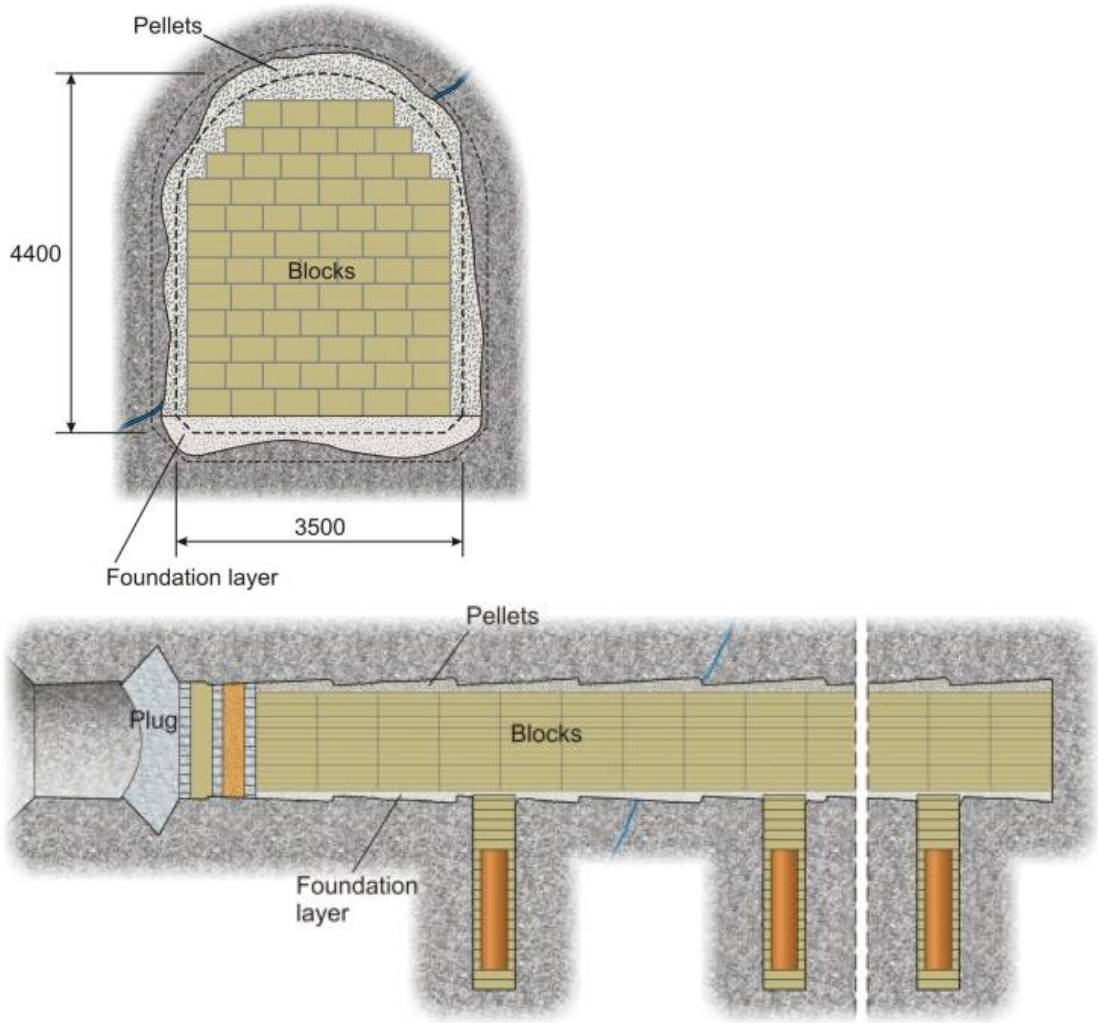

Figure 14. *Schematic images of the tunnel. In the upper image, the inner black dotted line shows the theoretical excavation profile and the outer line shows the maximum possible cross-section of the tunnel assuming tolerances of 400 mm for the floor and 300 mm for the wall and the roof. In the lower image, location of the deposition tunnel plug is shown. (Edited from Autio et al. 2013)*

The current reference material for backfill blocks is Friedland clay, originated from Germany, with the montmorillonite content of 30-38 %. The blocks are pressed using uniaxial compaction method which is described by Koskinen (2012). The compaction pressure in this method is determined prior to pressing and it is affected by grain size distribution and water content of the material. (Keto et al. 2013)

Material for the foundation layer and for the pellets consists of bentonite with the montmorillonite content of 75-90 %. An example for the foundation layer material is Minelco granules which will be compacted in situ. Water content of the material needs to be defined, for example by Proctor compaction tests, to achieve high density and thus provide a stable base for the blocks. For the pellets, an example of suitable material is Cebogel QSE pellets. Minelco granules and Cebogel QSE pellets are both originated from Milos, Greece. A possible manufacturing method for the pellets is extruding the raw material as cylindrical, rod-shaped pellets. (Autio et al. 2013; Keto et al. 2013)

The current reference design for the tunnel plug includes a concrete dome, a watertight seal and a filter layer. This multi-component structure provides sufficient hydraulic isolation capacity and structural strength. The main functions of the tunnel plug include: keeping the tunnel backfill in place and isolating the deposition tunnel hydraulically from the central tunnel. The operational lifetime requirement of the plug will end after the central tunnel has been backfilled. (Keto et al. 2013)

Design specifications for the deposition tunnel components are based on performance targets and design requirements presented in *Design Basis 2012* (Posiva 2012a). The design specifications are presented in Table 3. The limits for the montmorillonite content and dry density of the backfill materials are set so that the system is able to homogenize, self-heal and provide a hydraulic conductivity of $<1*10^{-10}$ m/s. (Keto et al 2013) This value is the average hydraulic conductivity at the repository level of the Olkiluoto bedrock (Posiva 2012c).

The worst-case scenario for the installation of backfill might be an inflow of water from a single flow path collecting water from several inflowing fractures located near each other. Probe holes are used for detecting leakages and if the leakages in a probe hole are over 0.2 l/min, pre-grouting will be done before the tunnel excavation. The maximum local fracture related inflow to a deposition tunnel is 0.25 l/min and if this limit is still exceeded after the grouting, post-grouting might be done. (Autio et al. 2013) The expected groundwater inflow conditions to open repository tunnels and deposition holes are presented by Autio et al. (2013) and by Keto et al. (2013).

The main uncertainty in long-term backfill performance is homogenization of the system. With sufficient block installation techniques and appropriate backfill component properties, the estimated initial state can be achieved. (Autio et al. 2013)

Table 3. *Design specifications for the backfill and deposition tunnel end plug (Keto et al. 2013).*

1 PERFORMANCE
1.1 BACKFILL
Montmorillonite content:
The montmorillonite content of Friedland clay blocks shall be 30-38%.
The foundation layer and pellets shall consist of bentonite with montmorillonite content between 75-90%
Dry density:
The dry density of Friedland clay blocks shall be within the range of 1990-2070 kg/m^3.
The dry density of the foundation layer shall be within the range of 1150-1350 kg/m^3.
The dry density of the pellet fill shall be within the range of 900-1100 kg/m^3
Geometry:
The backfill blocks shall have following dimensions: 550 x 470 x 330 mm. The manufacturing tolerance shall be -1 mm / +2 mm.
The block filling degree (from the theoretical/nominal cross-section) shall be >80%.
The gap width between the blocks and the theoretical tunnel wall/roof shall be 100 mm. The pellet fill shall fill the remaining open gap between the blocks and rock.
The thickness of the foundation bed shall be maximum +150 mm above the theoretical floor layer. Considering excavation tolerance of +400 mm, the maximum thickness of the foundation layer is 550 mm.
1.2 PLUG
The plug shall consist of a concrete dome, bentonite seal and a filter layer. The thickness of the sealing and filter layers is 750 mm. The thickness of the concrete dome is 1500 mm measured from the centre of the plug.
The concrete shall be watertight after installation. The hydraulic conductivity of the concrete mass shall be <1x10^{-11} m/s.
The bentonite seal shall consist of bentonite with montmorillonite content of 75-90%. In order to ensure sufficient sealing capacity the dry density shall be >1400 kg/m^3. The sealing layer shall be pre-saturated to ensure water tightness after installation of the plug.
The filter layer shall consist of sand or crushed rock with grain size distribution optimised for filtering.
The plug shall maintain its hydraulic isolation capacity for at least 100 years.
2 CHEMICAL PROPERTIES
2.1 BACKFILL
The organics content in the backfill shall be lower than 1 wt-%.
The total sulphur content in the backfill shall be less than 1 wt-%, with sulphides making, at most, half of this.
2.2 PLUG
The cementitious materials that are used in plugs shall have a calcium to silica mass ratio less than 1:6.
The organics content in the plug shall be lower than 1 wt-%.
The total sulphur content in the plug shall be less than 1 wt-%, with sulphides making, at most, half of this.
3 SUPPORT OF OTHER COMPONENTS OF THE DISPOSAL SYSTEM/MECHANICAL PROPERTIES
3.1 PLUG
The mechanical strength of the plugs shall correspond to a pressure load of at least 7.5 MPa including the ambient hydrostatic pressure.
The main material component in the plug shall be quartz sand or crushed rock.

2.2.3 Buffer and backfill interaction

The design boundary between the buffer and the backfill is presented in Figure 15. The buffer thickness above the canister is 2500 mm and there is a 400 mm gap between the uppermost block and the theoretical excavation line of the tunnel. The thickness of this gap varies depending on the level of the actual tunnel floor. The gap will be filled with a buffer type of block material. To facilitate the emplacement of the OL1, OL2 and OL3 canisters, notched chamfers are made to the upper part of the deposition holes. These chamfers are also filled with the buffer type of block material. (Juvankoski et al. 2012)

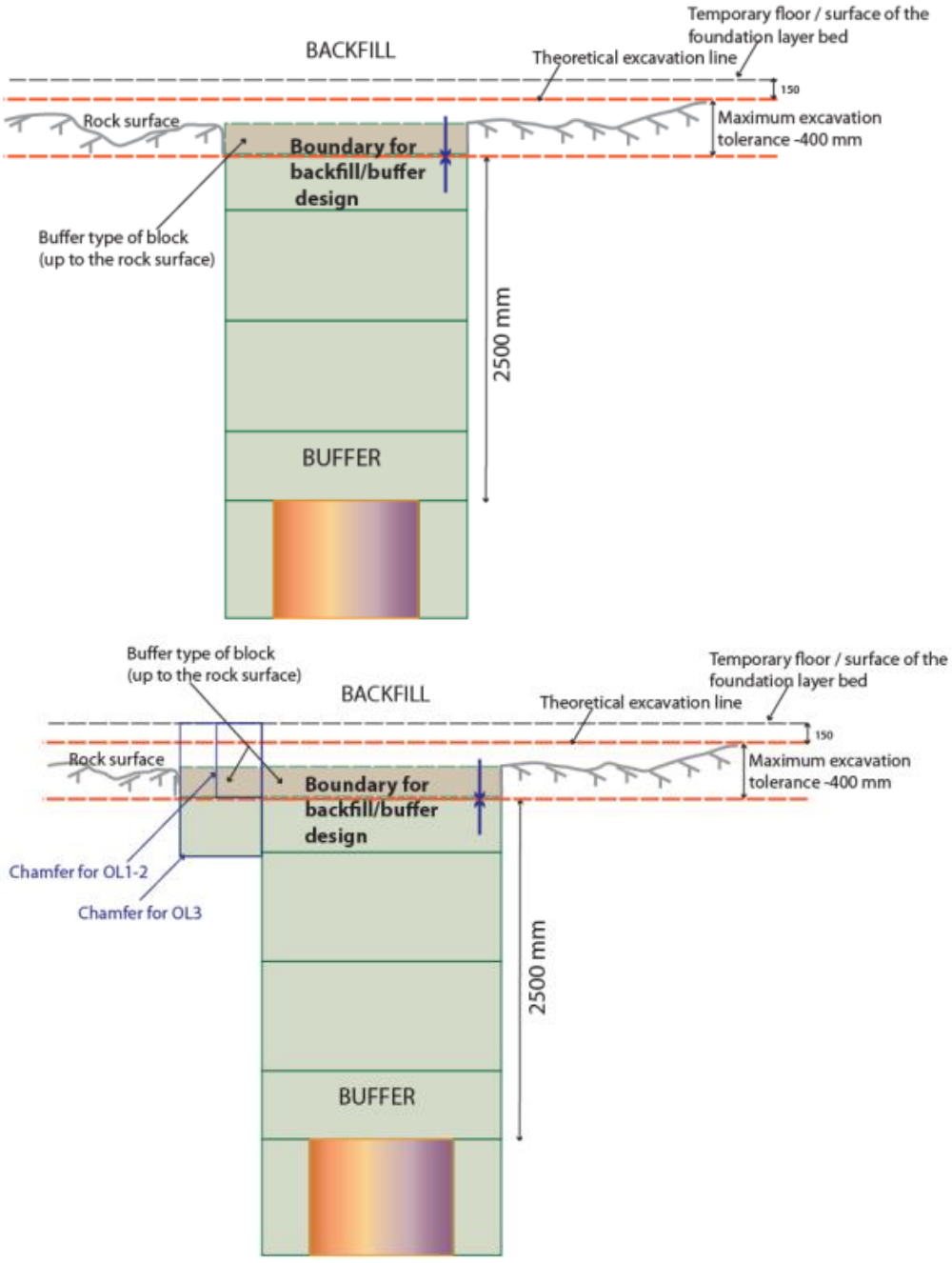

Figure 15. *The design boundary between the buffer and the backfill for the LO1-2 (upper image) and OL1-3 (lower image) spent nuclear fuel canisters (Juvankoski et al. 2012; Keto et al. 2013).*

Swelling pressure of the buffer is higher than swelling pressure of the backfill, so it is expected that the buffer intrudes into the deposition tunnel. The magnitude of this vertical displacement depends on various factors including the initial swelling pressure of the buffer, friction angle between the buffer and the rock, saturation state of the buffer and the backfill, and composition of the backfill. Swelling of the buffer into the backfill will end when a mechanical balance is reached between the buffer and the backfill. (Keto et al. 2009)

Consequently, one of the main requirements for the backfill is to limit swelling of the buffer into the backfill which decreases the density of the buffer. Decrease in the buffer density has various consequences including increase of the buffer permeability, increase of the microbiological activity and decrease of the mechanical strength. Increased permeability and microbiological activity may lead to canister corrosion and failure which further lead to migration of radionuclides through the buffer. Decrease of the mechanical strength might lead to canister movements deteriorating the performance of the EBS. (Keto et al. 2009)

A possible worst-case scenario concerning the upwards swelling of the buffer is when the buffer is fully saturated and the backfill is still unsaturated (Keto et al. 2009). Therefore it is important that the backfill has rigidity to prevent the upwards swelling also in the unsaturated state.

To decrease the upwards swelling the inflowing water should be distributed evenly and the swelling process should be controlled. In the current design the deposition tunnels are declined towards the central tunnel by 2 %. However, earlier saturation and possibly more even distribution of water in the backfill might occur if the inclination would be towards the rear portions of the tunnels which will be backfilled first. (Hansen et al. 2010)

Some modelling studies about the buffer and backfill interaction have been accomplished during recent years. Although modelling requires many assumptions and simplifications, modelling can give new insight about the interaction. Based on some modelling studies (Börgesson & Hernelind 2009; Korkiala-Tanttu 2009; Toprak et al. 2013; Leoni 2013) it has been concluded that the vertical displacement of the buffer due to swelling will be in a range between 20 mm and 150 mm. This variance is a result, for instance, from different assumptions regarding the saturation state of the buffer and backfill. The supposed worst-case scenario with respect to upwards swelling of the buffer, where the buffer is completely saturated and the backfill is completely dry, has been used in many modelling studies to find the highest possible vertical displacement and also the highest reduction in the buffer density.

As a result of the modelling, Korkiala-Tanttu (2009) found that the buffer density does not exceed the criterion of 1950 kg/m^3 if the loosening of the buffer occurs evenly. Le-

oni (2013) had a similar conclusion with a criterion of 1990 kg/m^3 for the saturated density of the buffer above the canister. Börgesson & Hernelind (2009) found that the friction angle between the buffer and its surroundings has a strong influence on the upwards swelling. Other critical parameters for the upwards swelling were stiffness and swelling of the backfill. In a study by Toprak et al. (2013), thermal behavior of the canister was modelled. They found that the maximum temperature in the interface of the canister and the buffer was 80°C and it was reached after 30 years. After 1000 years the model reached conditions at which both the canister and the buffer had the same temperature which was about 42°C. Toprak et al. (2013) also found that the buffer space between the canister and the rock wall was fully saturated in less than 10 years if the rock permeability equaled 10^{-18} m^2 and with the rock permeability of 10^{-20} m^2 the full saturation was reached after 50 years. Vertical displacements of the buffer and backfill materials during 1000 years are shown in Figure 16. These FEM calculations were made by Toprak et al. (2013).

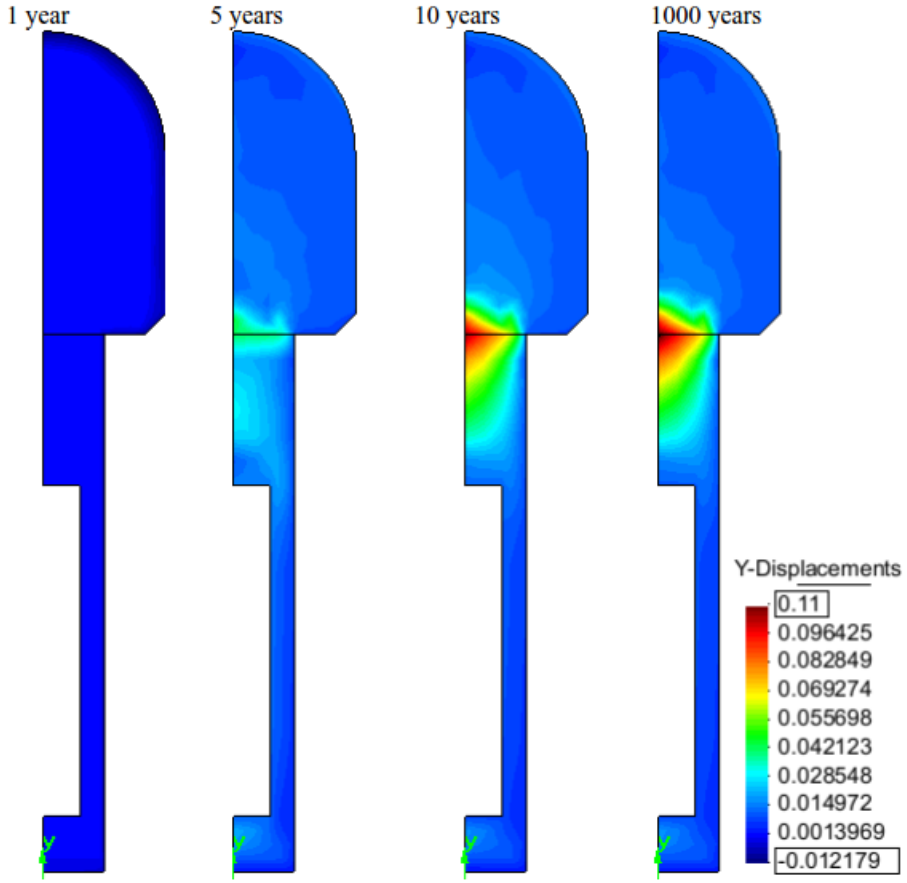

Figure 16. *Modelled vertical displacement (m) of the buffer and backfill system (Toprak et al. 2013).*

In a study by Åberg (2009) where full-scale buffer with reduced height was used to test effects of water inflow on the buffer, heaving of the bentonite rings were measured. In a test with MX-80 bentonite rings and with water inflow of 0.01 l/min, vertical displacement of over 50 mm was measured in the uppermost ring after about 17 days (Figure 17). More heaving occurred in the uppermost ring compared to the lowermost ring. Ab-

sence of overburden pressure for the uppermost ring needs to be taken into account when considering the results.

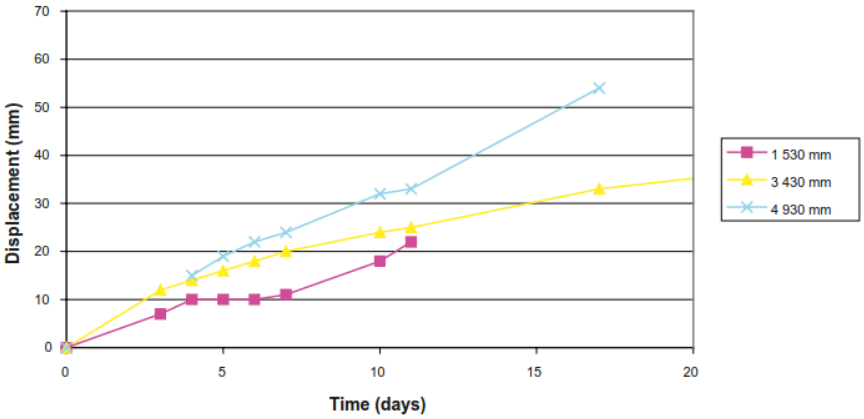

Figure 17. *Vertical displacements of three different positions of the uppermost ring in the buffer test by Åberg (2009).*

Vertical displacement of a full-scale buffer in a time scale of almost ten years has been studied by Åkesson (2012) and Johannesson & Hagman (2013). Artificial wetting and heating with temperatures over 100 °C were used by Åkesson (2012) and as a result, 47 mm of vertical displacement of the uppermost block was found (Figure 18). Vertical displacement of 176 mm of the uppermost block with no artificial wetting at a test depth of 450 m was found by Johannesson & Hagman (2013) (Figure 19).

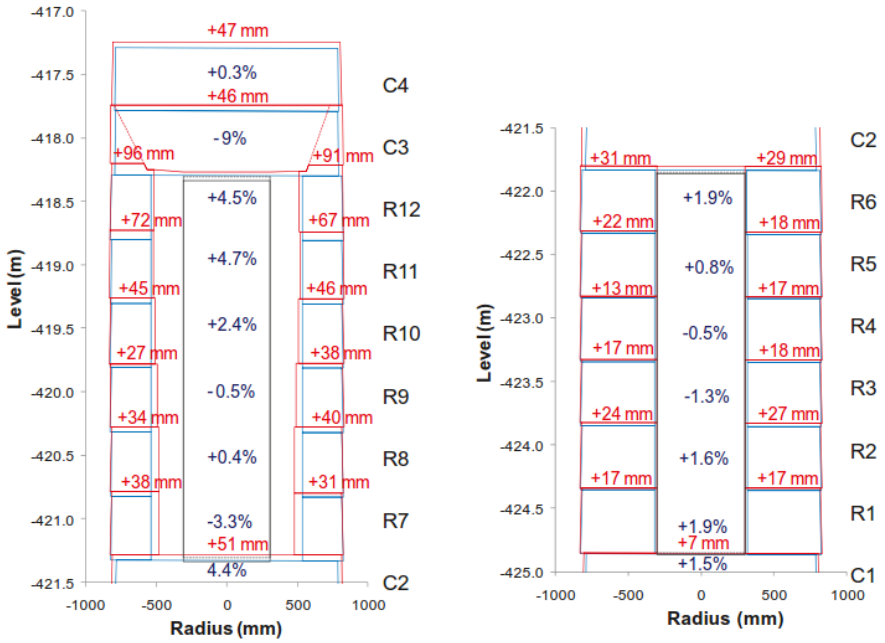

Figure 18. *Contours of bentonite blocks at installation (blue lines) and at dismantling (red lines) of a full-scale deposition hole studied by Åkesson (2012). Absolute changes in height (red numbers) and relative changes in thickness (blue numbers) are shown for each block. The lower heater was surrounded by compacted MX-80 bentonite rings and the upper heater was surrounded by a composite barrier with a sand shield between the heater and the bentonite. The upper part of the gap between the bentonite and the rock wall was filled with pellets (MX-80) to seal the sand filling below.*

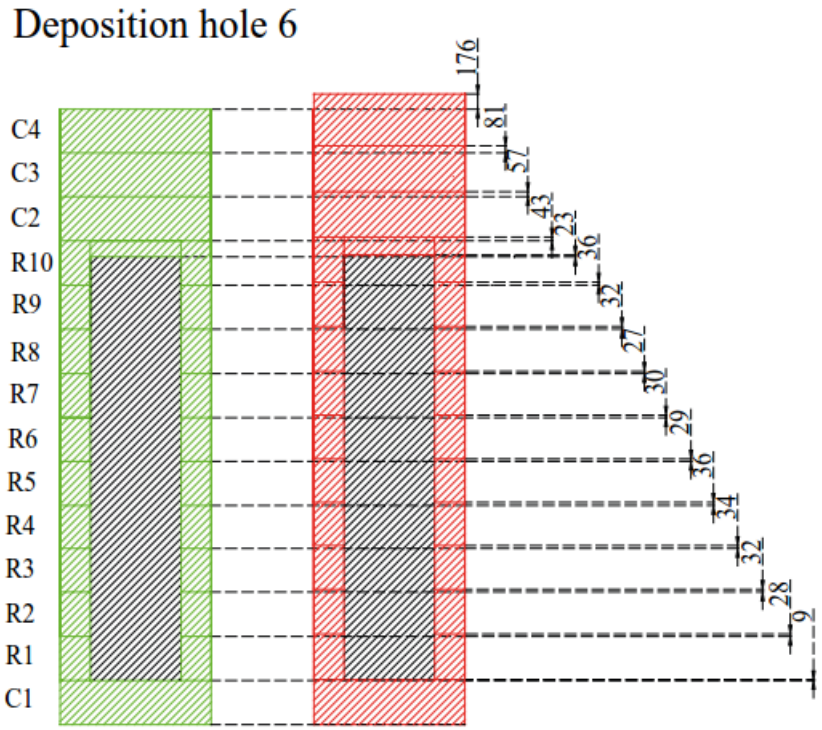

Figure 19. *Relative displacements of the upper surfaces of each block in the study by Johannesson & Hagman (2013) in which full-scale canisters were used.*

2.3 Bentonite

2.3.1 Material properties

Bentonite clay, a material with special properties, is used for many purposes in geotechnics. Bentonite is a soil material with a high content of swelling mineral. Usually this swelling mineral is montmorillonite which belongs to a smectite mineral group. The montmorillonite and other smectite minerals have an articulated layer structure. High-quality bentonite normally contains over 80 % of montmorillonite. The remaining part of the bentonite may vary substantially in mineralogy and depends basically on the geochemical conditions during the formation of the bentonite. Accessory minerals in bentonites might include other clay minerals, quartz, feldspars, gypsum, prite, various oxides/hydroxide, and also amorphous and organic compounds. (Karnland et al. 2006; Karnland 2010) A schematic image of bentonite microstructure is presented in Figure 20.

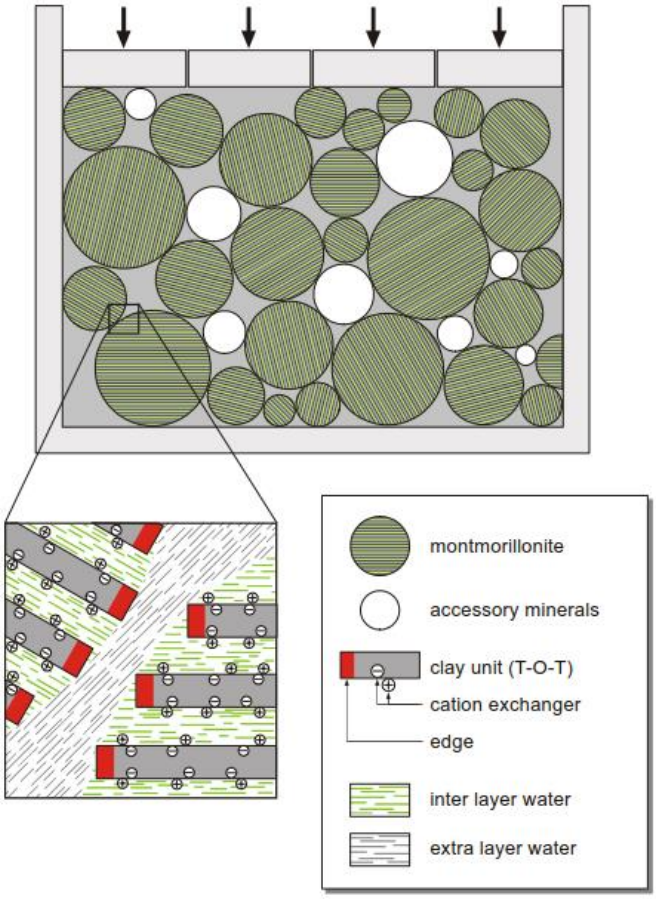

Figure 20. *Microstructure of bentonite under compaction (Wersin 2003, cited in Pastina & Hellä 2006).*

Bentonite has the ability to absorb water accompanied by a large increase of volume (Ahonen et al. 2008). The wetting process, also called saturation, occurs when compacted and unsaturated bentonite is in contact with water. Bentonite swells together with wetting due to penetration of water into the interlamellar space of montmorillonite. Faster wetting results in faster swelling of the bentonite. Wetting occurs when water invades pore spaces either as liquid or as vapor and water can also be transported bound to montmorillonite within the solid phase. The relative importance of these transport mechanisms might depend on conditions such as porosity and composition of the bentonite and electrolyte content of the water involved. Suction and the surrounding water pressure are the most important driving forces for the bentonite wetting process. (Sane et al. 2013) Dry and wetted MX-80 bentonite pellets are shown in Figure 21.

Figure 21. *Dry and wet MX-80 pellets in a test performed to study effects of water inflow on the buffer (Åberg 2009).*

Swelling pressure of the bentonite is affected by density, degree of saturation, water salinity, type of adsorbed cation in montmorillonite, montmorillonite content and degree of cementation. The swelling pressure increases with increasing density and decreasing salt concentration. The effect of the salt concentration is relatively small at high densities. At very low densities the effect on the swelling pressure can be deleterious. (Pastina & Hellä 2006) The effect of the increasing density and decreasing salt concentration on the swelling pressure is shown in Figure 22. A comparison of swelling pressures between different bentonite types, sodium (MX-80) and calcium (Milos), is also shown in Figure 22. At saturated densities over 1800 kg/m^3, swelling pressures of calcium and sodium bentonite are similar. Thus, at high densities the swelling pressure is relatively independent of the adsorbed ion if montmorillonite contents are equal. At lower densities the swelling pressure is lower in calcium bentonite. (SKB 2004)

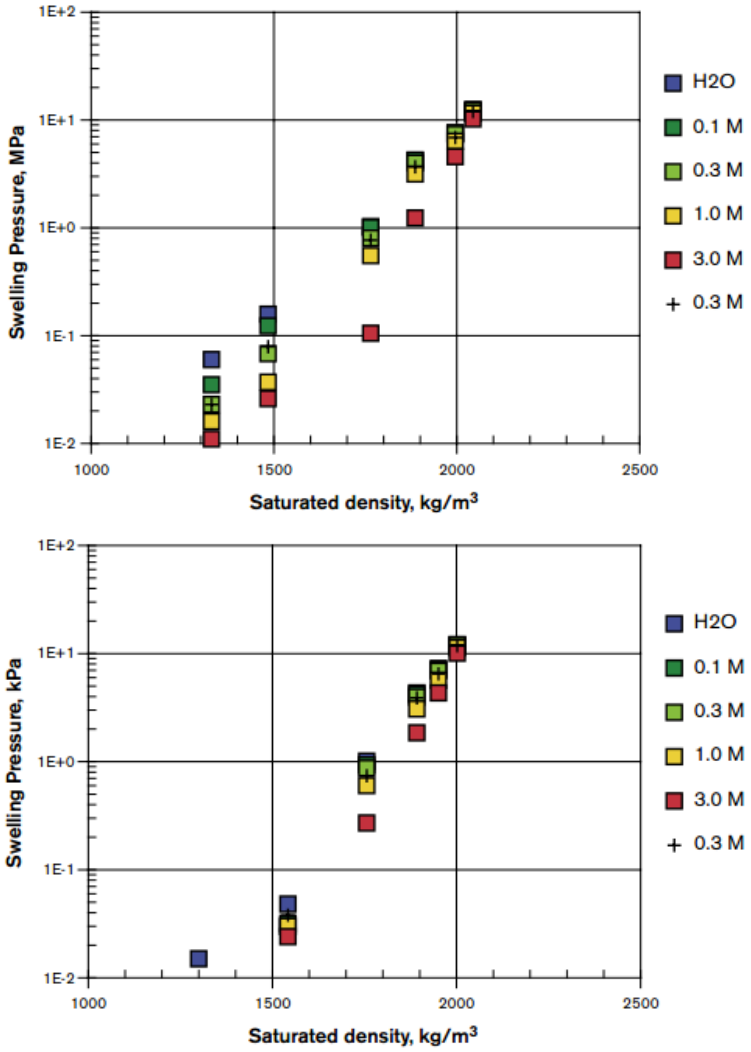

Figure 22. *Swelling pressures of MX-80 bentonite (upper) and Milos bentonite (lower) at different densities and molar concentrations of NaCl (for MX-80) and $CaCl_2$ (for Milos) (SKB 2004).*

2.3.2 Bentonite in nuclear waste disposal

Bentonite is a crucial part of the engineered barrier system, securing the long-term safety of the final disposal. Bentonite is used as a buffer material surrounding the canister, and also as a material for backfilling the deposition tunnels. Bentonite has several properties supporting its usage as the buffer and backfill material: high swelling pressure, low hydraulic conductivity, retardation capacity and plastic behavior. (Ahonen et al. 2008) The swelling of the bentonite is essential to protect the canister from minor rock displacements and in case of a release, slow down the transport of radionuclides. Development of swelling pressure along with water saturation is important also for dissipating the heat from the canister. Artificial wetting could be an option to shorten the time to reach the desired swelling pressure. (Pastina & Hellä 2006) Based on the results from a small-scale buffer material study by Holt et al. (2011), artificial wetting could potentially induce rapid and homogeneous swelling of the buffer bentonite.

The swelling of the bentonite is important also for sealing water channels and thus preventing circulation of the water and erosion of the bentonite. The erosion of the bentonite by flowing groundwater is a process called mechanical erosion. During the operational phase of the repository, high groundwater pressure gradients in the open excavations might cause erosion. Consequences of the erosion might include: reduced density of the bentonite, reduced swelling pressure, accessibility of the canister surfaces to sulfides which increases the copper corrosion rate, and transport of radionuclides in case of an accidental release. (Pastina & Hellä 2006) To avoid erosion, maximum allowable inflow of 0.1 l/min to the deposition hole has been set as rock suitability criteria (Posiva 2010).

There are different factors affecting the bentonite erosion. A summary of small-scale erosion studies is presented in *Current Status of Mechanical Erosion Studies of Bentonite Buffer* by Sane et al. (2013). Based on the small-scale erosion studies, effective montmorillonite dry density (EMDD) correlates well with erosion rates. Higher EMDD increases erosion. Optimal water ratio is needed to achieve optimal compaction density and proper erosion resistance. Too high and too low water ratio increases the erosion which is attributed to slaking (very fast mass detachment occurring when dry bentonite interacts with solution) and also to generally decreased cohesion forces keeping the material intact. The erosion is affected also by montmorillonite content and salinity. Higher erosion rates have been found with lower montmorillonite content and higher salinity. The effect of the salinity on the erosion is stronger in early phases. The effect of the salinity is also non-linear. (Sane et al. 2013)

In a study by Pintado et al. (2013), early saturation behavior of a small-scale buffer system (Figure 23) was investigated. Water inflow rate of 0.1 l/min was used. Sampling of outflowing water for erosion rate was performed at regular intervals. With salinities ranging from tap water (0.0315 g/l) to 35 g/l, the accumulated erosion after 2000 hours was approximately three times larger with the salinity of 35 g/l compared to the tap water. Concentrations of the eroded bentonite during the tests are presented in Figure 24.

Figure 23. *Test cylinder comprised of a PVC cylinder fitted with plastic pistons at the bottom and top. The diameter of the test cell was 269 mm and the height was 800 mm. Flow inlet and outlet ports (inner diameter 6 mm) were found at the bottom and top of the test cylinder, respectively. (Pintado et al. 2013)*

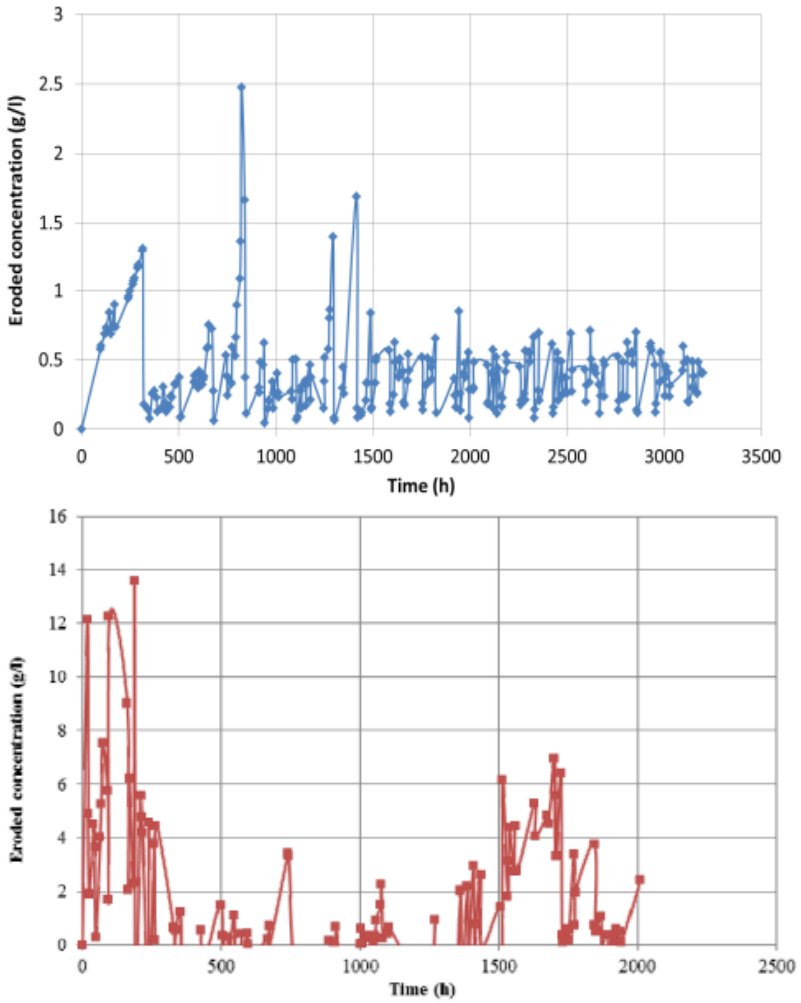

Figure 24. *Eroded bentonite concentrations (g/l) in tests with the small-scale buffer system. The samples were taken from outflowing water at regular intervals. Salinity of inflowing water in the test 1 was 0.0315 g/l (upper graph) and in the test 2 it was 35 g/l (lower graph). (Pintado et al. 2013)*

Excessively high groundwater flows and inadequate compaction may result in formation of water channels which is called piping erosion (Pastina & Hellä 2006). The occurrence of the piping might depend on variables including groundwater salinity, flow rate and pressure head (Sane et al. 2013).

The ability of the bentonite to swell is crucial for the piping erosion. Swelling material like bentonite has a tendency to push itself into the channel. The channel will close if the swelling is strong and the water flow is low enough. It is expected that erosion occurs in a piping channel with a constant water flow when the bentonite swells towards the channel. In the EBS, containing both bentonite blocks and pellets, the initial creation of the piping channels occurs at the pellet filling due to the large air volume between the pellets and absence of swelling pressure to oppose piping. Under the worst-case conditions with large point-like inflows to the deposition holes, the filling of the void spaces is estimated to require some tens of years. After a deposition tunnel is sealed and the void spaces are filled with groundwater, it is expected that the piping erosion process ends due to equal overall pressure between the water in the EBS and the surrounding groundwater. (Sane et al. 2013) A possible worst-case condition for the piping erosion in the buffer is presented in Figure 25.

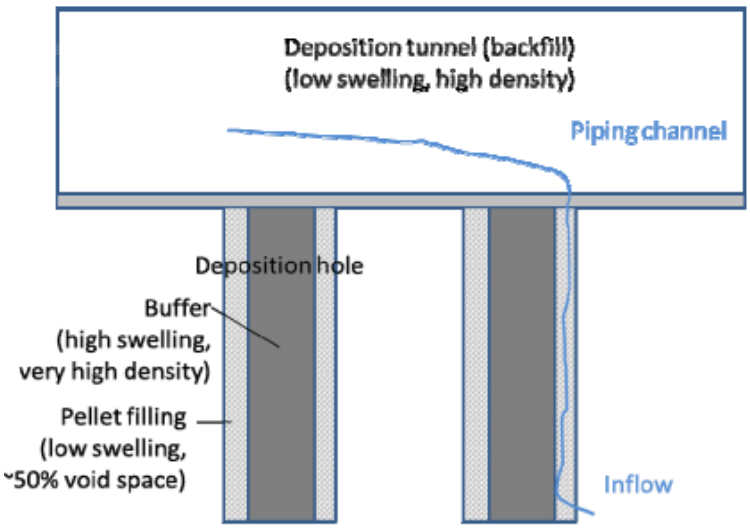

Figure 25. *A schematic presentation of a worst-case piping erosion for the buffer where the groundwater flow transports bentonite from the deposition hole into the deposition tunnel (Edited from Sane et al. 2013).*

In the small-scale buffer system test by Pintado et al. (2013), with the inflow rate of 0.1 l/min, water flow channels were continuously observed at the sample/test cylinder interface (Figure 26). In addition, no significant resistance to water inlet pressure was observed which indicated that flow pathways in the buffer system remained open. In the full-scale buffer test with the reduced height by Åberg (2009) it was concluded that bentonite pellets do not have the ability to seal water pathways if there is a continuous inflow of water (Figure 27).

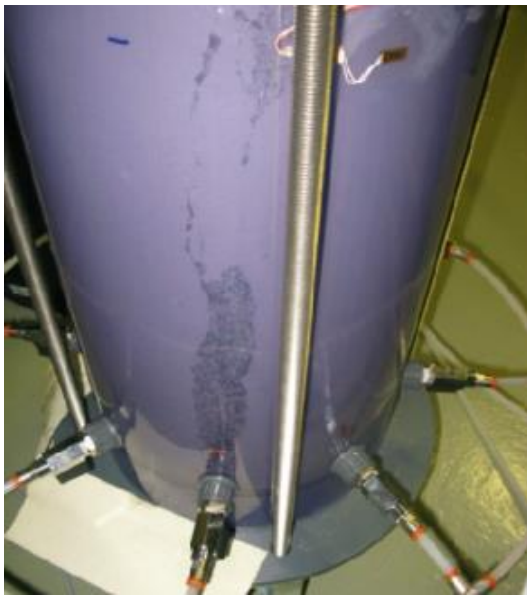

Figure 26. *Water flow channels visible at the sample/test cylinder interface of the small-scale buffer system study by Pintado et al (2013).*

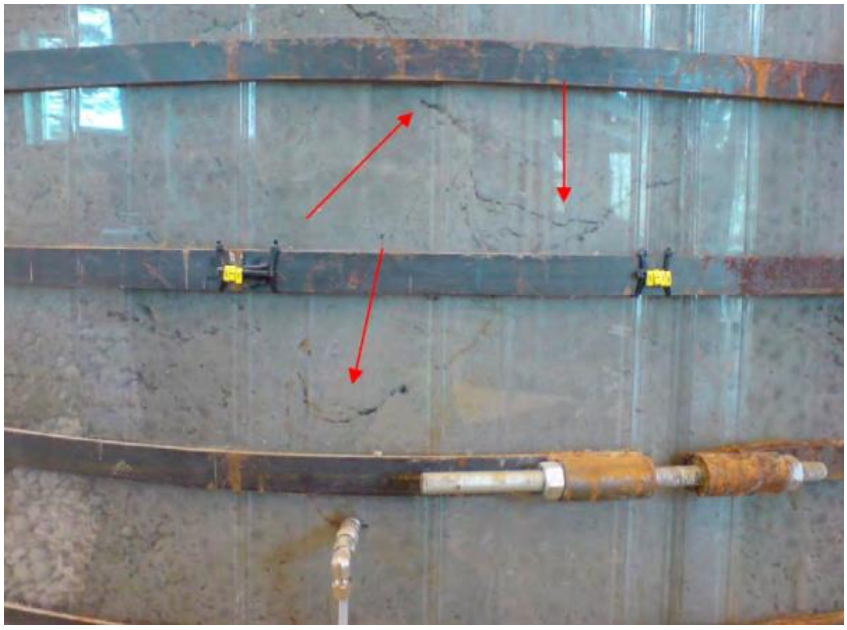

Figure 27. *Water channels in the test with the full-scale buffer with the reduced height (Åberg 2009).*

3. EXPERIMENT

This 1/6 scale experiment was carried out to get a new insight of the bentonite behavior in the initial phase of the final disposal, after the bentonite blocks and pellets have been installed and natural or artificial wetting of the bentonite begins. In the experiment, buffer and backfill components were both included to investigate their interaction. This experiment gave data about the scale effect and with the use of the small-scale test system the test was less time-consuming and less expensive. However, small-scale test probably do not simulate full-scale situations perfectly. Despite the smaller scale the pellet layer thicknesses nearly corresponded to the full-scale buffer and backfill, making the erosion behavior and possible formation of water channels possibly similar compared to larger scale systems. The main interests in the experiment were water distribution, flow channels, swelling of the bentonite, erosion of the bentonite, and the interface and the interaction between the buffer and the backfill. The buffer system used in this test was similar to the buffer system used in the test series performed by Pintado et al. (2013).

The 1/6 scale test system simulated a vertical deposition hole and a horizontal deposition tunnel that were filled with bentonite blocks and pellets. No canister or heating system was included in this experiment. Saline water flowed through the test system and samples were taken from the outflowing water for erosion and outflow rate analyses. Swelling of the bentonite was monitored and follow up of wetting of the bentonite was performed through the partly transparent test system. After the test was stopped, samples were taken for water content and density analyses. Visual observations of the wetting and water channels were done during the dismantling. Also, a vertical displacement of the buffer was investigated.

The test was initiated on May 5, 2015, and it was stopped on July 6, 2015, when the sampling and dismantling work started. Duration of the test was 62 days corresponding to approximately 1448 hours.

3.1 Test equipment

3.1.1 Tunnel and tube

For this project, new laboratory test equipment was manufactured in 2014 at about 1/6 scale dimensions of the deposition area planned in Olkiluoto. The test equipment was composed of two main parts, the tunnel and the deposition hole simulating tube. Dimensions of the tunnel and the tube were based on the deposition hole designed for the nu-

clear waste produced by OL1 and OL2. The tunnel, about 3400 mm in length, 760 mm in height and 650 mm in width, was manufactured from stainless steel. Steel was used due to internal swelling pressure of the tunnel. FEM calculations were used in the design. The tunnel was also equipped with polycarbonate windows, covering about 40 % of the tunnel walls. The tube was manufactured from transparent PVC. The inner diameter of the tube was 269 mm, outer diameter 280 mm and height 950 mm. The tube was connected into the bottom of the Middle unit. The tunnel was lying on a steel frame whose adjustability was utilized to set the tunnel to horizontal position. There were three overflow basins (1500 mm x 1500 mm x 400 mm) under the test system for possible leaking of the system. The basins were made from stainless steel and they were connected to the drainage system by a hose. The tunnel, the tube, the tunnel support frame and the overflow basins are shown in Figure 28. More precise dimensions of the test equipment are presented in Appendix 1.

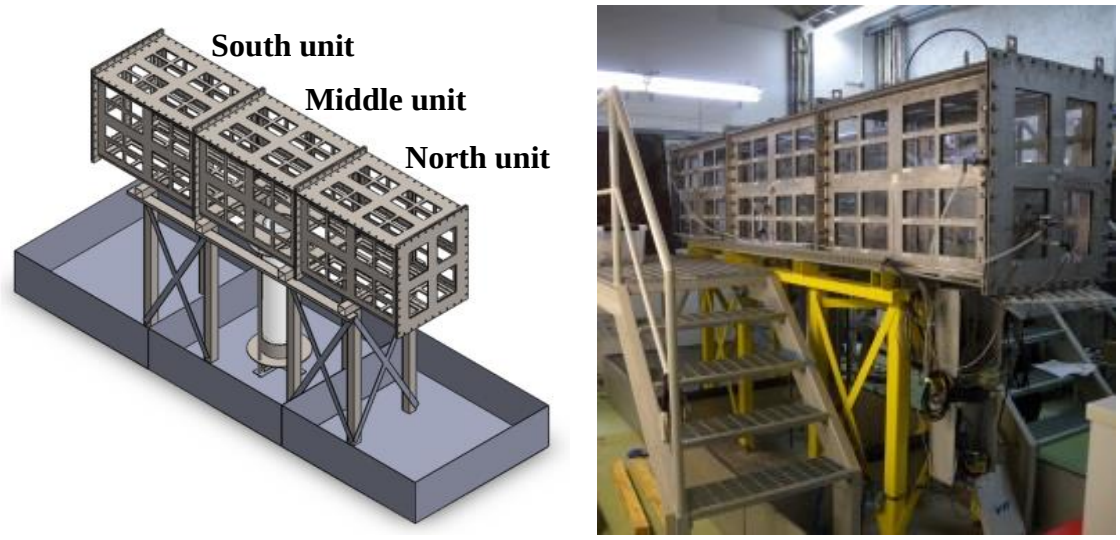

Figure 28. *Schematic view of the test equipment with overflow basins (left), and a photo of the test equipment (right).*

3.1.2 Water flow system

Water solution simulating Olkiluoto's groundwater flowed through the test equipment. The water was stored in two 2500 liter tanks from where the water was delivered to a pump unit which had its own water reservoir of about 200 liters. The pump unit operated as a screw pump and it was controlled by an AC drive. The pump unit had internal measurements of water flow and counter pressure which were constantly monitored and used as controlling parameters of the pump. The maximum allowed counter pressure of the pump was 500 kPa. The pump was set to supply water into the test equipment at a constant rate of 0.1 l/min which is the maximum rate of inflow to the deposition hole according to the rock suitability criteria, presented by Posiva (2012a). The rate of the water inflow was constantly monitored. Water inlet located in the tube, 150 mm above the bottom of the tube. A scheme of the water flow system is presented in Figure 29 and photos of the water inflow system are shown in Figure 30.

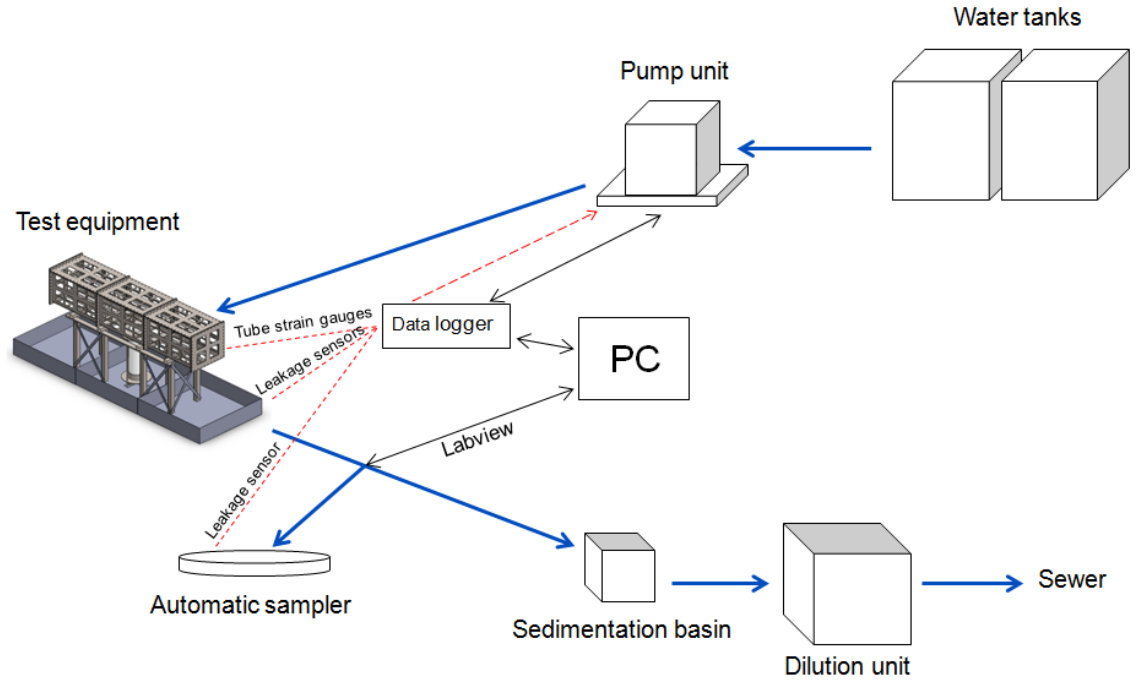

Figure 29. *A schematic view of the water flow system where blue lines indicate the water flow, red dashed lines indicate an automatic switch off system of the pump, and black lines indicate a controlling system of the pump unit and an automatic sampler.*

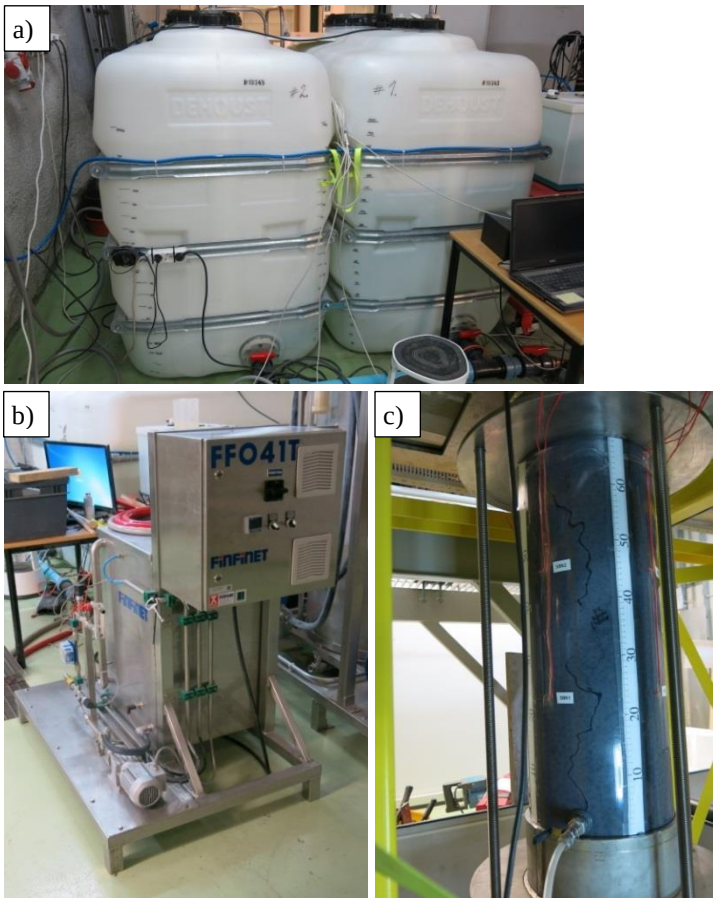

Figure 30. *Different parts of the water inflow system: a) two water tanks, b) the pump unit, c) the water inlet connected to the tube.*

The tunnel was equipped with eight open outlets for the outflowing water and solid material. Four of these outlets were in the North unit and four in the South unit. Locations of the outlets are shown in Appendix 2 in which also labelling of the tunnel windows is presented. All eight outlet pipes were channeled towards a collecting pipe which was located in the North end of the tunnel. The collecting pipe was channeled past an automatic sampler which took a seven minute sample from the outflowing water in four or five hour intervals. Outside the sampling time the outflowing water went through a three chamber sedimentation basin where eroded bentonite was separated from the water. Before disposal to the sewer the water was diluted with tap water in a dilution unit. Photos of the parts of the outflow system are presented in Figure 31.

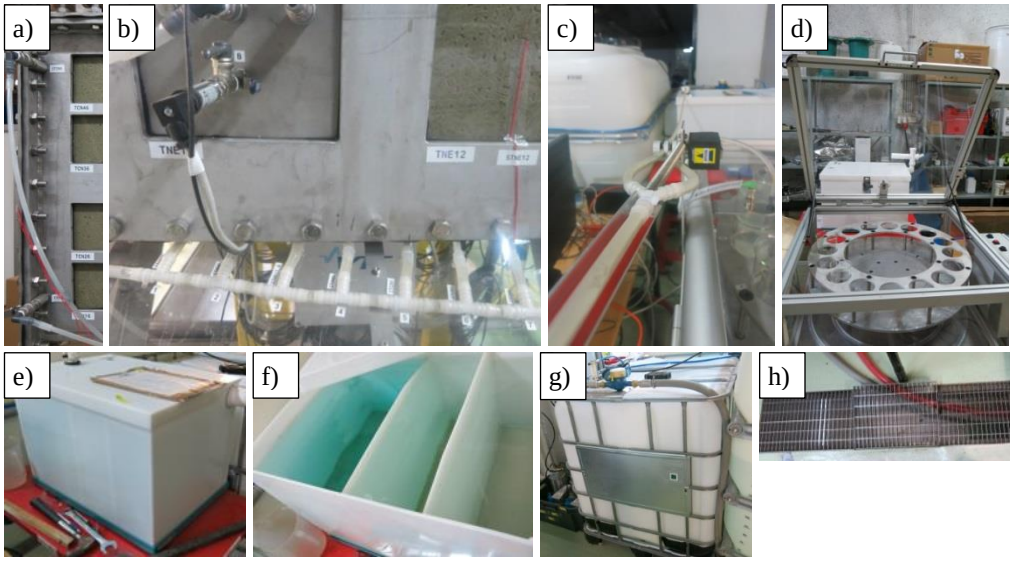

Figure 31. *The outflow system: a) two outlets in the North unit (ITCN5 and ITCN6), b) the collecting pipe, c) a branch in the outflow pipe where the water was directed either to the automatic sampler or to the sedimentation basin, d) the automatic sampler with a collar for 16 beakers, e), f) the sedimentation basin, g) the dilution unit, h) the sewer.*

3.1.3 Instrumentation

Swelling of the bentonite was monitored with different instruments. Strain gauges (Kyowa, KFG-5-120-C1-11L1M2R), total pressure sensors (Tokyo Sokki Kenkyujo's KDE-PA Soil Pressure Gauges) and dial gauges were installed for the swelling pressure monitoring. These instruments were mainly used for safety aspects by setting maximum limits for the stresses. To the outer surface of the tunnel, 22 strain gauges and two dial gauges were attached. Four total pressure sensors were installed into the tunnel: above the tube against the bottom of a tunnel backfill block (1), above the tube on the top pellet layer of the tunnel (2), in the center of the North end (3), and in the center of the South end (4). Total pressure sensors 1 and 2 were positioned horizontally and sensors 3 and 4 vertically. On the outer surface of the tube there were eight strain gauges attached to measure radial stress in the tube. There was also a force transducer (Utilcell load cell M750) under the tube to measure axial stress in the tube. Locations of the strain gauges

and the dial gauges are presented in Appendix 2. Photos of some of the gauges and sensors are shown in Figure 32.

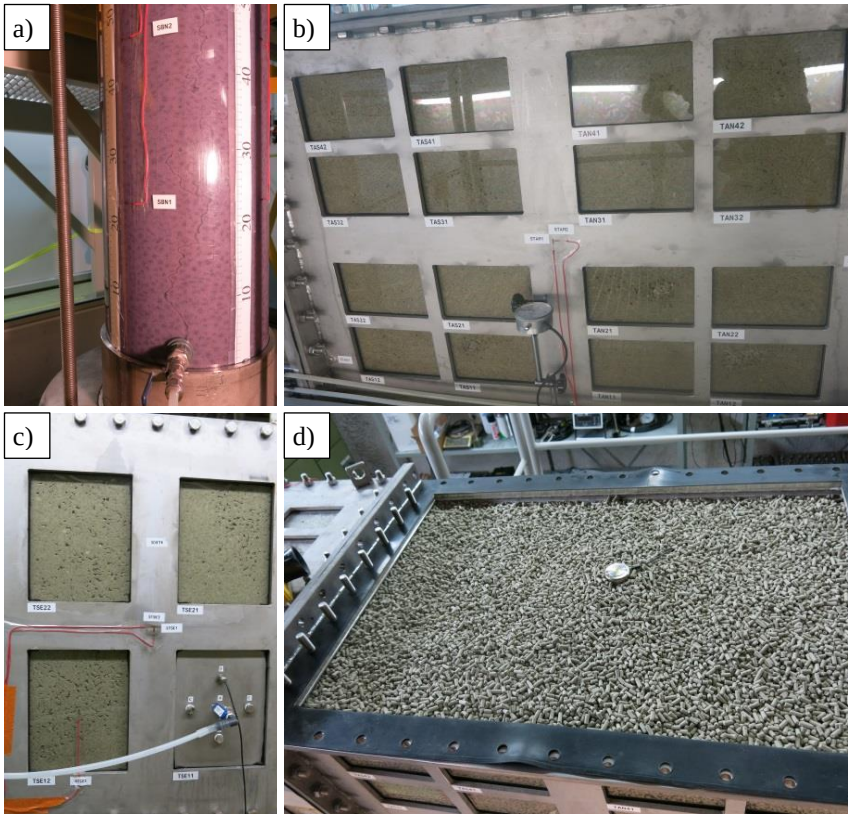

Figure 32. *Some parts of the test system instrumentation: a) strain gauges on the outer surface of the tube (SBN1 and SBN2), b) strain gauges (STAM1 and STAM2) and a dial gauge in the Middle unit of the tunnel in the A-side, c) strain gauges in the South end of the tunnel (STSE1, STSE2 and STSE12), d) pressure sensor on the top pellet layer of the Middle unit.*

Collection of the measured data by the gauges and sensors was managed by a data logger (DataTaker DT85G-3, see Figure 33a). The data was automatically stored by a NAS server (Linkstation 220 4T Networked Access Server). The data was collected in five second intervals and it was observable from the data logger's web server (Figure 33c).

Alarm events were connected to 14 channels of the data logger (Pump counter pressure, STAM1, STAN1, STAS1, STBM1, STBN1, STBS1, STCM1, STCN1, STCS1, STNE1, STNE2, STSE1, and STSE2). The pump counter pressure was set to log an alarm in a pressure of 190 kPa. Exceeding a maximum limit pressure of 200 kPa was set to induce a shutdown of the pump. Strain gauges connected to the alarm system (listed above) had a maximum limit stress of 250 kPa and exceeding this limit was set to shut down the pump. In an alarm situation a SMS message was programmed to be sent to a person involved in the test. The limit stress of 250 kPa was set for safety reasons and it was based on a yield point of the tunnel material and results of a pressure test which is described later in the text. Placement of the strain gauges to the middle parts of the tunnel units was based on the FEM calculations done before test.

Also, possible leakage of the test system was monitored with an alarm system. Two open conductors were used for detecting the leakage, and with a NetBiter EC220 communication gateway, SMS message was sent. Conductors for the leakage detection were located in the overflow basins and under the automatic sampler (see Figure 29).

The automatic sampler was operated by a motor drive which was controlled by a custom LabVIEW 2014 program used by a PC. A relay module controlled magnetic valves (Figure 33d) which directed the outflowing water either to the automatic sampler or to the sedimentation basin. Ultrasonic sensor measured the water level in a beaker when sampling was under way.

Two types of video cameras were used in the test. Two recording cameras (Brinno TLC200 Pro, see Figure 33e) were installed to take images in one minute intervals. This enabled to make a time lapse video of bentonite wetting and development of water channels. Also, a surveillance IP-camera (Milesight MS-3366, see Figure 33f) was installed to give an overall view of the test equipment, video image being accessible from the web browser.

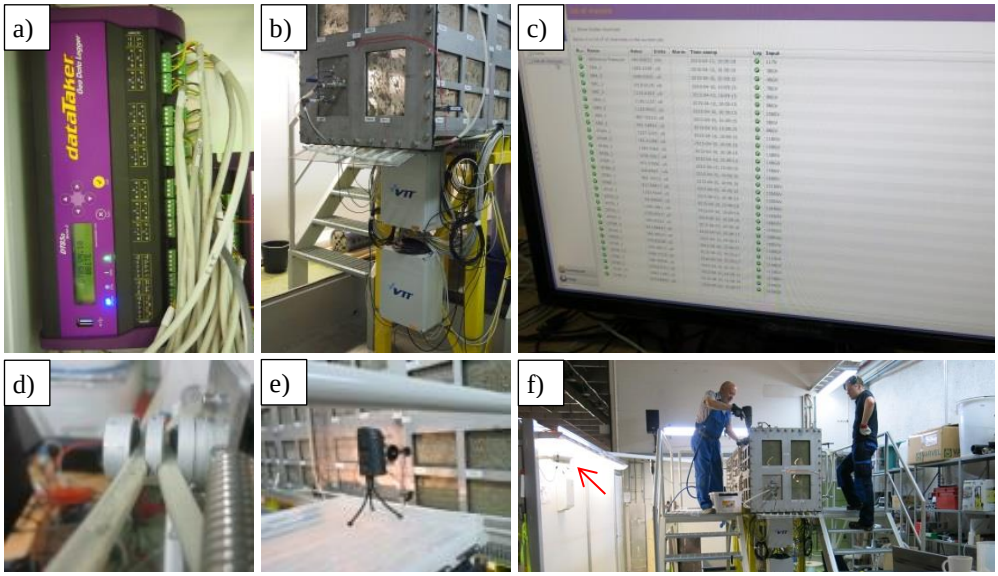

Figure 33. *Parts of the test system instrumentation: a), b) parts of the data logger system, c) a view from the data logger's web server in the laboratory's PC, d) magnetic valves controlling the water flow either to the automatic sampler or to the sedimentation basin, e) a time lapse camera, f) the IP camera pointed by a red arrow.*

Before the start of the test, functioning of the test equipment, the gauges and the sensors were checked in a water pressure test. Also, the calibration of the instrumentation was done by the pressure test. In the pressure test, tap water was supplied into the test equipment. Pressure inside the tunnel was increased to a maximum value of 220 kPa while possible leaks from the equipment were detected and the strains were followed. Maximum relative strain of the tunnel was specified (0.15 %) to prevent permanent deformations of the steel tunnel. In a case of leaking, bolts of the tunnel lids were tightened.

3.2 Materials

Bentonite blocks and pellets were used to fill the tube and the tunnel (Figure 34a-d). The blocks and the pellets arrived to a VTT's Research Hall one month before the start of the test and they were stored in climate rooms with a relative humidity of 65 % and a temperature of 20 °C. Most of the blocks had small defects in their edges (Figure 34e-f).

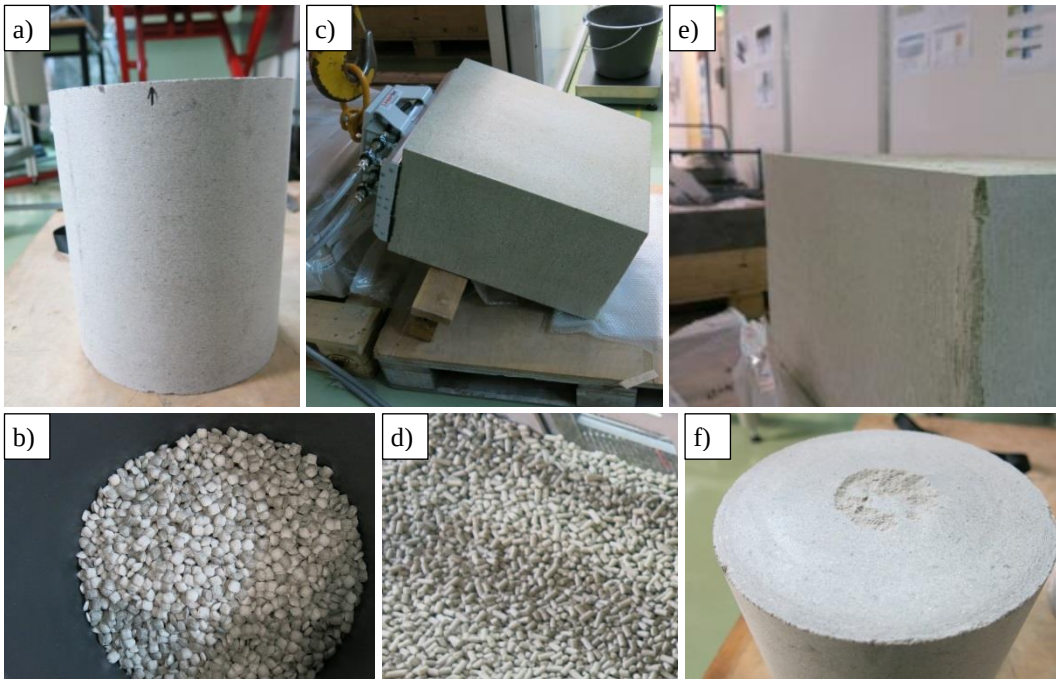

Figure 34. *Bentonite materials used in the test: a) buffer blocks (MX-80), b) pillow shaped buffer pellets (MX-80), c) tunnel backfill blocks (Ibeco RWC BF), d) extruded tunnel pellets (Cebogel), e) defect in the edge of a tunnel backfill block, f) defect on the top of a tube buffer block due to machining.*

3.2.1 Tube

MX-80 bentonite was used as the buffer block and pellet material. Four cylindrical blocks, manufactured by isostatic compression of 100 MPa, were installed into the tube (Figure 35). A 50 mm gap between the blocks and the inner surface of the tube was filled with pillow shaped pellets, manufactured by roller compaction. Each block was weighed and the dimensions were measured before the installation.

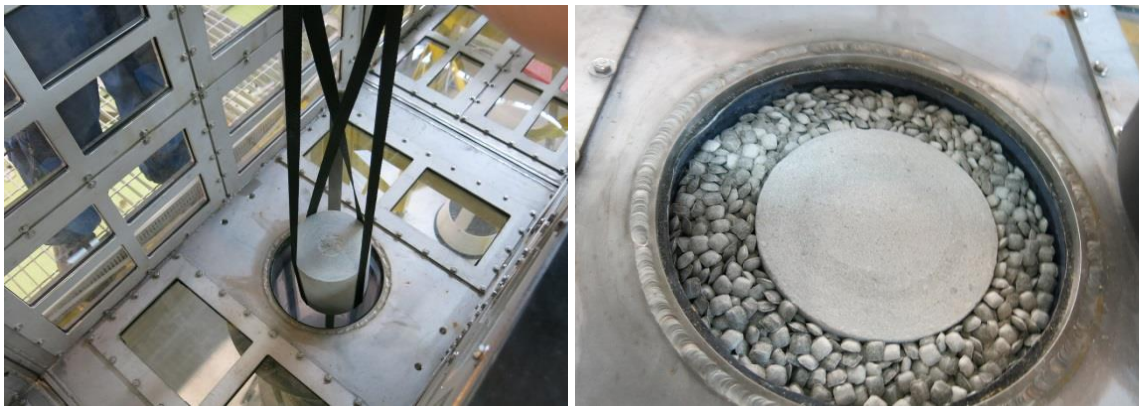

Figure 35. *The buffer blocks were installed into the tube by straps and they were centered with the help of custom-made wooden sticks. The blocks and the pellets were installed in turns so the pellets stabilized the blocks that were already in the tube. The level of the top of the uppermost block was 30 mm below the tunnel floor level.*

Bulk density, dry density and water content of the tube materials are presented in Table 4. For the blocks, these properties were analyzed from an extra block not used in this experiment. Weights and dimensions of the buffer blocks are presented in Appendix 3.

Table 4. *Properties of the buffer materials.*

Material	Bulk density (kg/m^3)	Dry density (kg/m^3)	Water content (%)
Blocks (MX-80)	2051	1768	16,0
Pellets (MX-80)	1078	925	16,6

3.2.2 Tunnel

The tunnel was filled with six Ibeco RWC BF backfill blocks and Cebogel QSE pellets (Figure 36). The blocks were manufactured by uniaxial compression and the pellets by extruding. The blocks were weighed and their dimensions were measured before they were installed. Approximately 37 % of the tunnel volume was filled with the blocks and 63 % with the pellets.

Figure 36. *The floor of the tunnel was filled with a 95 mm thick pellet layer and six backfill blocks were installed into the tunnel with a vacuum lifting device. After the blocks were installed, the rest of the tunnel was filled with the pellets.*

Bulk density, dry density and water content of the materials are presented in Table 5. For the backfill blocks, these properties were the averages of the six blocks used. Weights and dimensions of the tunnel backfill blocks are presented in Appendix 3.

Table 5. *Properties of the tunnel materials.*

Material	Bulk density (kg/m^3)	Dry density (kg/m^3)	Water content (%)
Blocks (Ibeco RWC BF)	2041	1760	16,0
Pellets (Cebogel)	1119	936	19,5

3.2.3 Water solution

For the experiment, water solution was prepared into two water tanks before the test. The solution consisted of tap water, sodium chloride and calcium chloride. The salinity of the water solution was 10 g/kg and Na/Ca relation was 2. Properties of the solution are presented in Table 6.

Table 6. *Properties of the artificial groundwater solution.*

	Tap water (%)	NaCl (%)	$CaCl_2$ (%)	Salinity (%)	Na/Ca
Water solution	99,0	0,65	0,35	1,00	2,00

3.3 Test implementation

There were different routines during the test. Every working day, different checks were done: function of the test system, pressure values, inflow rate of the pump and water consumption. Also, samples from the outflowing were taken and photos were taken from the tube and the tunnel to investigate the wetting of the system as well as development of possible water channels. All observations were documented.

Samples from the outflowing water were analyzed every working day. The samples were collected with the automatic sampler generally at four hour intervals. In the weekends the sampling interval was five hours but in the first two days, the sampling interval was occasionally one or two hours. The sampling time was seven minutes throughout the test. The beakers containing water samples were weighed and placed into an oven (120 °C) for evaporation. The automatic sampler was then refilled with weighed and labelled empty beakers, and the automatic sampler was restarted. First sample after filling and restarting of the sampler was collected immediately, thus making the sampling interval to be less than four hours. The samples were held in the oven for four days after which they were weighed to define the dry material content and the outflow rate of the water. The beakers were washed in a dish washer before reusing them. In the automatic sampler there were three additional beakers filled with the water solution. These samples were weighed every working day to determine the evaporation of the water inside the automatic sampler. The average evaporation of the three additional water samples was used for determining the volume of the samples collected from the outflowing water, right after the collection.

Of the two water tanks used in the test, only one was in use at a time. The water inlet was switched between the tanks before the water ran out from the tank that was in use. New water solution was then prepared into the emptied tank. One pump was installed into the bottom of both tanks to mix the water solution after filling the tank with a new water solution. Salinity of the water in the tank in use was determined for reference in ten days intervals on average. The determination was done by drying a sample in the oven.

In the 59^{th} day, three days before the end of the test, a tracer was added into the water tank that was in use. This was done to color the inflowing water and thus enable to make observations of the water flow paths inside the test system. The tracer was Erioglaucine disodium salt and it was used 0.005 g/l.

After ending the test, the tunnel and the tube were dismantled from the bentonite. During the dismantling, a large amount of block and pellet samples were taken. The samples were analyzed for density and water content.

3.4 Sampling and dismantling

3.4.1 Progression of the sampling and dismantling work

The sampling and dismantling work started after the pump unit was switched off and the water inlet valve connected to the tube was closed. Also the outlet pipes were disconnected from the tunnel. The automatic sampler was disconnected and removed from the test area.

The work was done in two phases: first the tunnel, then the tube right after. Work in the tunnel was done in three phases: North, Middle and South units, respectively. To prevent drying of the bentonite inside the tunnel, a plywood board was placed on the top of the tunnel when the work paused.

In each tunnel unit, the work advanced from the top to the bottom. After removing the lid of a unit (Figure 37), top layer (B-side) pellet samples were taken. Some of the pellets were attached to the lid as shown in Figure 37. After the top layer of the pellets was removed, block samples were taken and then those blocks were dismantled and pellet samples from the sides (A-, C-, N- and E-sides) were taken. Lastly, pellet samples from the bottom of the tunnel (D-side) were taken. Locations of the tunnel pellet and backfill block samples are presented in Appendix 4 and 5. From the bottom layer of the tunnel, nine additional samples were taken above the buffer. These samples contained the approximately 100 mm thick tunnel bottom pellet layer and also a part from the uppermost buffer block or pellet. Locations of these samples are presented in Appendix 6. All of the pellet and the backfill block samples were packed in vacuum bags and labelled right after the sampling.

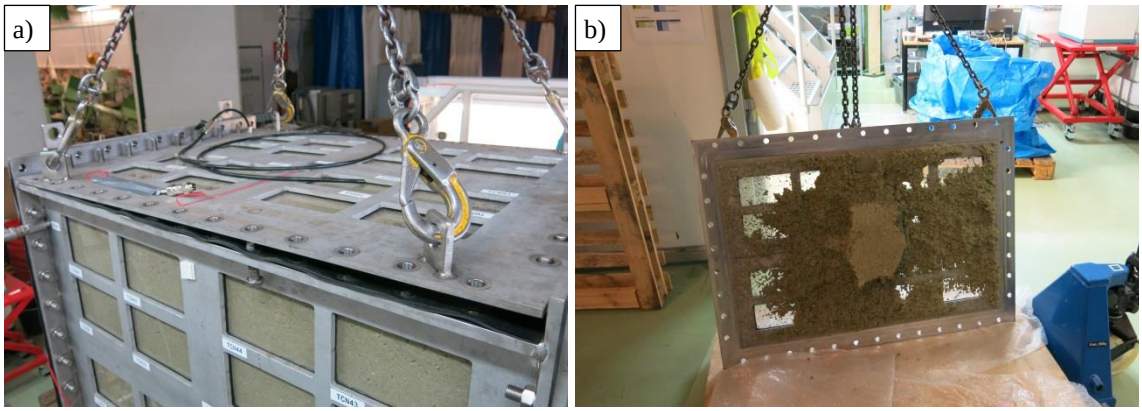

Figure 37. *Lifting the North unit lid with a hoist after unscrewing (a) and placing the lid on a pallet (b).*

After finishing the tunnel sampling, the interface between the backfill in the tunnel and the buffer in the tube was investigated closely. After that, the tube was disconnected from the tunnel (Figure 38) and taken to a specific room for sampling.

Figure 38. *Disconnecting the tube.*

3.4.2 Working techniques and tools

In the tunnel most of the backfill block samples were taken by drilling. Some samples were taken by using a chipping hammer and a chain saw. Progress of the drilling work is presented in Figure 39. The drilling from the top of the backfill block was done in two phases, due to the limited length of the drill. First, about 300 mm long drilled sample (diameter of 75 mm) was taken and then the bottom part was drilled with an extension.

Figure 39. *Backfill block drilling.*

From every tunnel pellet sample location, two samples were taken: one close to a window and one close to a block. Samples close to the blocks (Figure 40) were taken with an iron pipe (75 mm diameter) that was pushed into the pellet layer manually, possibly using an iron bar if more force was required.

Figure 40. *Pellet samples close to the blocks were taken by using an iron pipe (a), and custom-built instruments (b) were used to take the samples (c) out from the pipe.*

Pellet samples close to the windows were taken with a plastic pipe (35 mm diameter) that was pushed into the pellet layer manually (Figure 41). This was usually done three times in every sample location to get a big enough sample size.

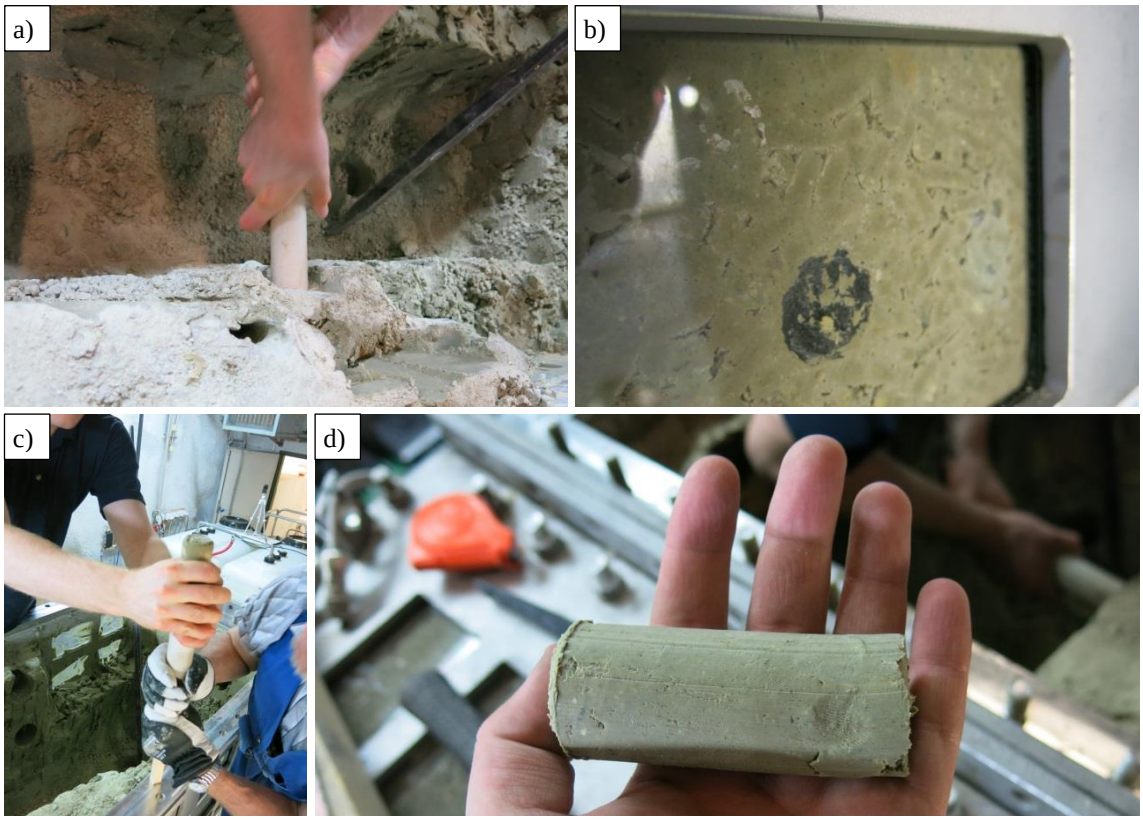

Figure 41. *A plastic pipe (a) was used to take samples close to the windows (b), and custom-built instruments (c) were used to take the samples (d) out from the pipe.*

Together with the sampling, the backfill blocks and pellets were dismantled and removed from the tunnel (Figure 42). A chipping hammer was the most used tool during the dismantling, especially with the backfill blocks. A plastic spatula was used close to the windows to prevent scratching them. Scoops and a vacuum cleaner were used to remove the material from the tunnel. In most parts of the tunnel, the block and the pellet materials were attached to each other due to wetting. Block material near its interface with the pellets was removed carefully. Usually a saw blade was used, and a thin layer of the backfill block material was left on the surface of the pellet layer to prevent disturbing the pellet material before sampling of the pellet layer. During the dismantling observations were made about wetting, block cracks and water flow paths.

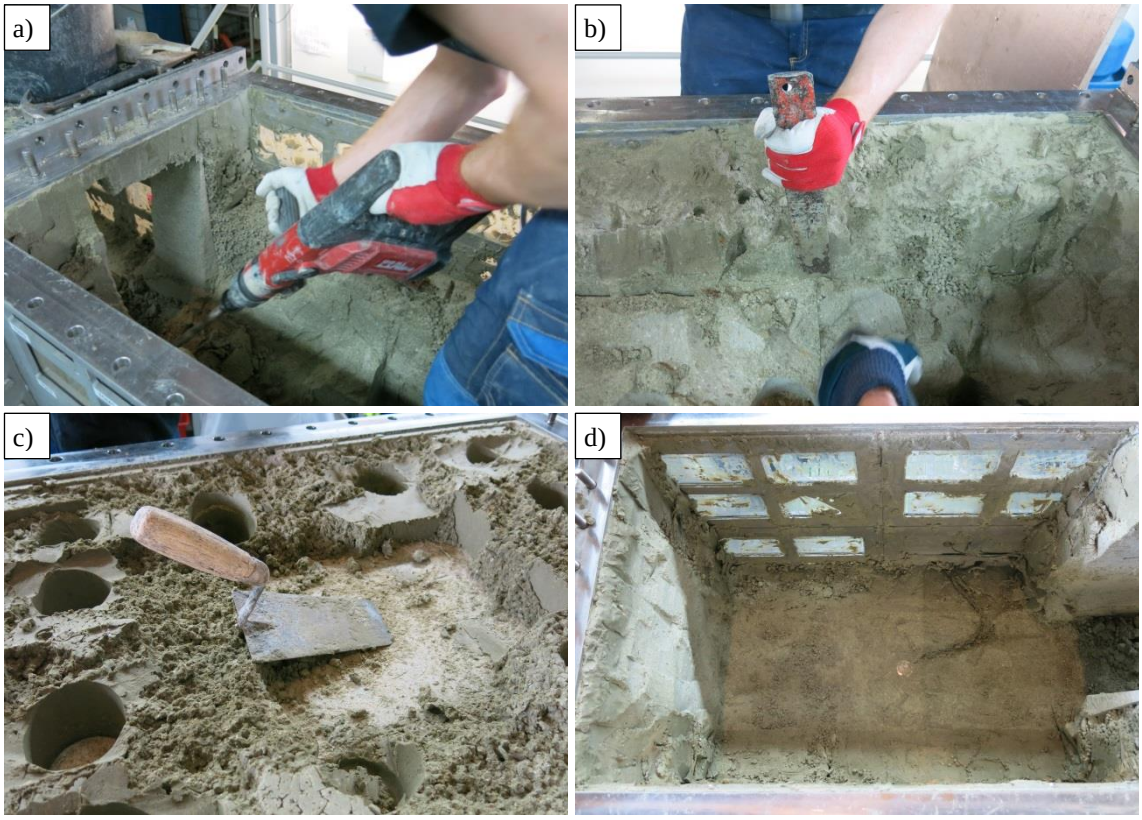

Figure 42. *Different tools were used during the dismantling: a) a chipping hammer, b) a saw blade, c) a trowel. In d) is shown the top of the bottom pellet layer in the Middle unit and a pressure sensor in the center of the unit.*

Some cracks were found from the backfill blocks during the dismantling work which may have been partly due to the drilling work (Figure 43). Most of the cracks were found from the backfill blocks 3 and 4 (block labelling is presented in Appendix 5). There were cracks especially in the area above the buffer, in the bottom parts of the backfill blocks 3 and 4. In the North unit, in the backfill blocks 5 and 6, cracks were found from the drilled samples. Also, during the dismantling the backfill block 6 was found to have a long vertical crack in a direction from A-side to C-side. In the South unit, in the backfill blocks 1 and 2, no significant cracks were found.

Figure 43. *Backfill block cracks were found during the dismantling work: a) the backfill block 4 and its interface with the backfill block 3, b) drilled sample from the backfill block 6 next to the North end, c) drilled sample from the backfill block 3 which was above the buffer. The bottom side of the sample is on the left.*

For the buffer sampling, the tube was placed on a pallet. The same drilling machine was used than in the backfill block sampling. However, a different drill bit was first used to remove the plastic cover of the tube to not damage the diamond drill bit that was used for the bentonite drilling. Inner diameter of the drill for the buffer was 50 mm. Progression of the work is presented in Figure 44 and the sample locations are presented in Appendix 7. Because of the wet pellet layer in the buffer, some problems occurred in the beginning of the sampling with the function of the drilling machine. Because of that a custom-built plastic pipe was taken in use to remove the pellet part of the sample before drilling the block part.

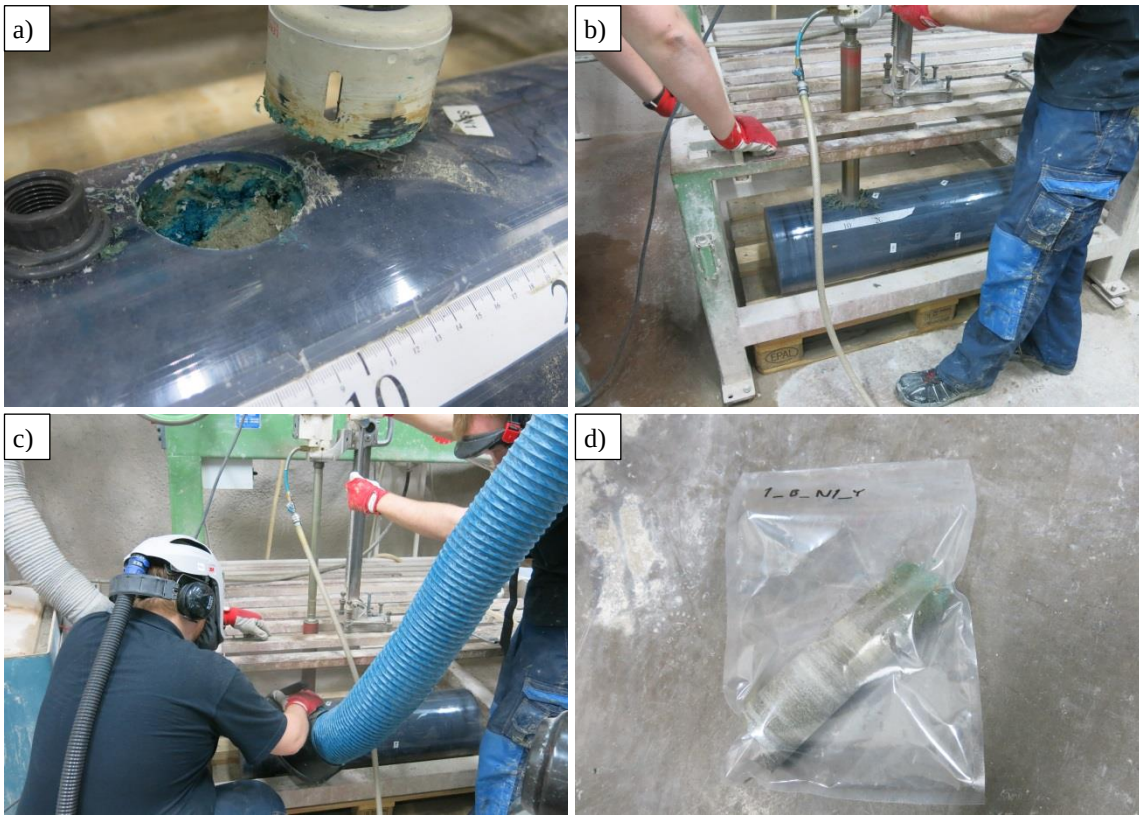

Figure 44. *Buffer sampling phases: a) removing the plastic cover, b), c) sample drilling, d) a drilled sample.*

3.5 Sample analyses

From the samples, water content, dry density, bulk density and saturation degree were analyzed. Some treatments were done for the samples before analyzing them. Cutting of the samples was done with a knife or a normal saw depending on the hardness of the sample. During the analyses, all the samples were labelled unambiguously.

The tunnel pellet samples were divided into three equally sized pieces. Two of the pieces were used for the water content analysis, using an average of the results. The third piece was used for the density analysis. Nine samples taken from above the buffer, contained 10-20 mm buffer block material and 20-40 mm tunnel pellet material. These samples were cut from the interface of the two materials. The tunnel backfill block

samples taken by drilling were sawed from their both ends to five 20 mm thick slices. The drilled samples taken from the buffer were sawed into 20-30 mm slices, in which one sawing was in the interface of the buffer and the backfill block material.

3.5.1 Water content

Water content was analyzed according to the standard *EN 1097-5:2008. Tests for mechanical and physical properties of aggregates – Part 5: Determination of the water content by drying in a ventilated oven.* Samples were weighed before and after they were placed into an oven (105°C) for 48 hours (72 hours in weekends). Small metal plates were used under the samples (Figure 45). After taking the dried samples out from the oven, the samples were held in the room temperature for 3-5 minutes before weighing them.

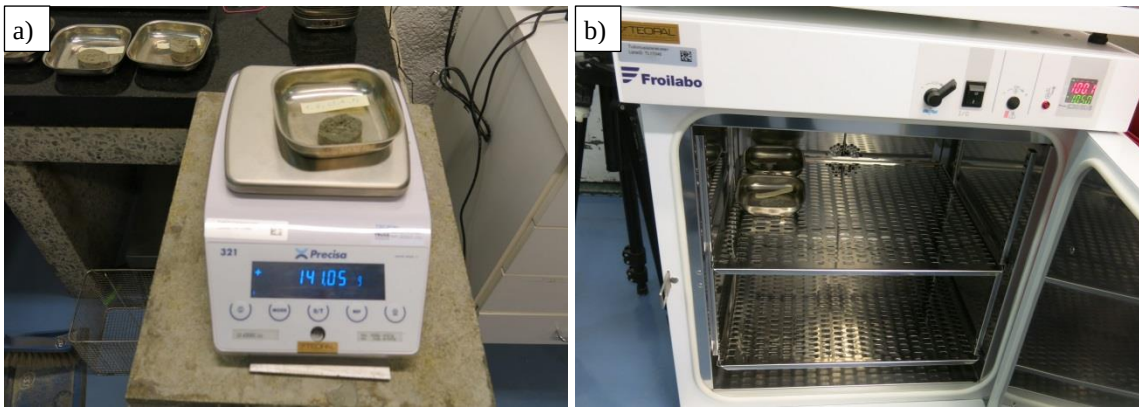

Figure 45. *For water content analyses, samples was weighed (a) and dried in the oven (b).*

Water mass (m_{water}) of a sample was the difference between the weight of the wet and the dried (m_{dry}) sample. The water content (w) was calculated in the following way:

$$w = \frac{m_{water}}{m_{dry}} \quad (1)$$

3.5.2 Density and saturation degree

For the density analyses, water immersion method was used. The analyses were performed following the principles of the standard *SFS-EN 12697-6: Bituminous mixtures. Test methods for hot mix asphalt. Part 6: Determination of bulk density of bituminous specimens.* Compared to the standard, the samples were put in vacuum bags. In the water immersion method, which is based on the Archimedes principle, the samples were weighed in the air (m_a) and in the water (m_w) (Figure 46).

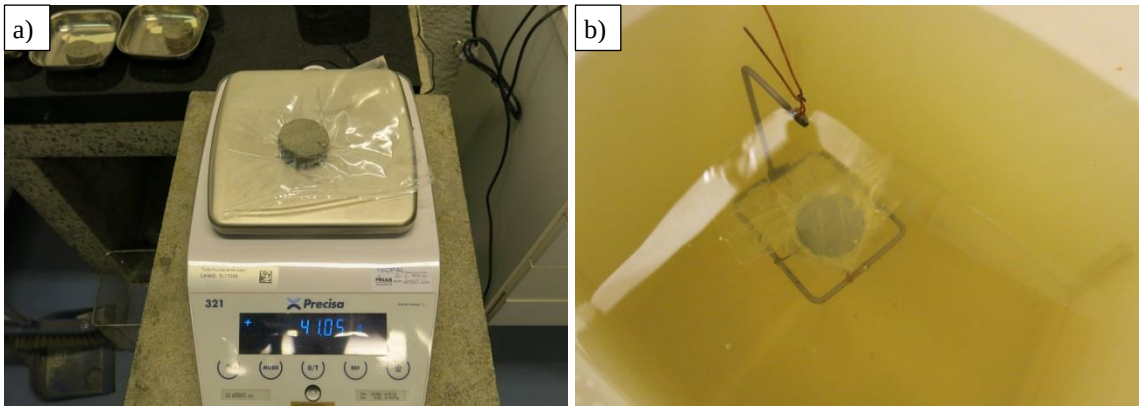

Figure 46. *For density analyses, samples were weighed in the air (a) and in the water (b).*

In the water immersion method, samples were put in vacuum bags whose weight (m_{bag}) and density (ρ_{bag}=1.05 g/cm^3) were measured. Water density value (ρ_{water}) in the prevailing water temperature was used. Bulk density (ρ_{bulk}) of a sample was calculated by dividing the mass (m_s) of the sample by the volume (V_s) of the sample:

$$\rho_{bulk} = \frac{m_s}{V_s}, where\ V_s = \frac{m_a - m_w}{\rho_{water}} - \frac{m_{bag}}{\rho_{bag}} \quad (2)$$

Dry density (ρ_{dry}) was calculated in the following way:

$$\rho_{dry} = \frac{\rho_{bulk}}{(1+w)} \quad (3)$$

For the calculation of saturation degree (S_r) and porosity ($\emptyset$), grain density (ρ_{solids}) of the bentonite material was assumed to be 2780 kg/m^3 (Karnland 2010). Equations for the calculations were the following:

$$S_r = \frac{{}^{w}/_{\rho_{water}}}{{}^{1}/_{\rho_{dry}} - {}^{1}/_{\rho_{solids}}} \quad (4)$$

$$\emptyset = 1 - \frac{\rho_{dry}}{\rho_{solids}} \quad (5)$$

4. RESULTS

A malfunction of the pump occurred during the test. Despite adjusting the pump settings during the test, the inflow rate decreased below the desired 0.1 l/min. The effect of the pump malfunction can be seen from the water outflow rate which is presented in chapter 4.3. The decreased water flow rate needs to be taken into account when considering the results. Also, a pause in the water supply while adding the tracer, on the 59th day, had a remarkable effect on the progression of the last few days of the experiment.

4.1 Wetting

Dry buffer pellets in the tube before the start of the water supply on May 5, 2015, at 11:05 are shown in Figure 47a. With a steady water flow rate of 0.1 l/min the water was seen in the tunnel bottom in less than two hours. Water channels were formed immediately in the beginning of the test (Figure 47b). Water paths were visible above the inlet during the whole test. Some paths disappeared after the first days. A photo taken after one month is shown in Figure 47c where a water path can be seen with a dark color which probably originated from a broken rubber component of the pump.

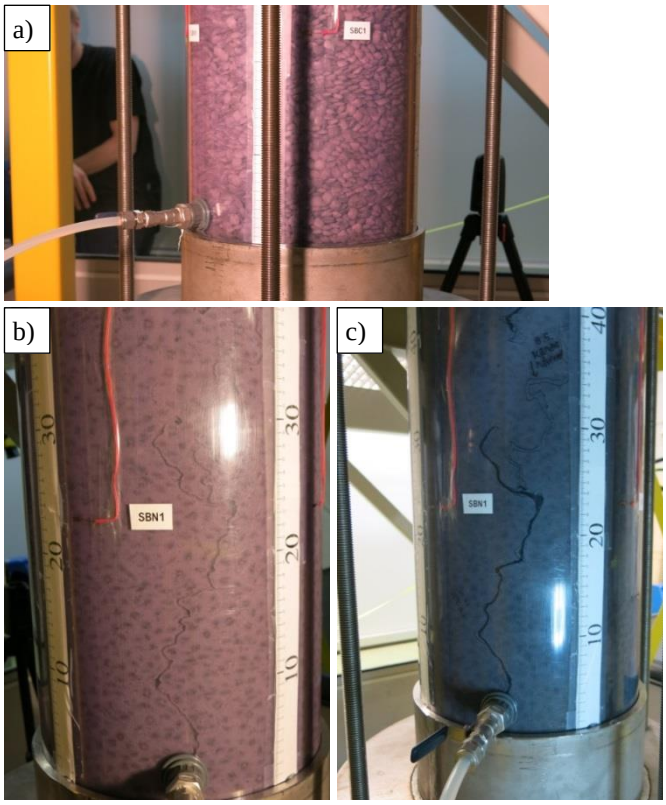

Figure 47. *Photos of the tube at different times: a) May 5, 2015, at 11:08 b) May 5, at 13:29 c) June 8.*

Observations of the wetting of the tunnel during the test were done through the tunnel windows from where the outer parts of the pellet layers could be seen. The wetting of the tunnel pellets began soon after the water supply started. After about one hour and forty minutes, about 1/4 of the windows TDN3/4 and TDS3/4 (Figure 48a) were wet. Ten minutes later about 3/4 of these windows were wet (Figure 48b). Also, pellets seen through the windows TDS1/2 and TDN1/2 had started to get wet. The bottom (D-side) of the Middle unit was almost completely wet in a few hours. The bottom of the North unit started to get wet before the South unit.

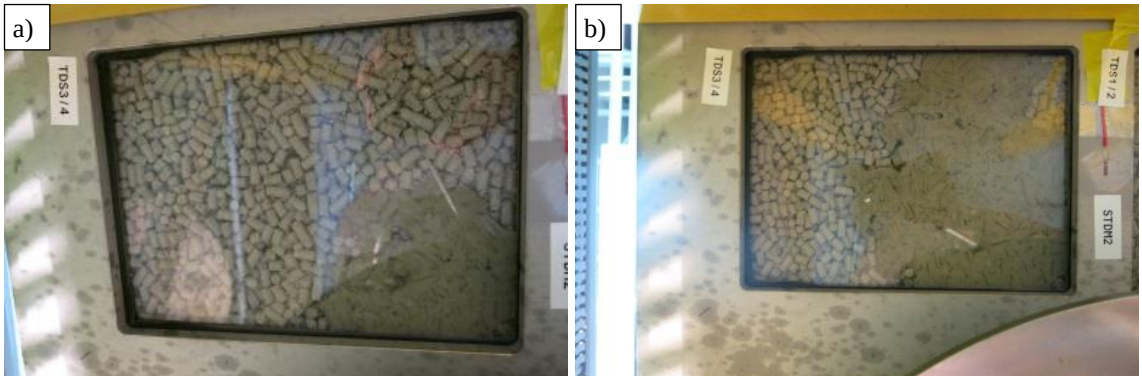

Figure 48. *Wetting of the window TDS3/4: a) May 5, at 13:45 b) May 5, at 13:50. The window located in the bottom of the Middle unit, south from the tube.*

After about six hours, wet pellets were seen in the C-side of the Middle unit (Figure 49a). After 24 hours, the bottom of the North unit was almost completely wet and wetting in the A- and the C-side had proceeded (Figure 49b). Also, half of the North end from the bottom was wet.

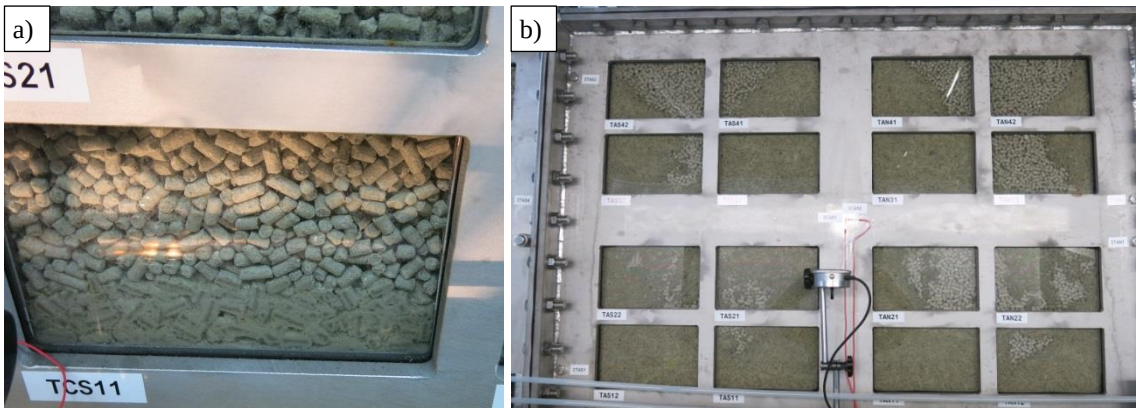

Figure 49. *Window TCS11 in May 5, at 17:30 (a) and A-side of the Middle unit in May 6, at 12:18 (b).*

After two days, the Middle unit and the North unit were almost completely wet. Also, half of the bottom and some of the A-side of the South unit were wet. After six days, the South unit was almost completely wet except from the top (B-side) where only a small part of the pellet layer was wet. Most of the B-side and also small parts of the A- and the C-side of the South unit remained dry until the pause in the water supply three days before the end of the test. After this, the A- and the C-side of the South unit got com-

pletely wet and also the top of the South unit got wetter (Figure 50). Development of the water distribution in the tunnel is visualizes in Figure 51.

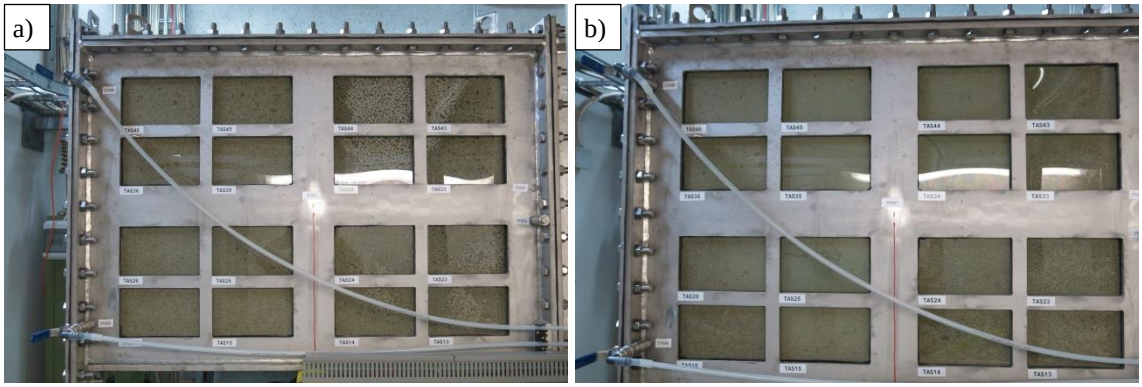

Figure 50. *The A-side of the South unit before and after the pause in the water supply: a) July 3 b) July 6.*

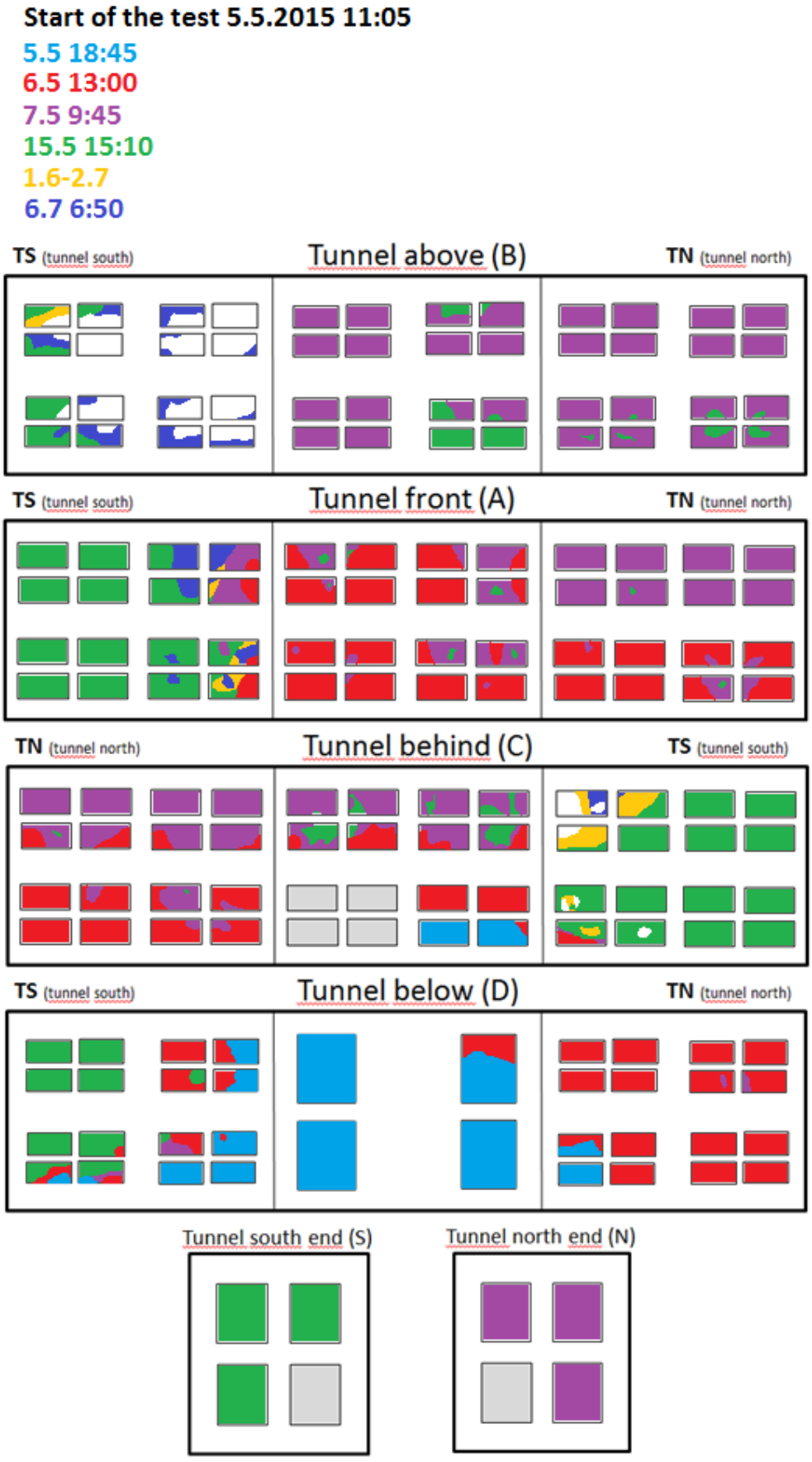

Figure 51. *Development of the water distribution in the tunnel. Each color represents wetted tunnel pellets found at dates and times listed above.*

Some water paths were seen through the tunnel windows during the test. A water path in the window TDN33 was seen throughout the test (Figure 52). Also, water paths were seen during the first days of the test in the windows TDN43, TCN24 and TCN34. During the last three days of test, new water paths had formed in the A-side of the South unit.

Figure 52. *A water path in the window TDN33.*

Water outflow from the tunnel via the outlets started after one day when drops of water were found in the ITAN6 outlet which was located in the A-side of the North unit. After two days, water had started to flow out via the ITCN6 outlet which was located in the C-side of the North unit. Water flowed out only via the ITCN6 outlet until the pause in the water supply three days before ending the test after which water flowed out only via the ITAS6 outlet which was located in the A-side of the South unit. In the sixth day, a burst of eroded bentonite occurred which blocked the pipes of the collecting system (Figure 53).

Figure 53. *Burst of bentonite caused blockages in the outflow pipes.*

Some cross sections from the tunnel photographed during the dismantling are shown in Figure 54. Most of the pellet material in the tunnel could be described as wet. However, some dryer pellets still in original shape were found from the long sides (A- and C-side) close to the backfill blocks and also from the top layer. Backfill blocks were found to be dry for the most parts except their outer edges in A-, C-, N- and E-sides and especially in the bottom of the backfill blocks where the interface between the backfill blocks and the pellets was not detectable. Wetter backfill block parts were also found from above the buffer.

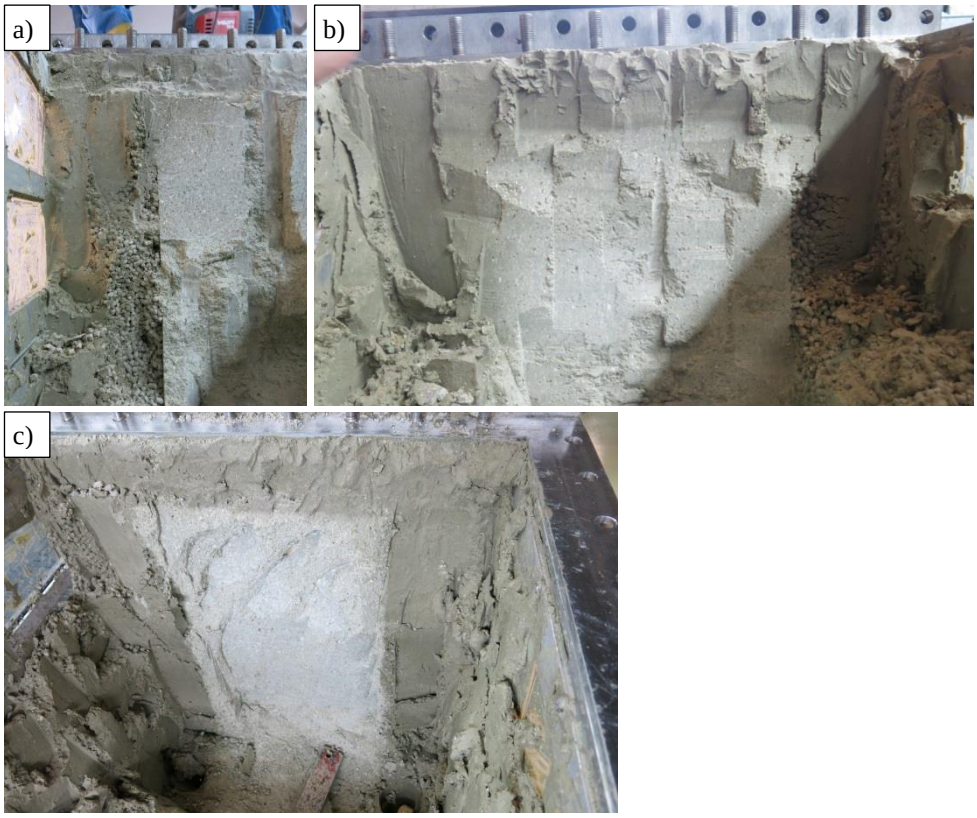

Figure 54. *Cross sections from the tunnel during the dismantling: a) between the North and the Middle unit in the A-side, b) between the Middle and the South unit, c) between the North and the Middle unit. Photos a) and c) are towards south and c) is towards north.*

During the dismantling of the tunnel, tracer and some other possible water path locations were found from different parts of the tunnel. The wettest pellet masses were found from the gaps between the window elements (Figure 55), especially in the C-side of the North unit from where water had flown out during the test, before adding the tracer. Also, pellet mass in junctions of the tunnel elements were found to be wetter. Any visible water paths close to the ITCN6 outlet were not found during the dismantling which may also be due to the disturbance of the pellet mass during the dismantling.

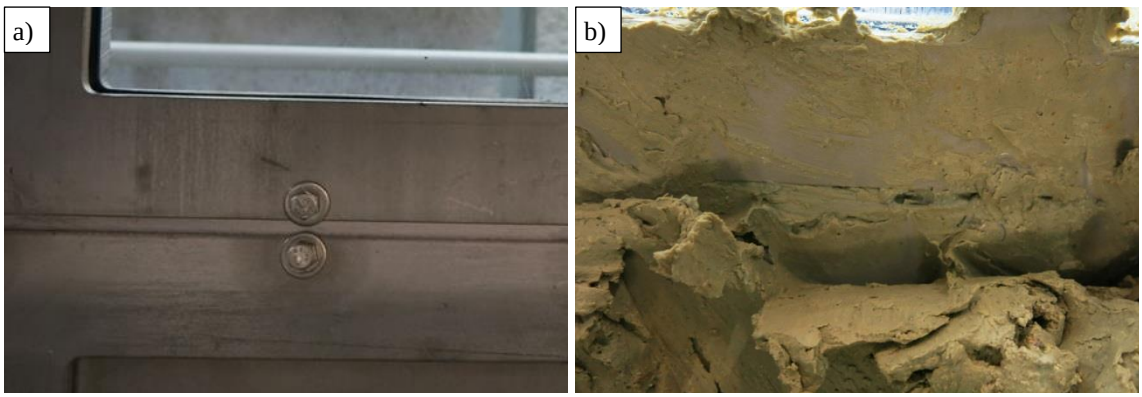

Figure 55. *A gap between window elements before the test (a) and wet pellet mass in a gap in the C-side of the North unit after the test (b).*

Most of the tracer that was found during the dismantling was located in the buffer (Figure 56a) and in the south side of the tunnel. Some tracer was found also from the north side of the Middle unit (Figure 56b).

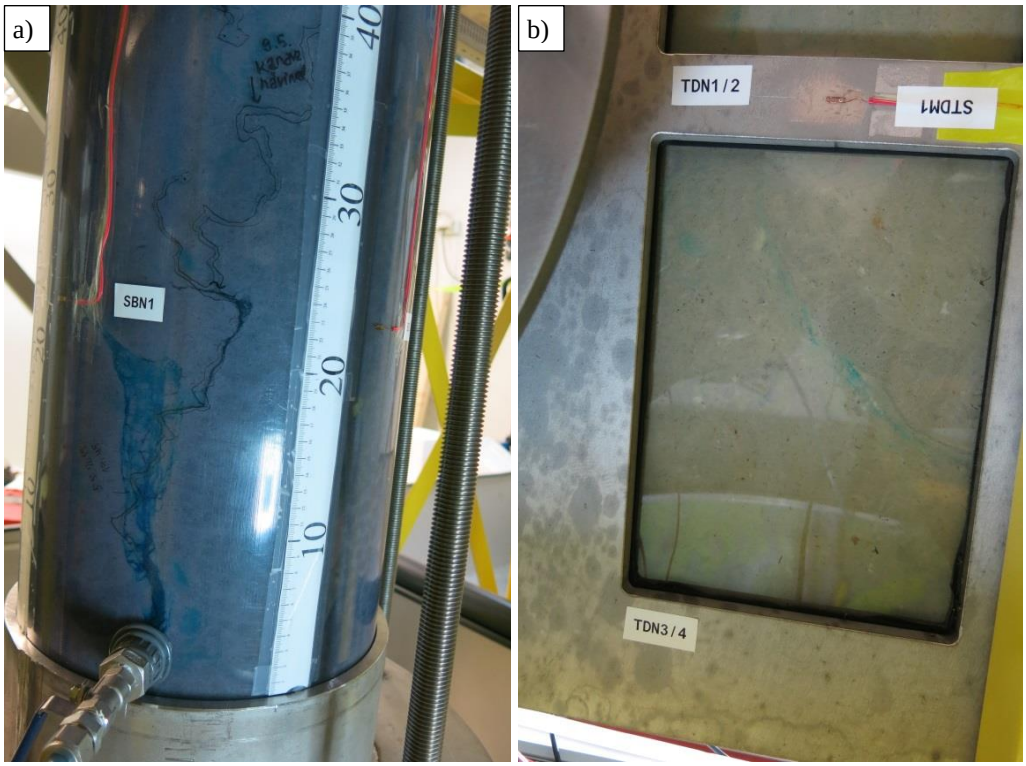

Figure 56. *Tracer visible in the buffer (a) and in the bottom of the tunnel, in the north side of the Middle unit (b).*

In the south side of the Middle unit, tracer was found from the pellet layer, especially close to the A-side and the bottom. In the South unit, tracer was found from many locations, also from the top of the tunnel which was obvious due to wetting of the top layer pellets during the last three days of the test. Photos of pellet mass containing tracer are shown in Figure 57.

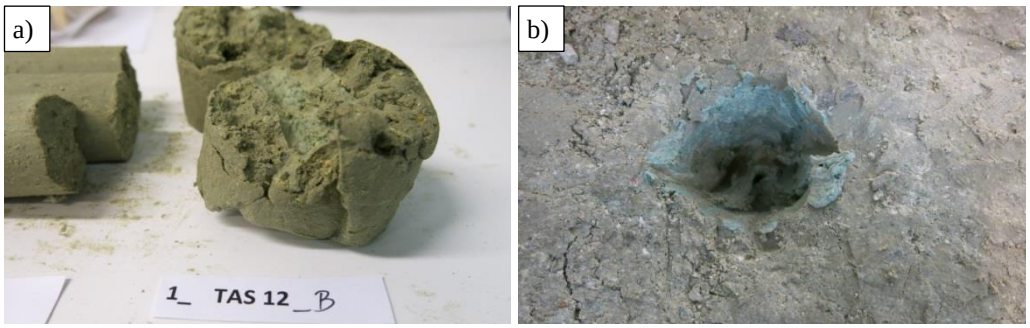

Figure 57. *A tunnel pellet sample close to a backfill block in the south side of the Middle unit (a) and a pellet sample hole in the bottom of the South unit (b).*

No dry buffer pellet mass was found from the buffer. Also, the outer edge of the buffer blocks had got wet. For the most part, the interface between the buffer blocks and the pellets was not detectable. Some tracer was found from the buffer pellet layer especially near the water inlet.

4.2 Swelling stresses

Development of counter pressure of the pump is shown in Figure 58. After the first days the pressure remained at an almost constant level for the first 20 days after which the pressure began to increase almost linearly. The high peak at the end of the test occurred after the pump was restarted after the tracer was added.

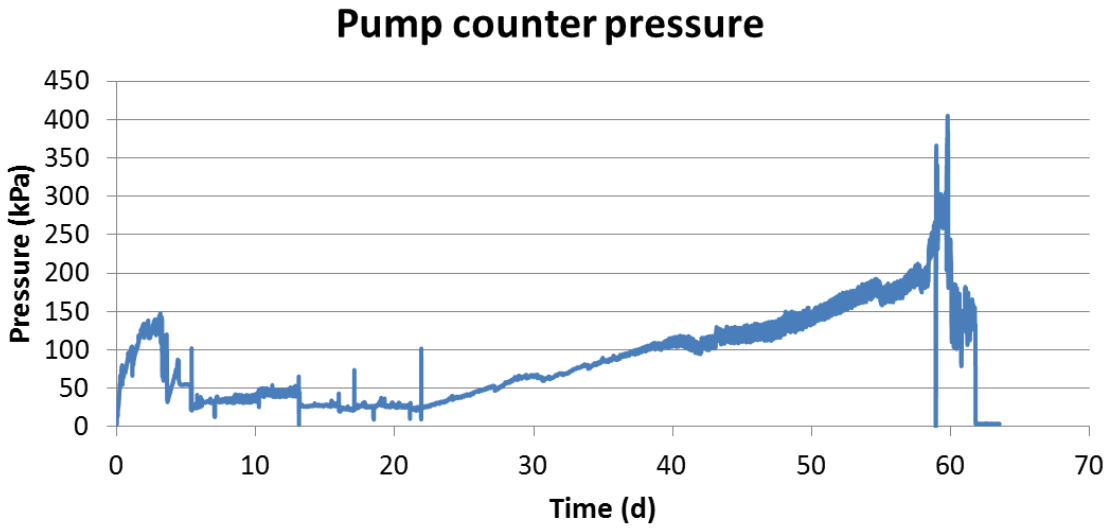

Figure 58. *Counter pressure of the pump.*

Axial force in the tube measured by the force transducer is presented in Figure 59 and radial stresses of the tube measured by the strain gauges are presented in Figure 60. It can be seen that the axial force remained at an almost constant level between the days 20 and 60. Radial stresses increased until the end of the test. The highest pressures were registered by the north side sensors (SBN1 and SBN2).

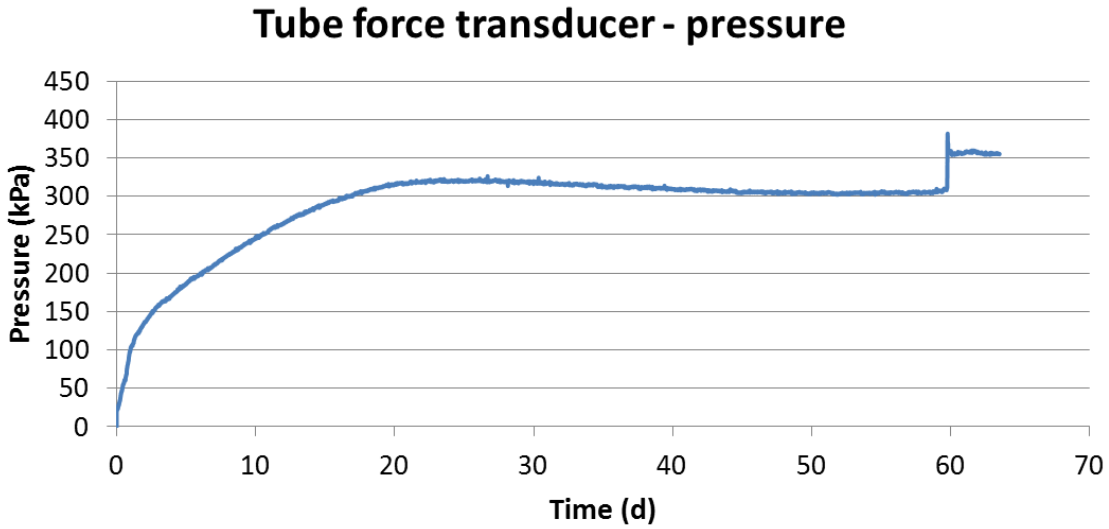

Figure 59. *Axial pressure measured by the force transducer under the tube.*

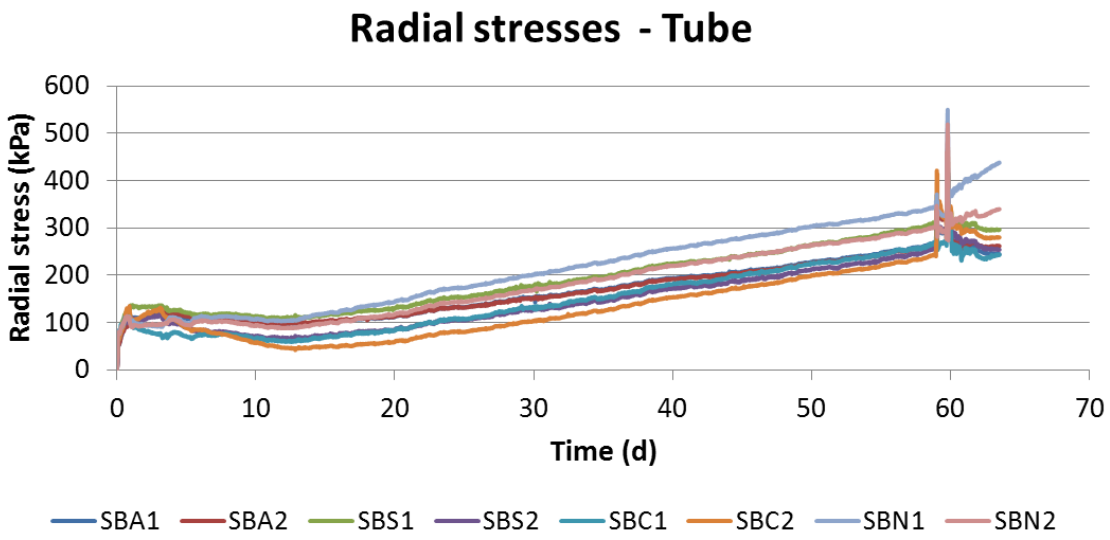

Figure 60. *Radial stresses of the tube measured by the strain gauges.*

Graphs showing the data measured by the total pressure sensors and by the dial gauges are presented in Figure 61 and in Figure 62. In the first day, a high peak in the pressure was registered by pressure sensor 1 which was located in the top of the Middle unit. Overall, slight increases in the pressures inside the tunnel were seen. The highest pressures were registered by the sensors 2 and 3, the sensors in the North end and in the interface between the tube and the tunnel. The restart of the pump in the 59th day induced a steep increase in the pressure of the sensor 2. No remarkable differences were seen in the displacements between the A- and C-sides measured by the dial gauges. Displacements for both sides were around 1.5 mm.

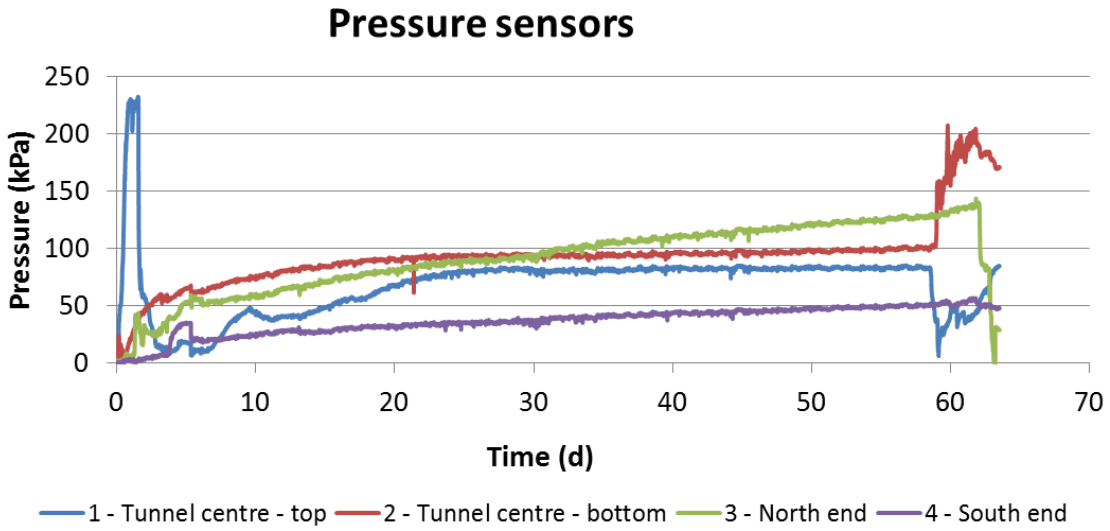

Figure 61. *Pressure inside the tunnel measured by the total pressure sensors.*

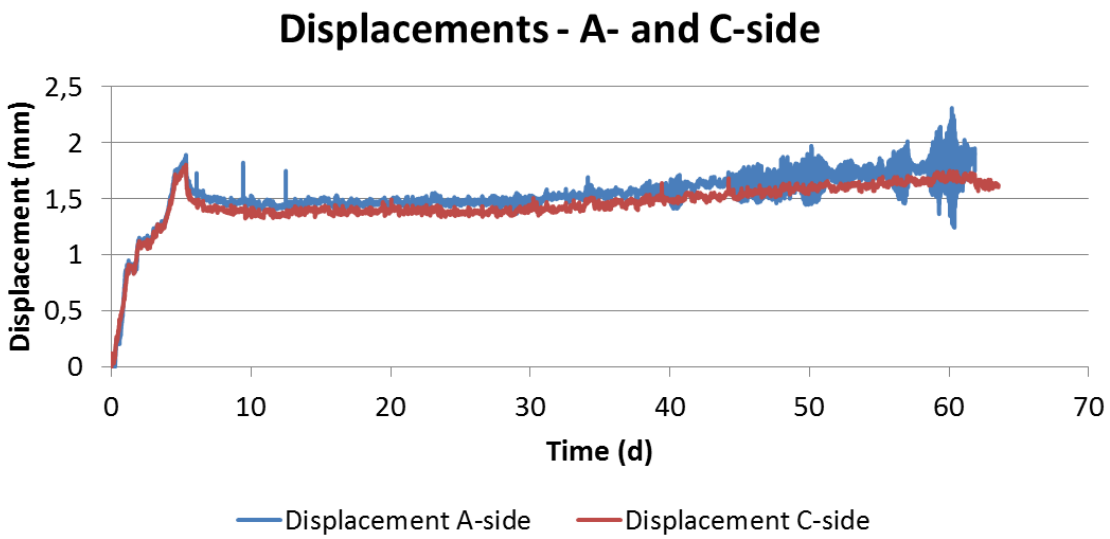

Figure 62. *Horizontal displacements of the center points of the A- and C-sides of the tunnel.*

Stresses of the tunnel frame registered by the strain gauges are presented in Figures 63-66. In general, the highest pressures were registered in the North unit (green curves) and the lowest pressures in the South unit (violet curves). Slight increases in the stresses were seen in most of the curves. Steep increases in the D-side pressures were seen after the pause in the water supply. Due to malfunction, strain gauges STAM2, STBM2 and STCM2 were left out from the graphs. Stresses measured by the strain gauges in the tunnel ends are presented in Figure 67 and Figure 68. Pressures were higher in the North end compared to the South end.

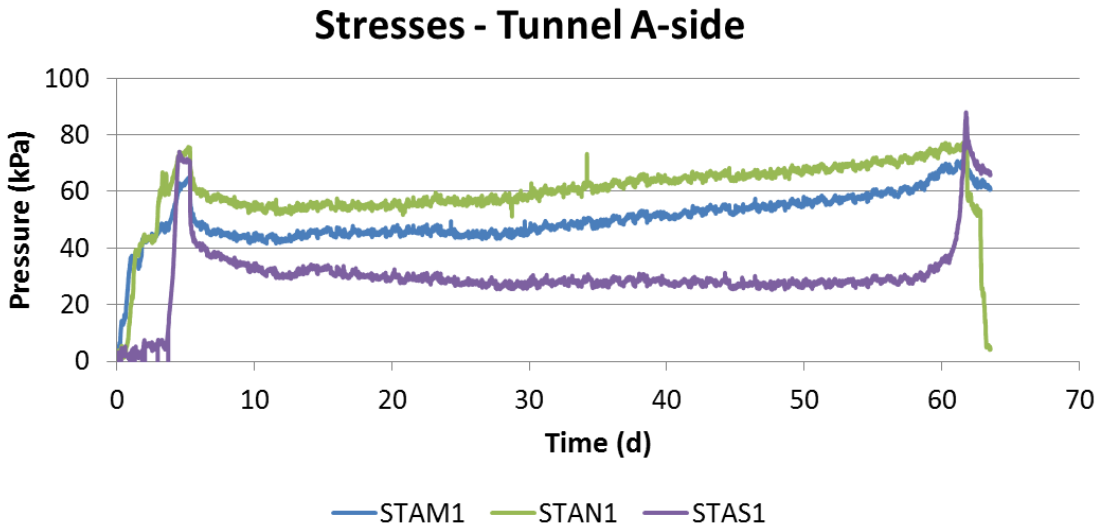

Figure 63. *Stresses in the tunnel A-side measured by the strain gauges.*

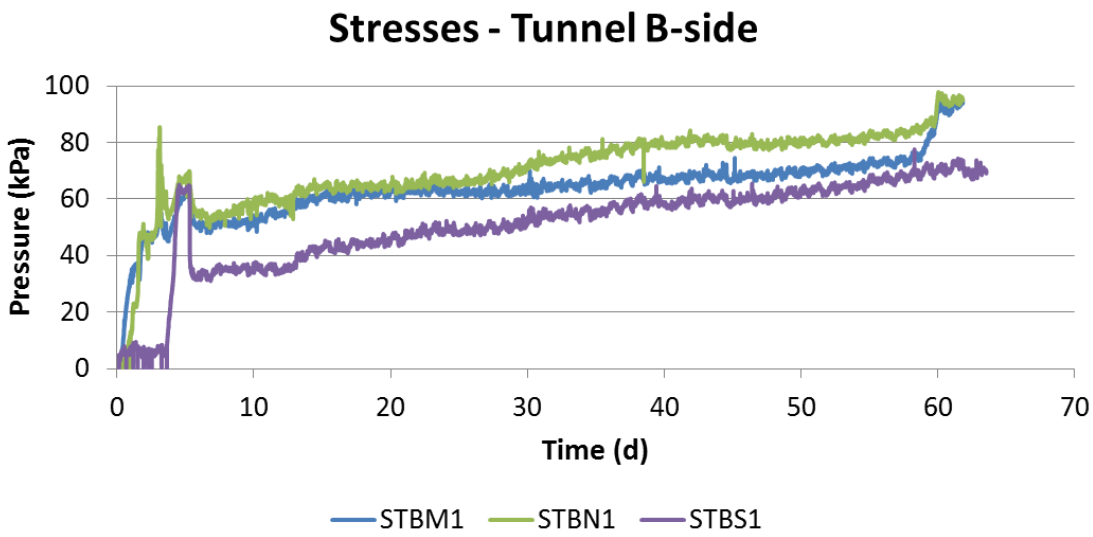

Figure 64. *Stresses in the top of the tunnel (B-side) measured by the strain gauges.*

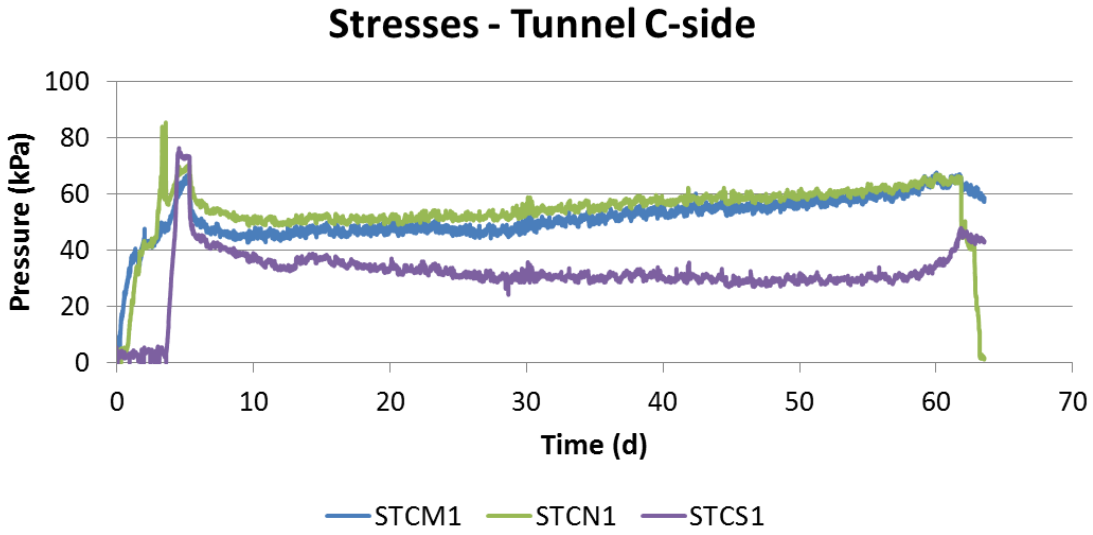

Figure 65. *Stresses in the tunnel C-side measured by the strain gauges.*

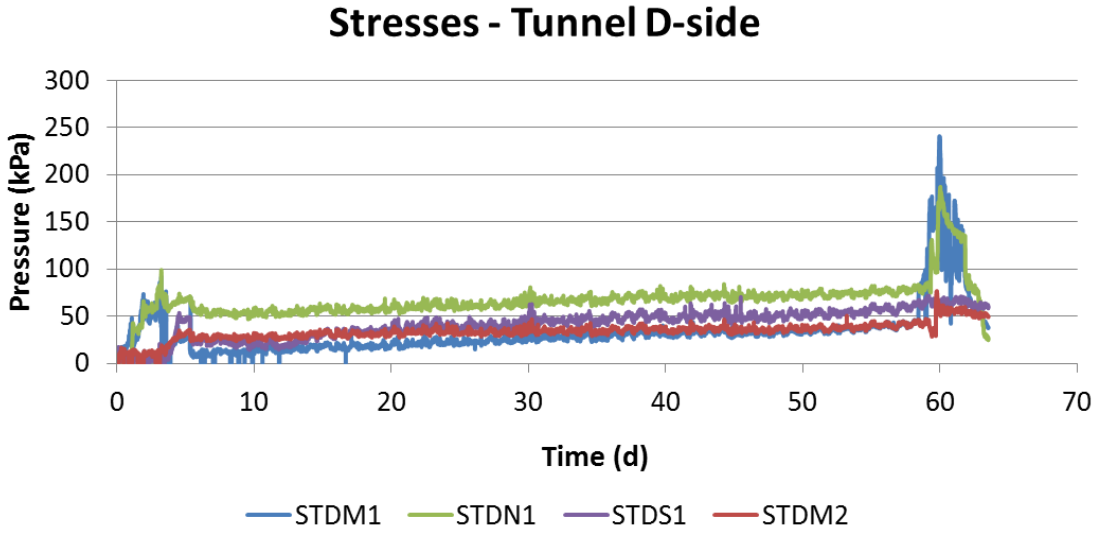

Figure 66. *Stresses in the bottom of the tunnel (D-side) measured by the strain gauges.*

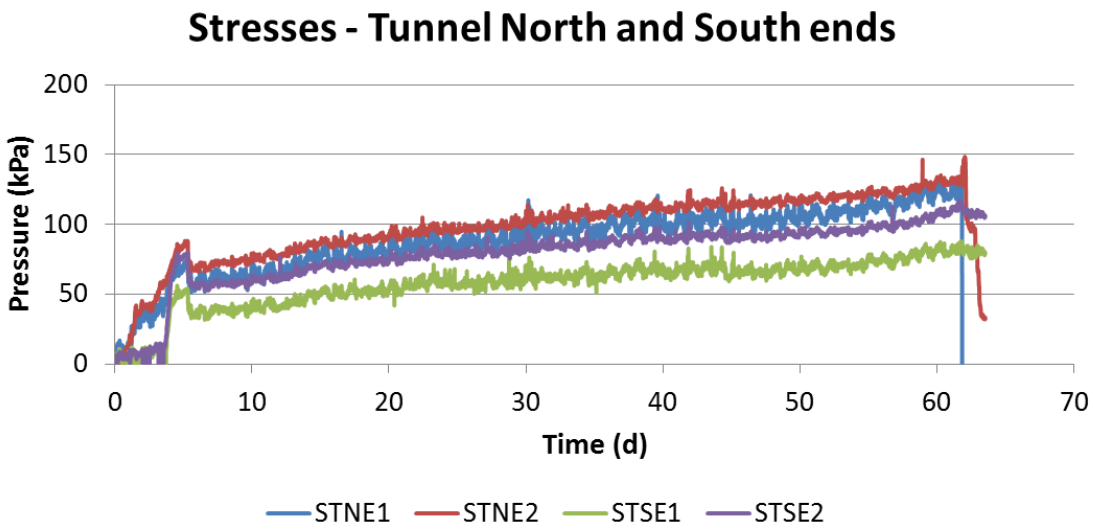

Figure 67. *Stresses in the North and South ends of the tunnel measured by the strain gauges.*

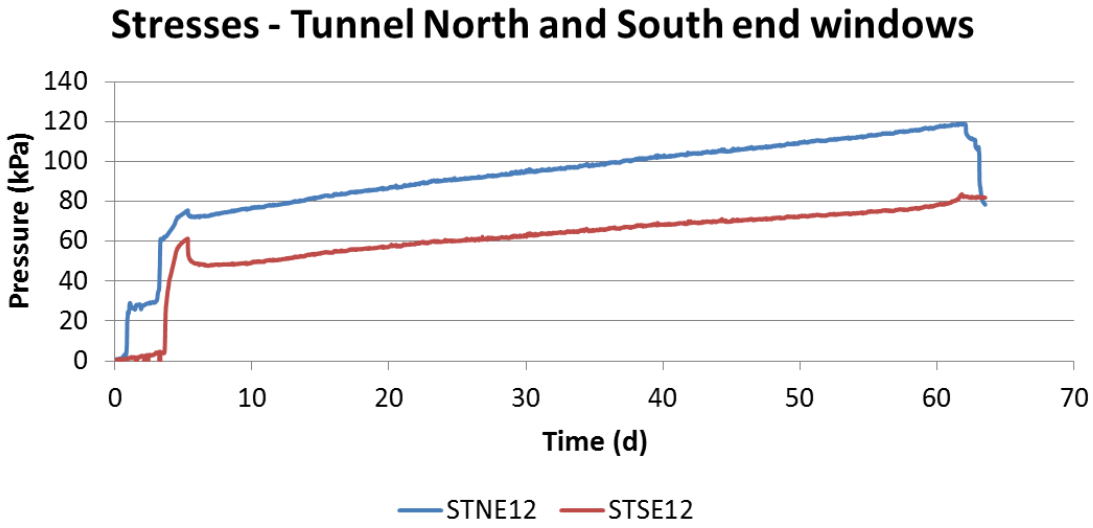

Figure 68. *Stresses in the North and South end windows of the tunnel measured by the strain gauges.*

4.3 Flow rate and erosion

The outflow rate of the water, the dry solid content of the outflowing water and the reference salinities are presented in Figure 69. The last three days were left out from the graph due to the negligible outflow rate.

The outflow rate varied especially during the first 20 days after which it briefly settled close to 0.1 l/min. After about the 25th day, the outflow rate began to decrease until the end of the test when it was already almost zero. The dry solid content, containing the salt and the eroded bentonite, varied during the first days of the test after which it settled to a level slightly over 1 %.

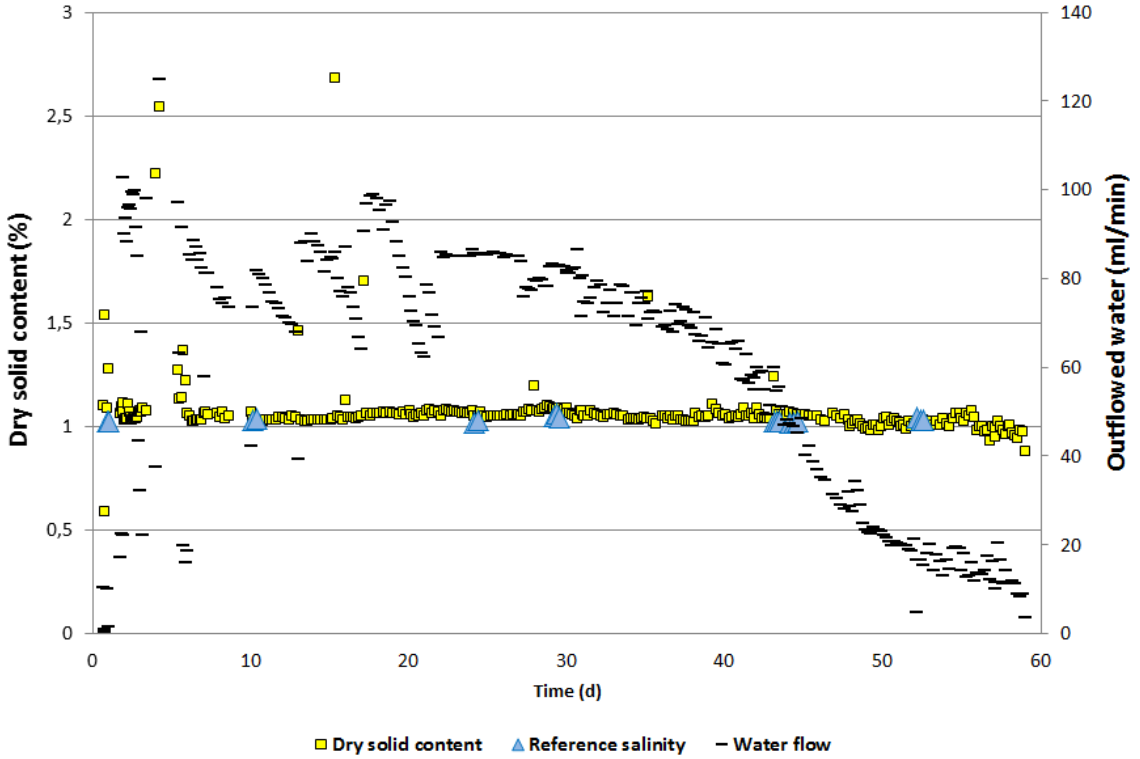

Figure 69. *The water outflow rate (right y-axis) and the dry solid content (left y-axis) of the water samples showing erosion products, and the reference salinities (left y-axis) analyzed from the samples taken from the water tanks.*

4.4 Buffer samples

Results of the buffer sample analyses are presented in Figure 70 and Figure 71 where graphs of the water content, saturation degree, bulk density and dry density are shown. Water contents were higher in the edges of the buffer whereas lower water contents were found close to the center of the buffer. Densities were higher in the center and lower densities were found from the edges of the buffer. Saturation degrees tended to have a slight trend where they were higher in the N- and A-sides and decreased towards the S- and C-sides. The highest saturation degrees were found from the north side of the buffer. Visualization of the buffer sample results accomplished by VisIt 2.9.2 software is presented in Figure 72. Pseudocolor plots were used for the visualization.

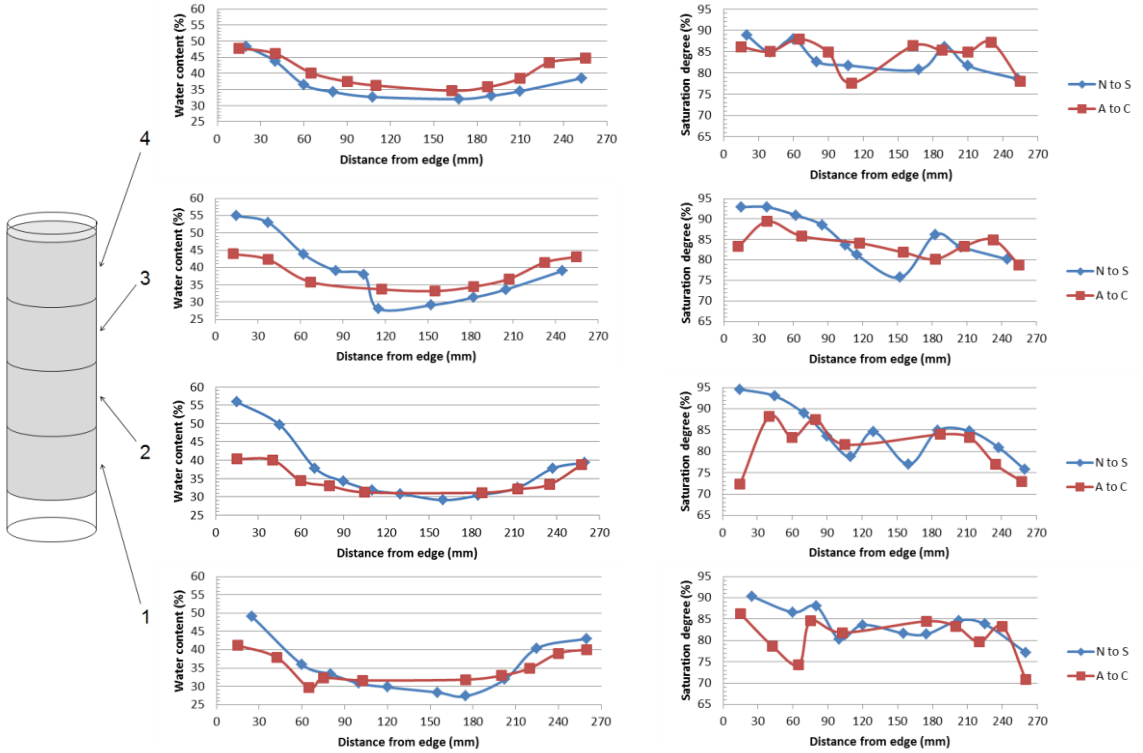

Figure 70. *Water content (left column) and saturation degree (right column) from four height levels of the buffer. The inner diameter of the tube was 269 mm and the samples were drilled through the buffer from two directions in each height level. Blue lines represent a direction from north (N) to south (S) and red lines a direction from A-side (A) to C-side (C). The squares represent the samples analyzed.*

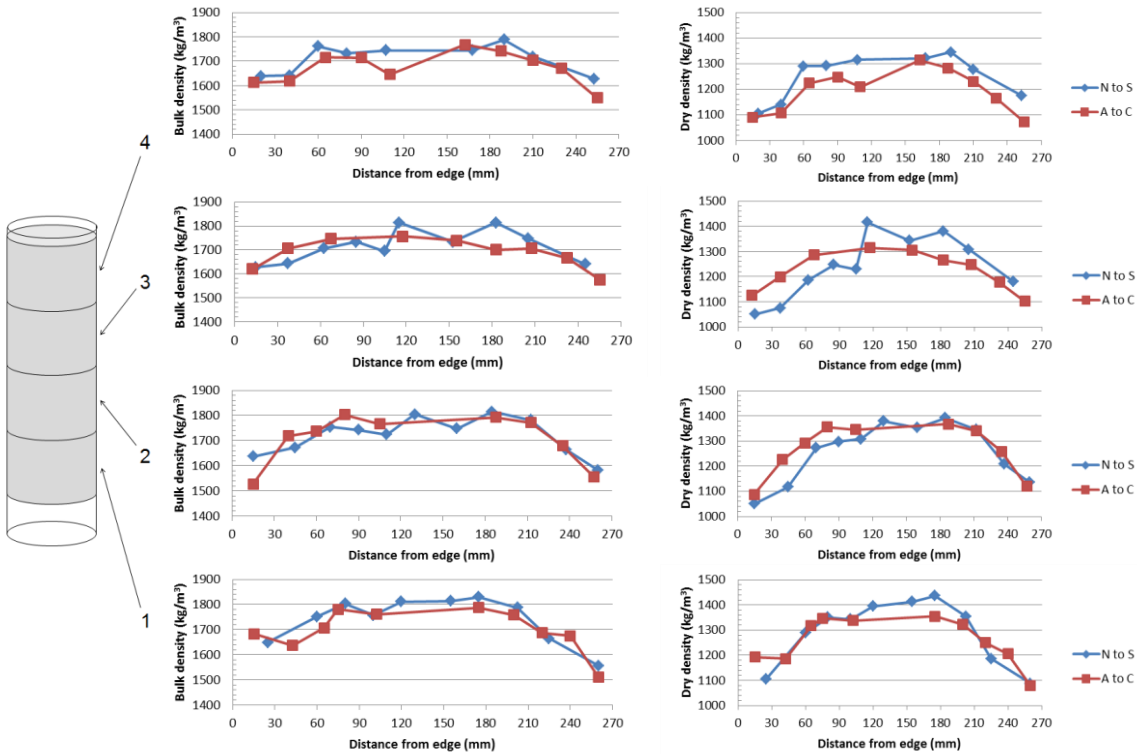

Figure 71. *Bulk density (left column) and dry density (right column) of the buffer samples.*

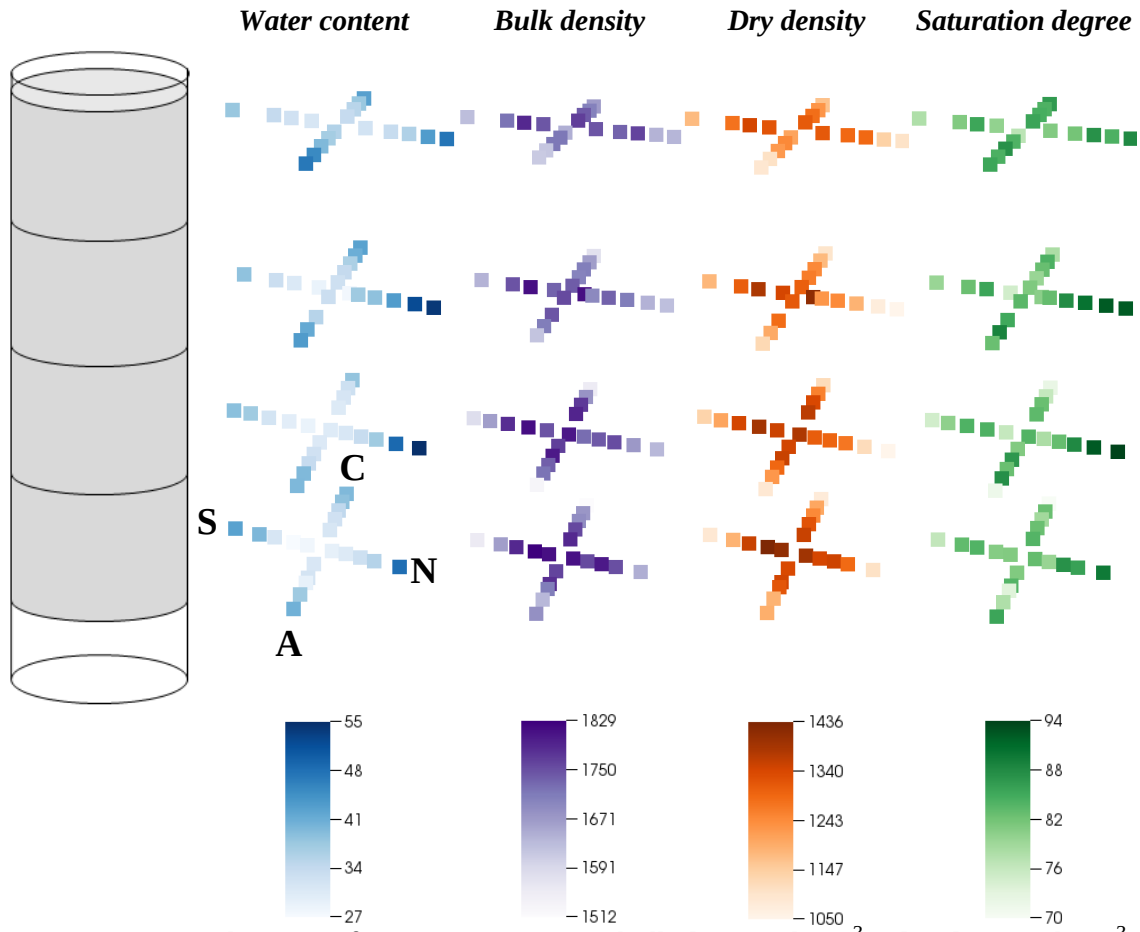

Figure 72. *Visualization of water content (%), bulk density (kg/m^3), dry density (kg/m^3) and saturation degree (%) of the buffer samples.*

4.5 Tunnel pellets

Visualizations of the tunnel pellet results were accomplished by VisIt 2.9.2 software, using Pseudocolor plots to visualize the values. Numeric values of the results are presented in Appendix 8.

Water contents of the tunnel pellets in different parts of the tunnel are presented in Figure 73. Overall, water contents were remarkably higher in the samples close to windows (w-samples) compared to the samples close to backfill blocks (b-samples). The wettest area in the tunnel was right above the buffer, in the north side. When comparing the long sides (A- and C-side) it was found that the A-side was wetter in the South unit and the C-side was wetter in the North unit. In the top pellet layer of the tunnel (B-side) the water content increased from south to north. Water content was higher in the north side of the tunnel also in the bottom (D-side). In the North end, the water contents were higher close to the bottom.

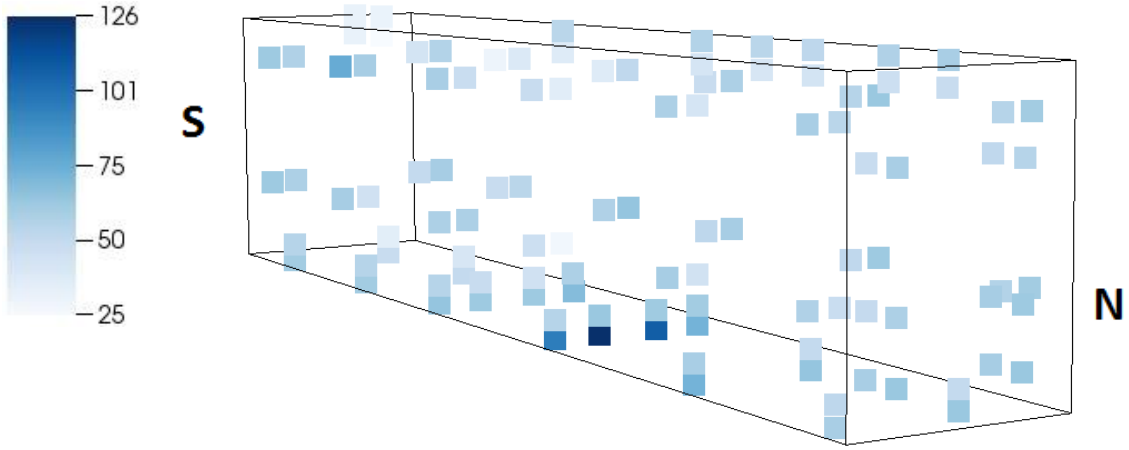

Figure 73. *Water content (%) of the tunnel pellets (S=south, N=north).*

Bulk densities of the tunnel pellets in different parts of the tunnel are presented in Figure 74. Compared to the b-samples, the w-samples mainly had higher bulk densities in the A-side of the North unit and in the south side of the C-side. In the north side of the C-side, bulk densities were higher in the b-samples. In the bottom, the b-samples had higher bulk densities. In the top and in the C-side, bulk densities were higher in the north side compared to the south side. In the bottom of the Middle unit, bulk densities were higher in the south side. The lowest bulk densities were found mainly from the south side of the top and from the north side of the Middle unit in the bottom.

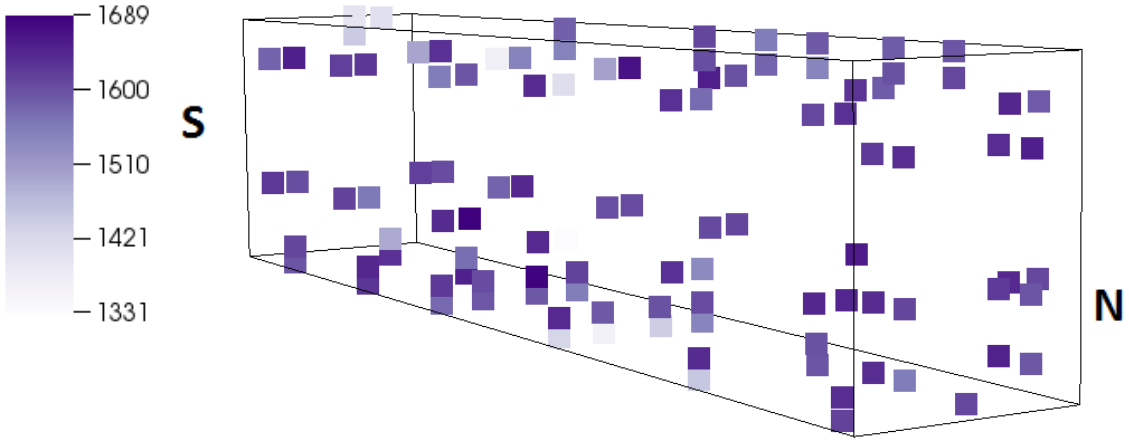

Figure 74. *Bulk density (kg/m^3) of the tunnel pellets.*

Dry densities of the tunnel pellets are visualized in Figure 75. The w-samples had lower dry densities than the b-samples, especially in the bottom of the tunnel. The lowest dry densities were found from the Middle unit of the bottom, especially in the north side of it. Low dry densities were also found from the south side of the A-side and from the north side of the C-side and the bottom.

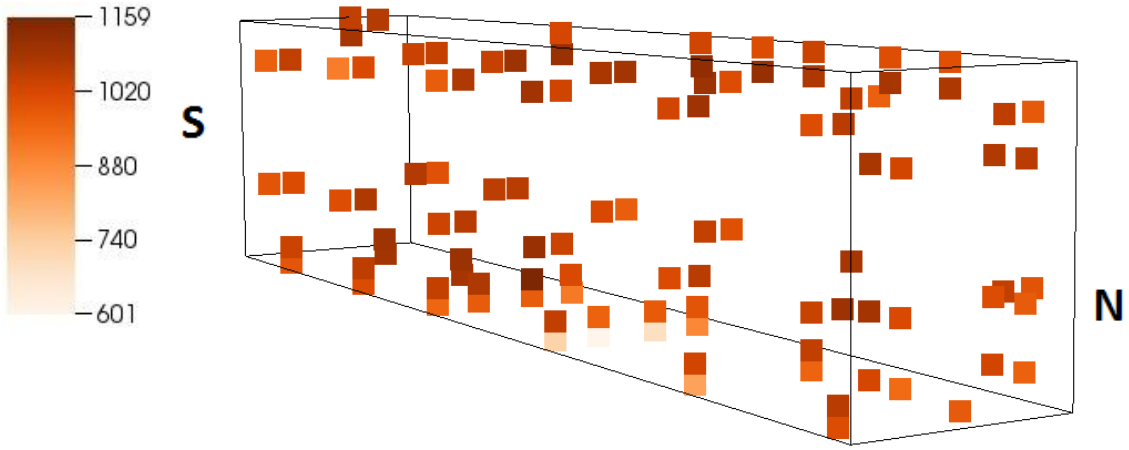

Figure 75. *Dry density (kg/m^3) of the tunnel pellets.*

Visualization of the tunnel pellet saturation degrees is presented in Figure 76. Saturation degrees were remarkably higher in the w-samples compared to the b-samples. Overall, high saturation degrees were found from the North unit of the A-side, from the Middle unit of the bottom, and from the Middle and the North unit of the C-side. Low saturation degrees were found from the top where saturation increased from south to north. In the North end, saturation degrees were higher closer to the C-side compared to the A-side.

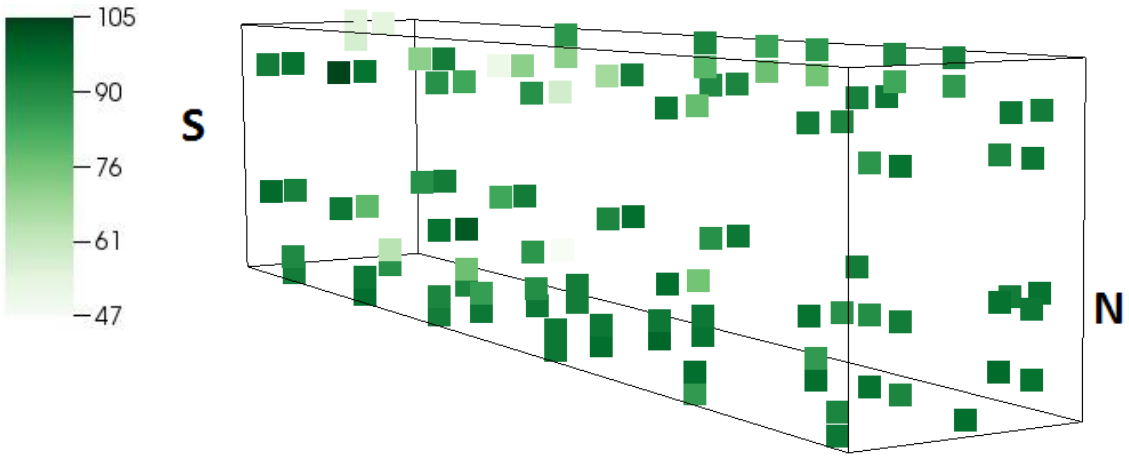

Figure 76. *Saturation degree (%) of the tunnel pellets.*

Relation between water content and density of the tunnel pellet samples is shown in Figure 77. Also lines representing full saturation are shown. With the water content lower than approximately 50 %, the bulk density increased with the increasing water content. With the higher water content, the bulk density decreased with the increasing water content. With the dry density, this limit value of the water content was approximately 45 %. Two samples had saturation degrees over 100 % which were probably results from inaccuracies in the analyses.

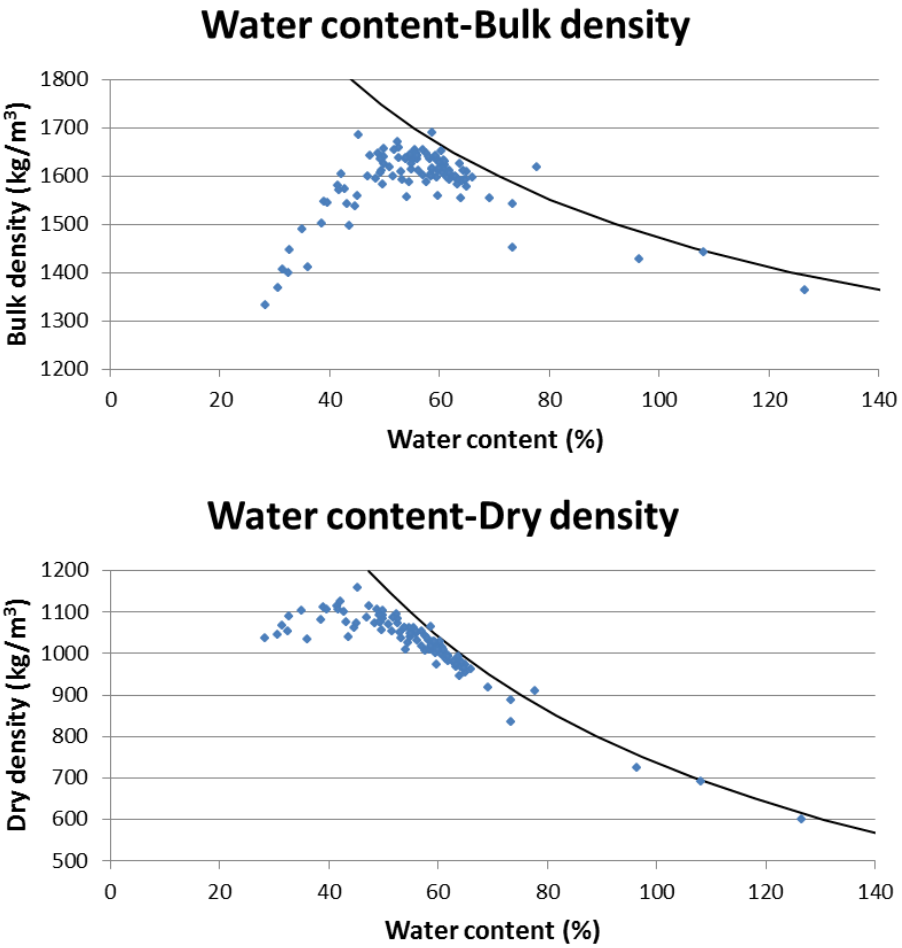

Figure 77. *A relation between water content and density of the tunnel pellet samples. Black lines represent the full saturation. The lines were calculated assuming the saturation degree to be 100 % and for different density values (50 kg/m^3 intervals), values for the water content were iterated.*

4.6 Tunnel backfill blocks

Locations of the drilled tunnel backfill block samples are presented in Figure 78. Results of the tunnel backfill block sample analyses are shown in Figure 79 and Figure 80. The highest water contents were found from the top and from the bottom of the samples, decreasing towards the middle part. Saturation degrees varied between 60 % and 80 % with no detectable trends. A possible trend can be seen with the densities which were lower in the ends, increasing towards the middle.

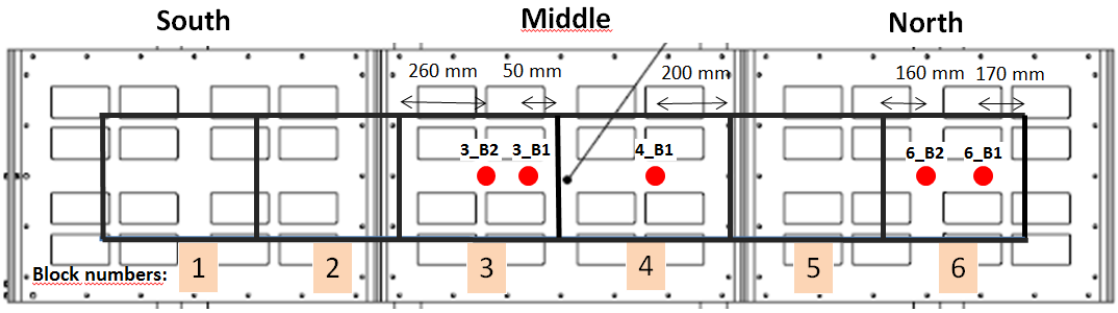

Figure 78. *Drilled backfill block sample locations presented from above the backfill blocks (B-side view), marked with red.*

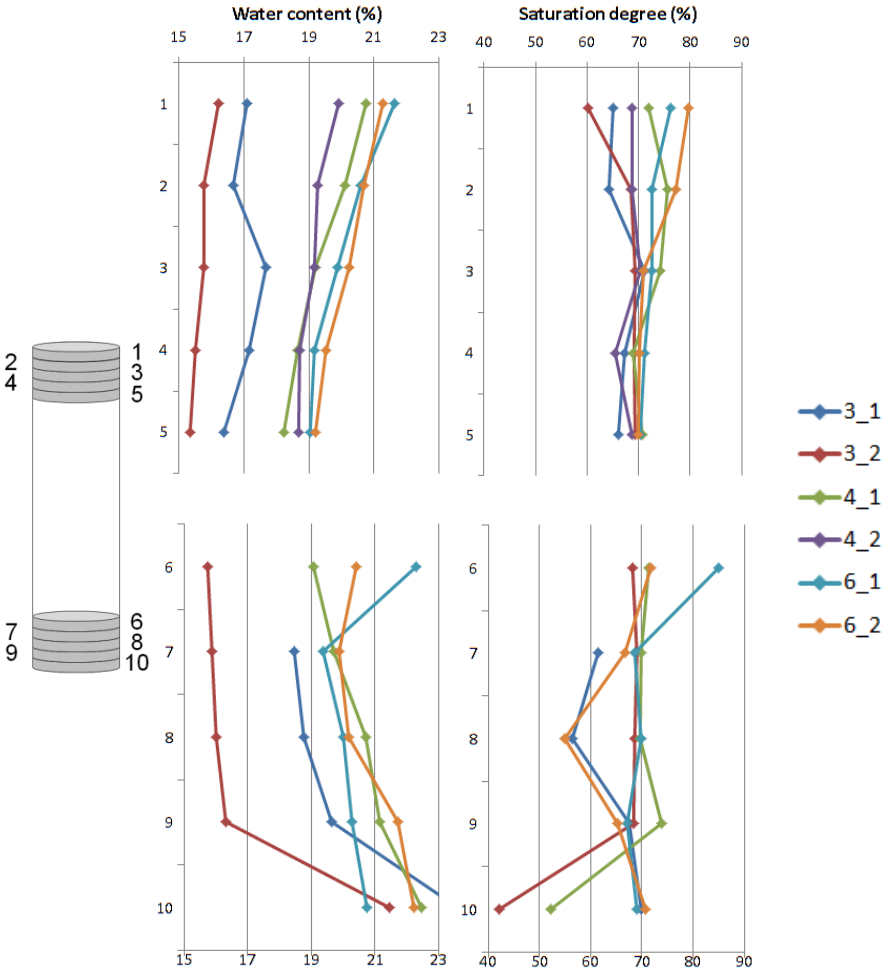

Figure 79. *Water content and saturation degree of the drilled tunnel backfill block samples. The squares represent the slices sawed from the samples, five from both ends. The samples were taken from the blocks 3, 4, and 6. The block 6 was the northernmost block in the tunnel (The block 1 being the southernmost).*

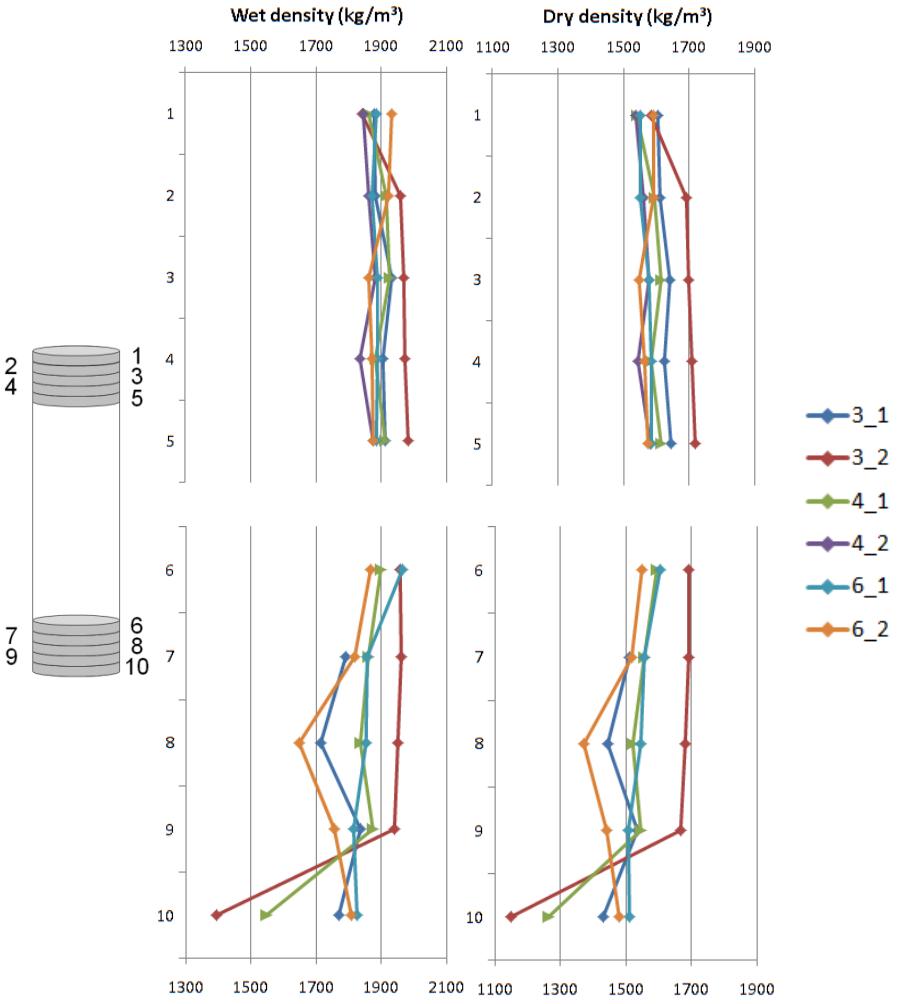

Figure 80. *Bulk density and dry density of the tunnel backfill block samples.*

4.7 Buffer and backfill interface

A sample taken from the interface of the tunnel pellets and the uppermost buffer block is shown in Figure 81a. The sample was taken from the center of the buffer. In the sample the tunnel pellet part was approximately 100 mm thick. The installed pellet layer part before the test was 130 mm so the pellet layer had compressed approximately 30 mm. It was also measured that the center of the buffer block was approximately 10 mm above the bottom of the tunnel (Figure 81b). Before the test the upper level of the uppermost buffer block was 30 mm below the bottom of the tunnel so approximately 40 mm of vertical displacement of the top surface of the uppermost buffer block had occurred during the test.

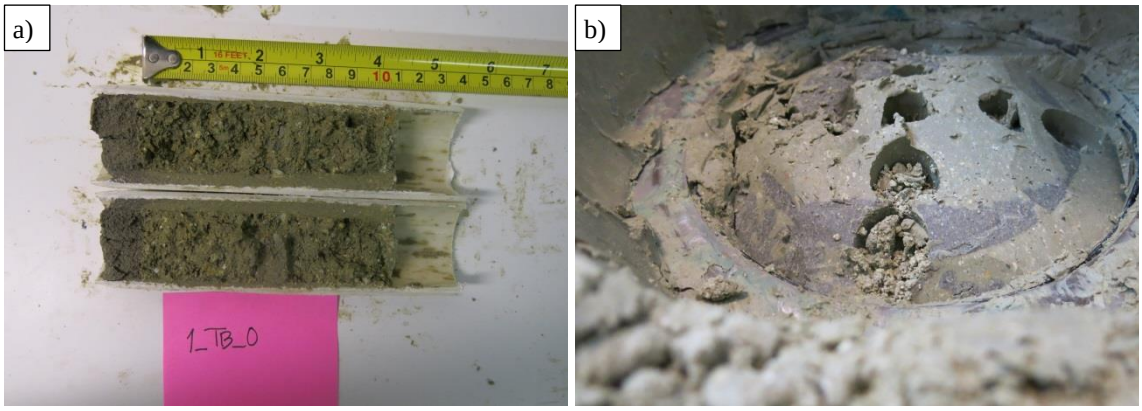

Figure 81. *In a), the sample above the center of the buffer is shown. About 20 mm thick buffer block part and about 100 mm thick tunnel pellet part can be seen in the sample. The plastic pipe was split because the sample was stuck inside. In b), the interface between the buffer material (darker color) and the tunnel pellet material is shown.*

Locations of the nine samples taken from the interface of the buffer and the tunnel pellets are presented in Figure 82. The samples were sliced from the interface and both parts, the buffer and the tunnel pellet, were analyzed. Results are shown in Figure 83 and Figure 84. Water contents were higher in the edges and the lowest water contents were found from the center of the buffer. A similar trend was found with the saturation degrees.

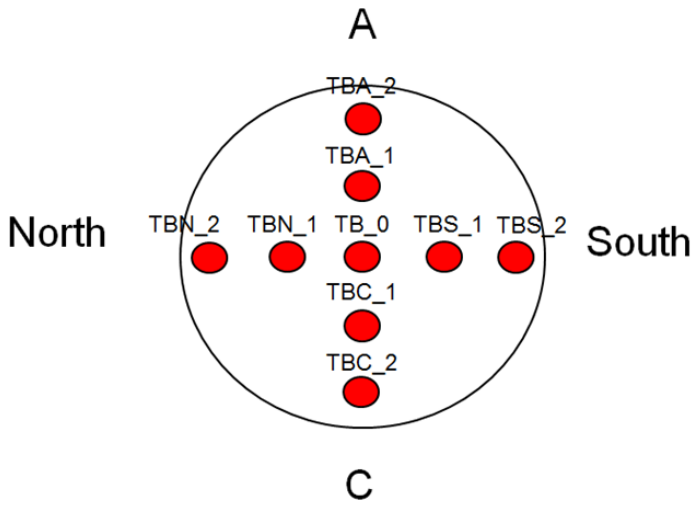

Figure 82. *Locations of the nine samples taken from above the buffer, containing the bottom pellet layer of the tunnel and a part of the uppermost buffer block.*

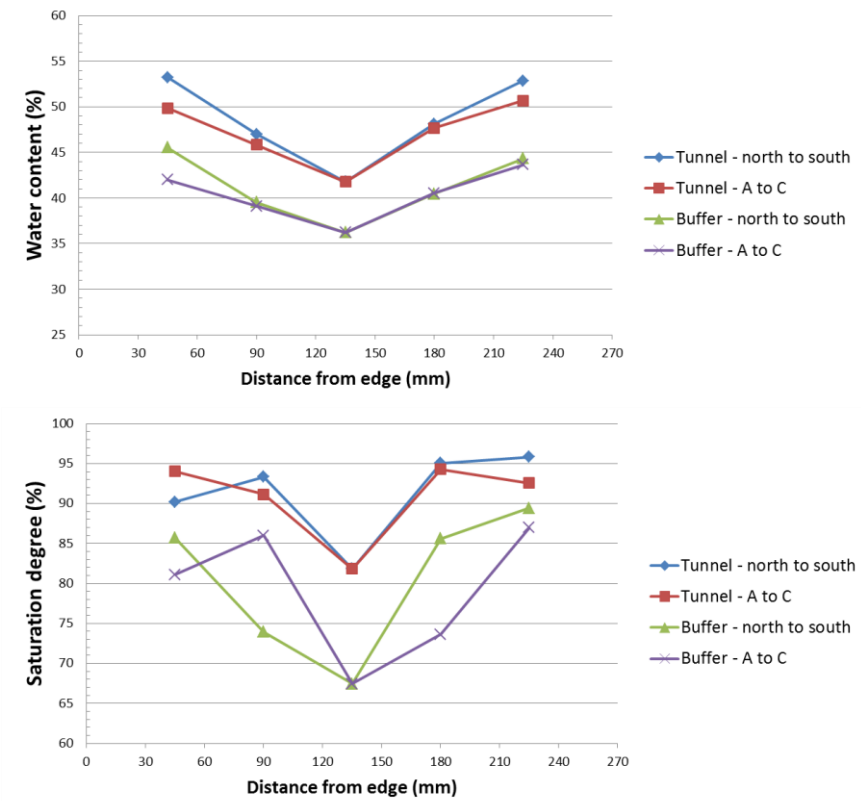

Figure 83. *Water content and saturation degree of the interface samples which were divided into a tunnel pellet part and a buffer part after which both parts were analyzed.*

Bulk densities of the tunnel pellet parts were lower in the edges and in the center. In the buffer parts, a possible trend is seen where the bulk density is lower in the center of the buffer and increases towards the edges. However, in the direction from A to C, the sample approximately 90 mm from the edge had a remarkably higher bulk density. This sample had also a remarkably higher dry density. Other dry densities of the buffer parts had a similar trend to what was found with the bulk densities. The dry densities of the tunnel pellet parts were lower in the edges compared to the center.

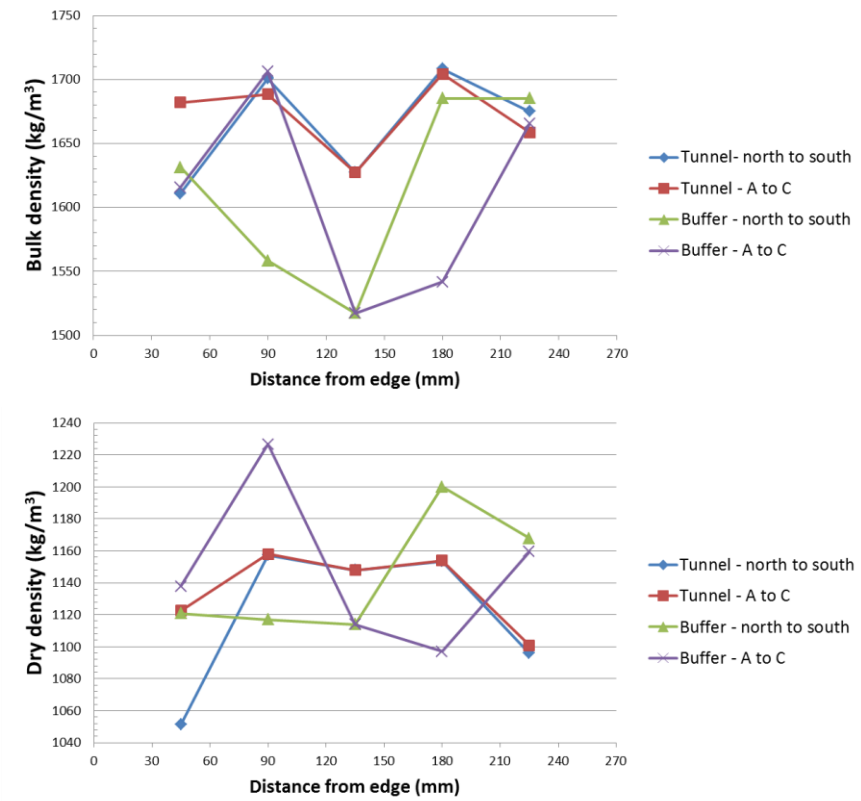

Figure 84. *Bulk density and dry density of the interface samples.*

When comparing the results of the buffer parts of the interface samples to the results of the drilled buffer samples from the center line of the uppermost buffer block (presented in Figure 70 and Figure 71), water contents in the A-C direction were slightly higher in the interface samples. Bulk density and dry density were slightly lower in the interface samples in both directions.

If the tunnel pellet parts of the interface samples are compared to the tunnel pellet samples taken from the bottom of the Middle unit of the tunnel (Figure 85), it can be seen that in the interface samples the water contents were lower and both bulk and dry densities were higher compared to the tunnel pellet samples. It should be noticed that the tunnel pellet parts in the interface samples were not divided into two samples: on sample close to a tunnel backfill block and one sample close to a window (buffer block in this case).

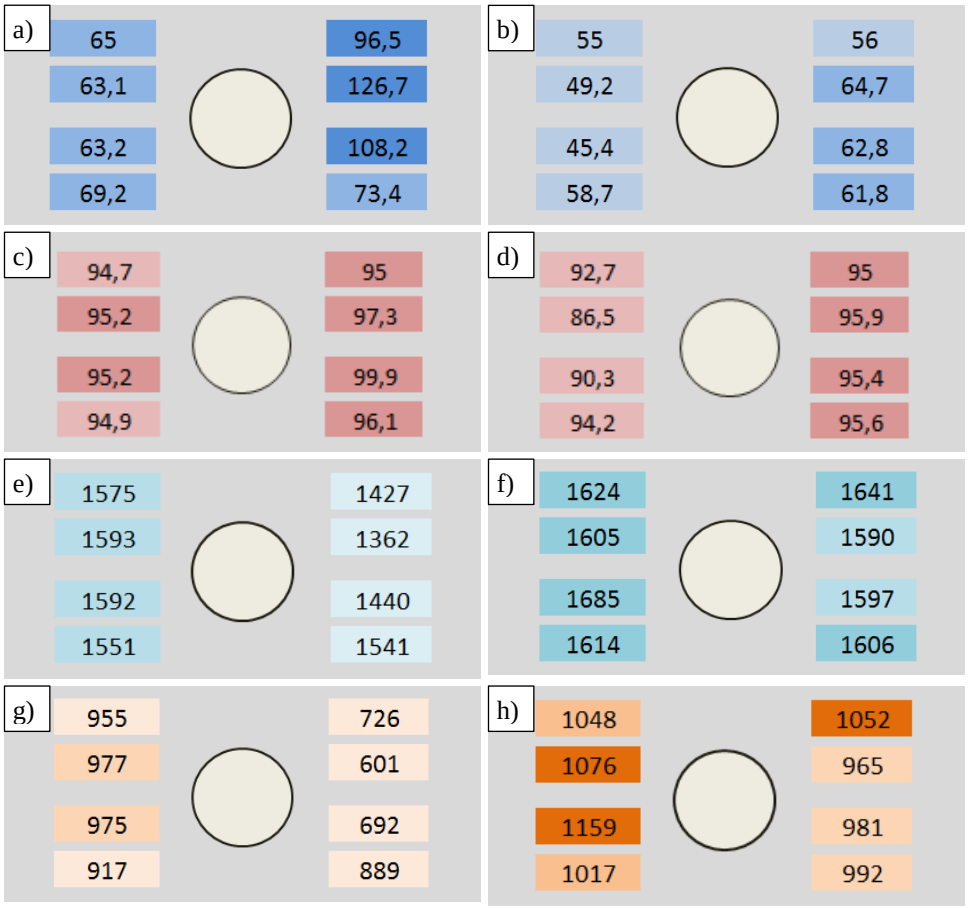

Figure 85. *Water content (a, b), saturation degree (c, d), bulk density (e, f) and dry density (g, h) of the tunnel pellet samples taken from the bottom of the Middle unit. Sample locations and labels can be found from Appendix 4. Images a, c, e, and g represent the samples taken close to the windows and images b, d, f, and h represent the samples taken close to the backfill blocks.*

High densities and saturation of the tunnel parts of the interface samples compared to the tunnel pellet samples is presented in Figure 86. In the graphs the results of the tunnel parts of the interface samples have been added to the graphs presented in Figure 77.

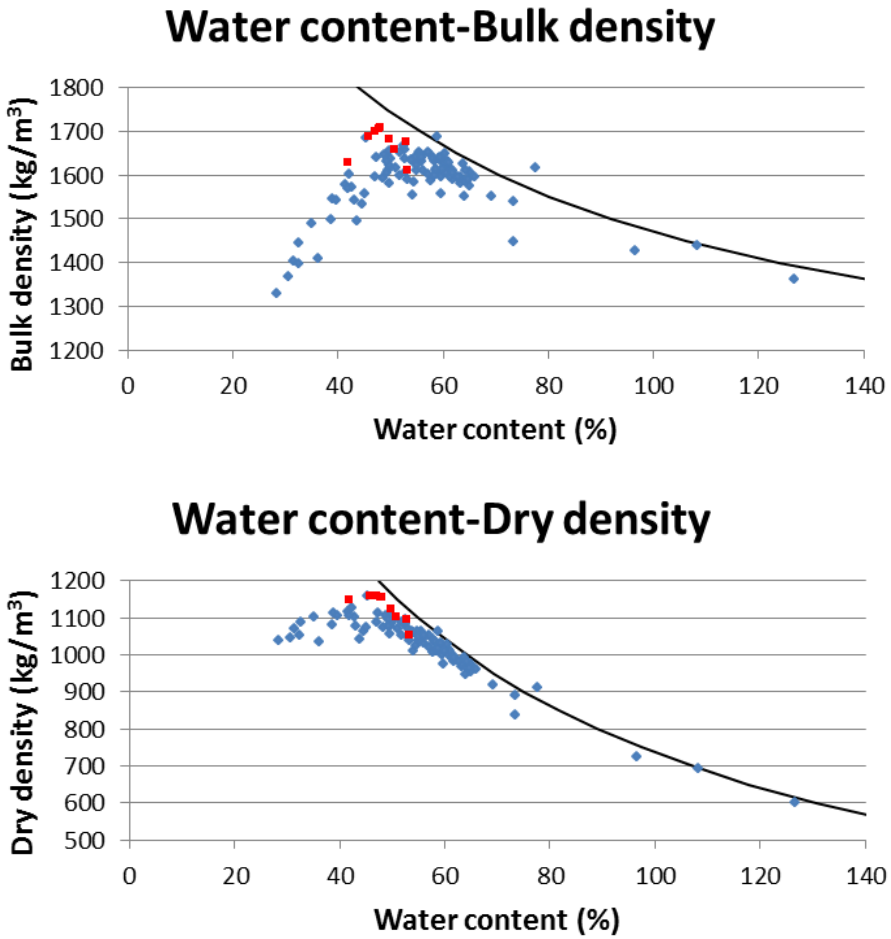

Figure 86. *Relation between water content and density of the tunnel pellet samples. In addition to Figure 77, red squares represent the tunnel pellet parts of the interface samples.*

5. DISCUSSION

Wetting and water channels

Most of the wetting of the tunnel pellets occurred during the first days of the test. After the 6th day, no dramatic change in the wetting pattern was observed until there was a pause in the water supply during which a tracer was added into inflowing water in the 59th day. After this, dry pellets in the South unit started to get wet. After two days of the start of the test, water started to flow out from an outlet in the North end of the tunnel. Water flowed out from the same outlet until the 59th day after which the location of the water outflow changed to the South end. These observations signify that water flowed in the tunnel using same channels and these channels were not closed with the continuous inflow of water. Similar conclusions were made in the study using an identical tube by Pintado et al. (2013) and in the study of full-scale buffer with reduced height by Åberg (2009).

The change in the water distribution pattern after the 59th day when there was a one hour pause in the water supply, indicates that at least some of the water channels were sealed due to the bentonite swelling and new channels were formed after the water supply started again. The water channel that was visible in the buffer pellet layer in the tube was not sealed during this pause. Thus, the changes occurred mainly in the tunnel. During the first days, some channels were visible through the tunnel windows but most of these channels were sealed shortly after they were observed. Also, in the buffer there were several branches in the channel but most of those were sealed after the first days. It is possible that in the initial phase, after the wetting of the pellets started, multiple channels existed but after some time all but one were sealed due to the bentonite swelling. It has to be taken into account that the water channels might have located in the gaps and junctions of the tunnel structure. Thus, the structure of the test equipment affected the flow paths to a great extent.

Uneven wetting of the tunnel backfill materials was observed in this test. The direction of the water distribution to the north part of the tunnel might have been due to the location of the water inlet and also due to the water channel which were located in the north side of the tube. The change in the water distribution in the tunnel after the possible sealing of the water channels in the 59th day might have been due to drier and less compacted pellets in the south part of the tunnel.

Sample analyses

The analyzed water contents supported the observations made during the test and the dismantling. Higher water contents were found from the north part of the tunnel. It is likely that a greater difference between the north and south parts would have existed without the change in the water distribution pattern after the 59th day. Tunnel pellet samples taken close to the tunnel walls had higher water contents than the samples taken close to the tunnel backfill blocks. This supports the observations that water flowed in the surface and in the gaps of the tunnel frame.

The bulk densities were dependent on the water content and the saturation degree. With the tunnel pellet samples it was found that with the water content lower than about 50 % the bulk density increased with the increasing water content. With the water content higher than 50 % the bulk density decreased with the increasing water content. In this limit, saturation degree was close to 100 %. It is probable that when the water content increased towards this limit of 50 %, void spaces in the pellet material were filled with water and consequently the bulk density increased.

When analyzing the results of the buffer samples, a possible trend could be seen where the water contents in the two uppermost buffer blocks were slightly higher compared to the two lowermost buffer blocks. In addition, the densities in the two uppermost buffer blocks were slightly lower. Thus, the two uppermost buffer blocks and pellets had possibly swelled more. This was probable also due to higher overburden pressure in the lowermost buffer blocks.

Monitored swelling pressure

Swelling of the bentonite was monitored by total pressure sensors inside the tunnel and by strain gauges attached to the outer surface of the tunnel and the tube. Also, two dial gauges were installed outside of the tunnel to measure horizontal displacement of the tunnel side walls. It has to be taken into account that the stresses measured, especially by the strain gauges and dial gauges, were dependent on the material and structure of the test equipment. These sensors were used mainly for monitoring the stresses of the test equipment.

As it was expected, based on the water distribution pattern, higher stresses were registered in the north part of the tunnel. Stresses in the long sides (A- and C-side) were similar. Some rapid changes occurred in the stresses, especially in the tunnel, during the first days of the test. These changes might have resulted from movements of the tunnel backfill blocks due to the bentonite swelling. Remarkable increases in the stresses were registered in the 59th day. This was probably due to sealing of the water channels during the pause in the water supply after which new water channels were formed and dry areas got wet and started to swell. Also, wetting and consequent swelling of the dry parts in the tunnel might have partly induced the sharp increases in the stresses.

Overall, many of the sensors showed continuous increases of stress during the whole test, especially in the tube which might have been a result from a less stiff material of the tube compared to the tunnel frame. Increased counter pressure of the pump might have been partly a result from the pump malfunction and partly from an increasing resistance of the water inflow.

Erosion

Continuous erosion of bentonite was found in the test. Variation in the erosion rate was seen during the first days of the test after which the erosion rate was mainly at a constant level. The effect of the pump malfunction needed to be taken into account when considering the erosion results. There is a possibility that the varying rate of erosion during the first days and the burst of the bentonite in the 6^{th} day were partly a result from the varying rate of the water inflow. The decreasing water flow rate might have sealed water channels at least partly and with the increasing water flow rate more erosion might have occurred when the channels were opened. A possible source for the eroded material in this test was also a bentonite dust included especially in the tunnel pellet bags.

Dry solid contents below 1 % in the last days of the test had to be considered as not realistic values. There might have been an error with the erosion analysis method with small water outflow rates. The error might have originated from the method used in estimating the evaporation of the water samples between the time of the sampling and the time of the sample weighing. In addition, with small sample sizes possible inaccuracies in measurements might have been emphasized.

In this test eroded bentonite was collected in seven minute sampling in four or five hour intervals so total amount of the eroded bentonite was not measured. An estimation of the total amount of eroded bentonite could have been done based on the water samples and assuming similar erosion behavior outside the sampling times. However, it needs to be noticed that some of the eroded bentonite got blocked in the outflowing pipes so the amount of erosion in the water samples did not always correspond the amount of the bentonite coming out from the tunnel during the time of the sampling.

Buffer and backfill interface

The vertical displacement of the center of the uppermost buffer block was approximately 40 mm. It is possible that most of this displacement was a result from swelling of the uppermost block. In the studies by Åberg (2009), Åkesson (2012), and Johannesson & Hagman (2013), it was found that heaving of the uppermost blocks were greater than heaving of the lowermost blocks. In this 1/6 scale test there might have been a water flow on top of the uppermost buffer block which has caused the slightly higher water contents and more swelling of the uppermost block. Also, smaller overburden pressure

of the uppermost block compared to the lowermost blocks supports the conclusion that the uppermost block swelled the most.

The materials and structure of the test equipment has to be taken into account when considering the upwards swelling. Swelling of the bentonite in the tube to horizontal direction might have also affected on the amount of the upwards swelling. In addition, in this test the water inlet was located in the tube so the test partly simulated the possible worst-case scenario where the buffer is saturated and the backfill is dry. With this kind of test scenario the vertical displacement was possibly greater than it would have been with different water inflow conditions.

In the interface, in the upper part of the uppermost buffer block, water contents were higher and densities were lower than lower in the uppermost buffer block. This probably indicates that the swelling of the uppermost block occurred mostly in the upper part of the block.

The tunnel pellet samples in the interface had higher densities and lower water contents than the samples taken from the bottom pellet layer of the tunnel. Higher densities were probably a result from the upwards swelling of the buffer and the compression of the bottom pellet layer above the buffer, from 130 mm to 100 mm. Lower water contents might indicate that water flowed along the tunnel floor to a great extent. Lower water contents of the interface samples might have also been due to the higher compression of the tunnel pellet layer above buffer which induced the higher densities. In Figure 86, it was seen that with full saturated tunnel pellet samples the water contents decreased when the densities increased.

Recommendations for future studies

New test scenarios with the 1/6 scale test equipment will possibly be carried out in the future. Modifications to the test equipment and test implementation will probably be made.

With different water inflow location or with multiple inflow points, the water distribution pattern and consequently the swelling development would be different. Supplying water from a different side of the buffer, water could possibly direct to a different side of the tunnel. One option for the water inflow location could also be the tunnel. In this option an interesting viewpoint would be to find out does the buffer get wet and in which time. With slower wetting of the buffer compared to the tunnel, the upwards swelling of the buffer blocks would probably occur in a lesser extent due to lesser saturation of the buffer blocks and greater swelling pressure originated from the tunnel backfill blocks and pellets. In addition, measuring the vertical displacements of individual buffer blocks should be considered in the future tests.

A tracer could also be used in the future tests for detecting the water flow paths. The tracer could be added into the water without switching off the pump so no changes in the water distribution would occur due to the tracer adding. Also, other possibilities to detect the water distribution in the system should be considered. One possible option for measuring the water distribution or flow could be non-destructive ERT (Electrical Resistivity Tomography) which has been used for instance by Korkealaakso & Kaila (2013).

More detailed erosion data could be collected in the future tests. The total amount of erosion could be collected as well as the amount of the inflowing water. Also, with the information of the outflowing water, the amount of water inside the test system could be calculated. With the total amount of the inflowing water and the total amount of eroded bentonite, a comparison could be made to an erosion model presented by Keto et al. (2009) where data from erosion tests performed by Sanden et al. (2008) and Sanden & Börgesson (2008) has been collected.

6. CONCLUSIONS

In this 1/6 scale laboratory experiment the aim was to get a new insight of the bentonite behavior in the initial part of the final disposal of spent nuclear fuel. Swelling of the bentonite was monitored and bentonite erosion was analyzed during the test. Also, wetting of the bentonite inside the test equipment was followed. After the 62 day test, samples were taken from the bentonite blocks and pellets. Due to the malfunction of the pump supplying water, the water inflow rate decreased gradually from the desired rate of 0.1 l/min to almost zero after which the test was stopped. The decreased inflow rate needed to be taken into account when the results were considered. Three days before the end of the test, a tracer was added into the inflowing water and the pump was switched off during the adding. The pause in the water supply and restart of the pump had remarkable effects on the water distribution pattern and bentonite swelling behavior.

Different conditions compared to the actual repository need to be taken into account, including for instance: the bedrock, different scale, canisters containing heat generating spent nuclear fuel, and water flow conditions. In addition, the duration of this test covered only the very early phases of the events in the repository.

The main findings in this study were:

- Wetting of the tunnel was inhomogeneous. Dry pellets were found after the test.
- Several water channels existed in the early phases of the test after which some of the channels were sealed.
- With a continuous water inflow from the same location, the main water channels were not sealed due to bentonite swelling.
- The pause in the water inflow induced sealing of the main water channels in the tunnel and after the water inflow started again, water flowed towards the dry parts of the tunnel.
- Continuous erosion occurred in the test.
- With water contents below approximately 50 %, bulk density of the tunnel pellets (Cebogel QSE) increased with the increasing water content. With higher water contents, the bulk density decreased with the increasing water content.
- A vertical displacement of approximately 40 mm of the center of the uppermost buffer block occurred, possibly mainly due to swelling of the uppermost buffer block.
- The tunnel pellet layer above the buffer compressed from 130 mm to 100 mm. Almost fully saturated tunnel pellets with high density were found from above the buffer.

REFERENCES

Ahonen, L., Korkeakoski, P., Tiljander, M., Kivikoski, H. & Laaksonen, R. 2008. Quality Assurance of the Bentonite Material. Working Report 2008-33. Posiva Oy, Eurajoki. 126 p.

Autio, J., Hassan, M., Karttunen, P. & Keto, P. 2013. Backfill Design 2012. Posiva 2012-15. Posiva Oy, Eurajoki. 96 p.

Börgesson, L. & Hernelind, J. 2009. Mechanical interaction buffer/backfill. Finite element calculations of the upward swelling of the buffer against both dry and saturated backfill. R-09-42. Svensk Kärnbränslehantering AB, Stockholm. 28 p.

Dixon, D., Hansen, J., Korkiala-Tanttu, L., Karvonen, T. H., Marcos, N. & Sievänen, U. 2013. Underground Disposal Facility Closure Design 2012. Working Report 2012-09. Posiva Oy, Eurajoki. 102 p.

Hansen, J., Korkiala-Tanttu, L., Keski-Kuha, E. & Keto, P. 2010. Deposition Tunnel Backfill Design for a KBS-3V Repository. Working Report 2009-129. Posiva Oy, Eurajoki. 113 p.

Hellä, P., Ikonen, A., Mattila, J., Torvela, T. & Wikström, L. 2009. RSC-Programme – Interim Report. Working Report 2009-29. Posiva Oy, Eurajoki. 123 p.

Holt, E., Marjavaara, P. & Löija, M. 2011. Artificial Wetting of Buffer Material – Small Scale. Working Report 2011-53. Posiva Oy, Eurajoki. 120 p.

Ikonen, K. & Raiko, H. 2012. Thermal Dimensioning of Olkiluoto Repository for Spent Fuel. Working report 2012-56. Posiva Oy, Eurajoki. 76 p.

Johannesson, L-E. & Hagman, P. 2013. Prototype repository. Method for opening and retrieval of the outer section. P-13-15. Svensk Kärnbränslehantering AB, Stockholm. 52 p.

Juvankoski, M. 2013. Buffer Design 2012. Posiva 2012-14. Posiva Oy, Eurajoki. 259 p.

Juvankoski, M., Ikonen, K. & Jalonen, T. 2012. Buffer Production Line 2012. Design, Production and Initial State of the Buffer. Posiva 2012-17. Posiva Oy, Eurajoki. 166 p.

Karnland, O. 2010. Chemical and mineralogical characterization of the bentonite buffer for the acceptance control procedure in a KBS-3 repository. Technical Report TR-10-60. Svensk Kärnbränslehantering AB, Stockholm. 25 p.

Karnland, O., Olsson, S. & Nilsson, U. 2006. Mineralogy and sealing properties of various bentonites and smectite-rich clay materials. Technical Report TR-06-30. Svensk Kärnbränslehantering AB, Stockholm. 112 p.

Keto, P., Dixon, D., Gunnarsson, D., Jonsson, E., Börgesson, L. & Hansen, J. 2009. Assessment of Backfill Design for KBS-3V Repository. Working Report 2009-115. Posiva Oy, Eurajoki. 162 p.

Keto, P., Hassan, M., Karttunen, P., Kiviranta, L., Kumpulainen, S., Korkiala-Tanttu, L., Koskinen, V., Jalonen, T., Koho, P. & Sievänen, U. 2013. Backfill Production Line 2012. Posiva 2012-18. Posiva Oy, Eurajoki. 181 p.

Korkealaakso, J. & Kaila, J. 2013. 3D time-lapse electrical imaging of processes and heterogeneities in the landfill body. International Conference on Final Sinks, pp. 231-231.

Korkiala-Tanttu, L. 2009. Finite Element Modelling of Deformation of Unsaturated Backfill Due to Swelling of the Buffer. Working Report 2008-88. Posiva Oy, Eurajoki. 40 p.

Koskinen, V. 2012. Uniaxial Backfill Block Compaction. Working Report 2012-21. Posiva Oy, Eurajoki. 94 p.

Kärki, A. & Paulamäki, S. 2006. Petrology of Olkiluoto. Posiva 2006-02. Posiva Oy, Eurajoki. 87 p.

Leoni, M. 2013. 2D and 3D Finite Element Analysis of Buffer-Backfill Interaction. Posiva 2012-25. Posiva Oy, Eurajoki. 81 p.

Marjavaara, P., Holt, E. & Sjöblom, V. 2013. Customized Bentonite Pellets: Manufacturing, Performance and Gap Filling Properties. Working Report 2012-62. Posiva Oy, Eurajoki. 76 p.

Pastina, B. & Hellä, P. 2006. Expected Evolution of a Spent Nuclear Fuel Repository at Olkiluoto. Posiva 2006-05. Posiva Oy, Eurajoki. 422 p.

Pintado, X., Adesola, F. & Turtiainen, M. 2013. Downscaled Tests on Buffer Behaviour. Working Report 2012-100. B+Tech Oy, Helsinki. 88 p.

Posiva. 2010. TKS-2009. Nuclear Waste Management at Olkiluoto and Loviisa Power plants. Posiva Oy, Eurajoki. 567 p.

Posiva. 2012a. Safety Case for the Disposal of Spent Nuclear Fuel at Olkiluoto - Design Basis 2012. Posiva 2012-03. Posiva Oy, Eurajoki. 177 p.

Posiva. 2012b. Safety Case for the Disposal of Spent Nuclear Fuel at Olkiluoto - Description of the Disposal System 2012. Posiva 2012-05. Posiva Oy, Eurajoki. 176 p.

Posiva. 2012c. Olkiluoto Site Description 2011. Posiva Oy, Eurajoki. 1039 p.

Posiva. 2013. Site Engineering Report. Posiva 2012-23. Posiva Oy, Eurajoki. 166 p.

Posiva. 2015. Posiva, web page. Available (accessed on 5.12.2015): http:www.posiva.fi/en.

Raiko, H. Canister Design 2012. 2013. Posiva 2012-13. Posiva Oy, Eurajoki. 164 p.

Raiko, H., Pastina, B., Jalonen, T., Nolvi, L., Pitkänen, J. & Salonen, T. 2012. Canister Production Line 2012. Posiva 2012-16. Posiva Oy, Eurajoki. 182 p.

Ritola, J. & Pyy, E. 2012. Isostatic Compression of Buffer Blocks – Middle Scale. Working Report 2011-62. Posiva Oy, Eurajoki. 74 p.

Saanio, T., Ikonen, A., Keto, P., Kirkkomäki, T., Kukkola, T., Nieminen, J. & Raiko, H. 2013. Design of the Disposal Facility 2012. Working Report 2013-17. Posiva Oy, Eurajoki. 196 p.

Sanden, T. & Börgesson, L. 2008. Deep repository-engineered barrier system. Piping and erosion in tunnel backfill. R-06-72. Svensk Kärnbränslehantering AB, Stockholm. 82 p.

Sanden, T., Börgesson, L. & Dueck, A. 2008. Deep repository-Engineered barrier system. R-08-136. Svensk Kärnbränslehantering AB, Stockholm. 50 p.

Sane, P., Laurila, T., Olin, M. & Koskinen, K. 2013. Current Status of Mechanical Erosion Studies of Bentonite Buffer. Posiva 2012-45. Posiva Oy, Eurajoki. 86 p.

Sievänen, U., Karvonen, T. H., Dixon, D., Hansen, J. & Jalonen, T. 2012. Design, Production and Initial State of the Underground Disposal Facility Closure. Posiva 2012-19. Posiva Oy, Eurajoki. 112 p.

SKB. 2004. Interim process report for the safety assessment SR-Can. R-04-33. Svensk Kärnbränslehantering AB, Stockholm. 138 p.

Toprak, E., Mokni, N., Olivella, S. & Pintado, X. 2013. Thermo-Hydro-Mechanical Modelling of Buffer. Posiva 2012-47. Posiva Oy, Eurajoki. 120 p.

Wersin, P. 2003. Geochemical modelling of bentonite porewater in high-level waste repositories. Journal of Contaminant Hydrology 61, pp. 405-422.

Åberg, A. 2009. Effects of water inflow on the buffer – an experimental study. R-09-29. Svensk Kärnbränslehantering AB, Stockholm. 41 p.

Åkesson, M. 2012. Temperature buffer test. TR-12-04. Svensk Kärnbränslehantering AB, Stockholm. 44 p.

APPENDIX 1: TEST EQUIPMENT DIMENSIONS

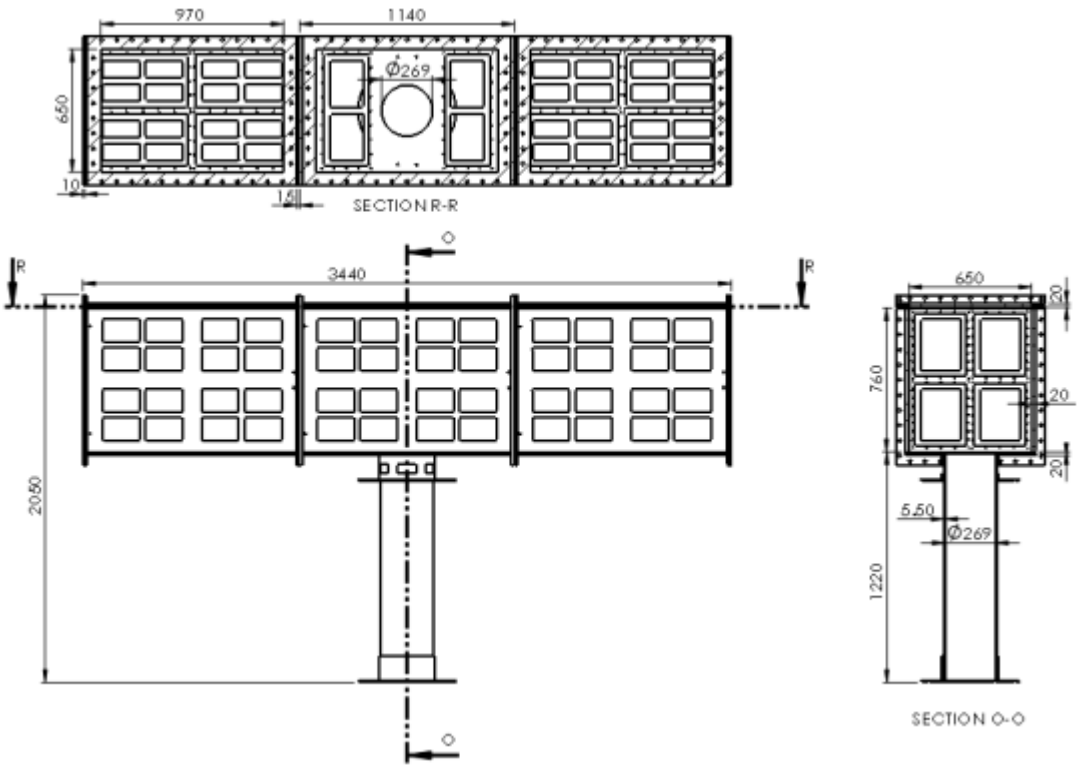

APPENDIX 2: TUNNEL WINDOW LABELLING, STRAIN GAUGES, AND OUTLETS

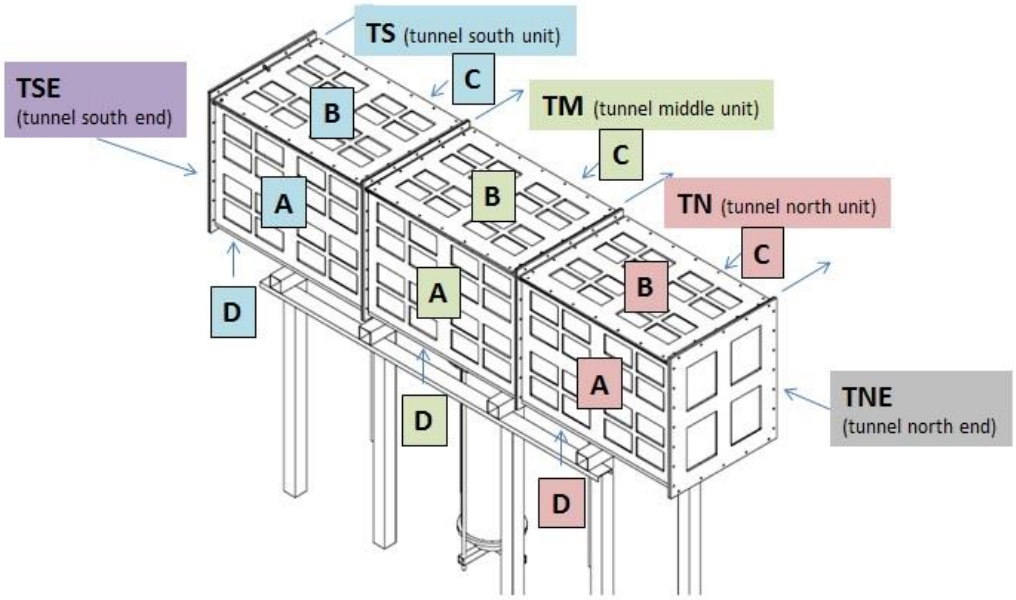

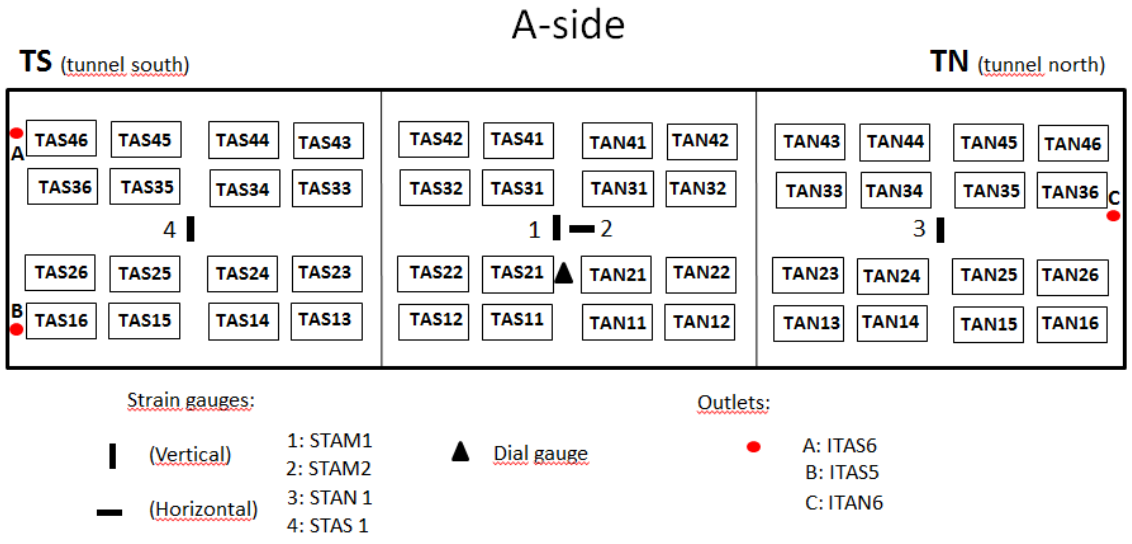

B-side

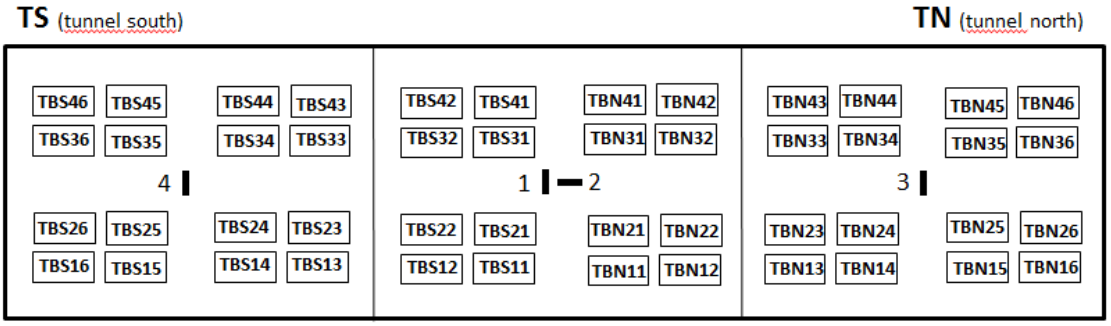

Strain gauges:

▮	(Vertical)	1: STBM1 2: STBM2
▬	(Horizontal)	3: STBN 1 4: STBS 1

C-side

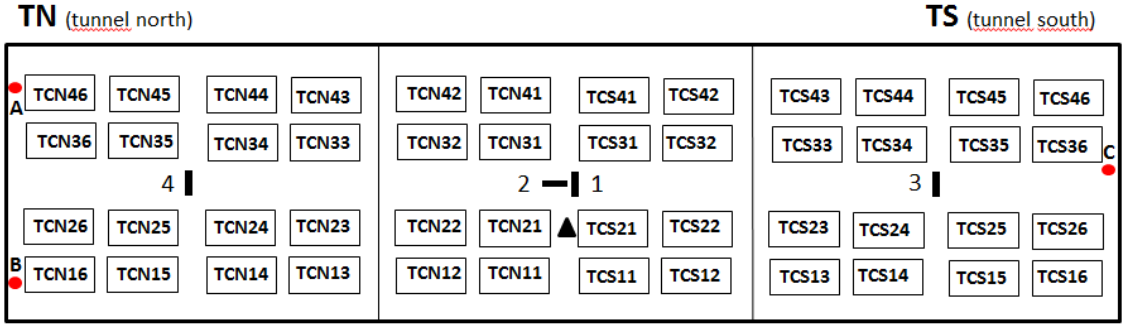

Strain gauges:

▮	(Vertical)	1: STCM1 2: STCM2
▬	(Horizontal)	3: STCS 1 4: STCN 1

▲ Dial gauge

Outlets:

●	A: ITCN6 B: ITCN5 C: ITCS6

D-side

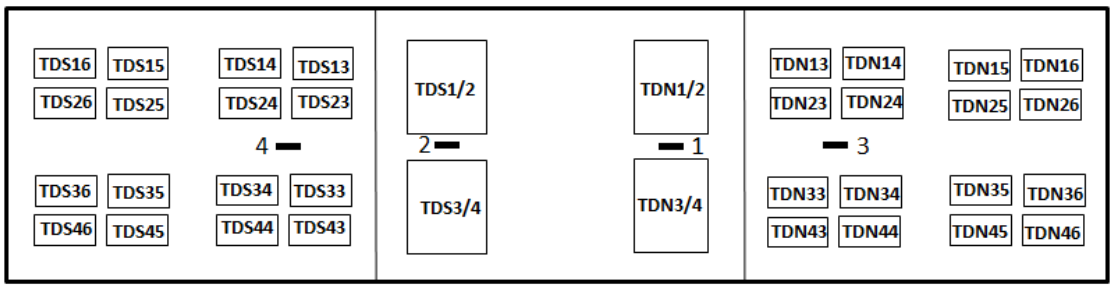

Strain gauges:

▮	(Vertical)	1: STDM1 2: STDM2
▬	(Horizontal)	3: STDN1 4: STDS1

South and North ends

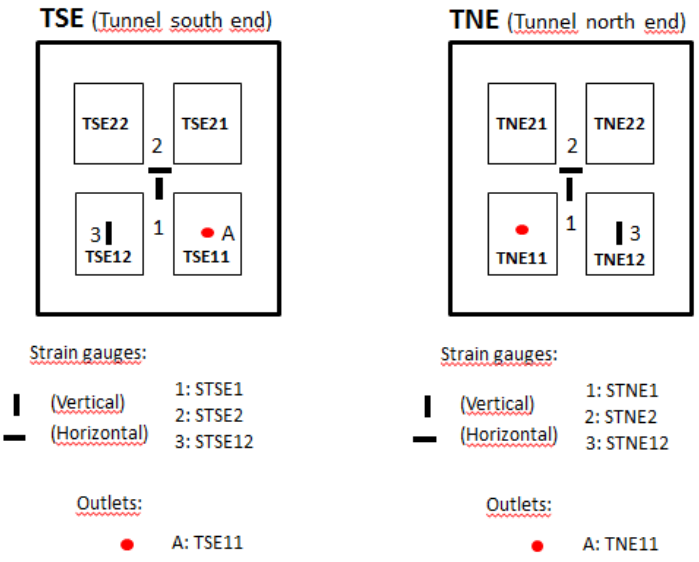

Tube

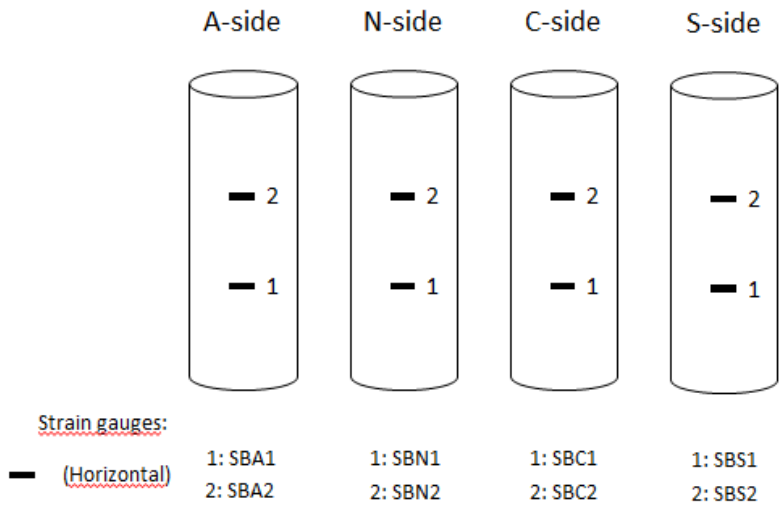

APPENDIX 3: BLOCK DIMENSIONS

Table A3-1. *Weights and dimensions of the buffer blocks.*

Buffer block number	Weight [kg]	Height [mm]	Height average [mm]	Diameter [mm]	Diameter (average) [mm]	Observations
1 (lowermost)	9.38	200.8	200.8	170.2 170.2 170.2	170.2	Roughness on the top of the block, diameter 56.6 mm
2	9.36	200.7 200.2 200.0 200.0	200.2	170.0 170.0 170.0	170.0	Roughness on the top of the block, diameter 34.4 mm
3	9.38	201.4 201.0 200.3 200.3 200.3	200.7	170.4 170.3 170.3	170.3	
4 (uppermost)	9.36	201.1 200.2 200.3 200.8 200.3	200.5	170.2 170.2 170.2	170.2	

Table A3-2. *Weights and dimensions of the tunnel backfill blocks.*

Backfill block number	Weight [kg]	Height [mm]	Height (average) [mm]	Width [mm]	Length [mm]	Length (average) [mm]
1 (north)	188.46	332.0 331.9 331.9	331.9	568.7	497.4 498.2 497.6	497.7
2	188.26	329.4 329.4 329.0	329.3	568.1	497.3 497.6 497.1	497.3
3	188.00	330.8 331.4 331.0	331.1	568.2	497.6 497.5 497.4	497.5
4	192.10	331.5 331.5 331.5	331.5	567.4	497.0 497.4 497.0	497.1
5	186.46	333.5 333.0 334.0	333.5	569.4	498.5 499.2 498.5	498.7
6 (south)	187.16	332.4 332.5 332.0	332.3	569.5	498.6 498.9 498.5	498.7

APPENDIX 4: TUNNEL PELLET SAMPLE LOCATIONS

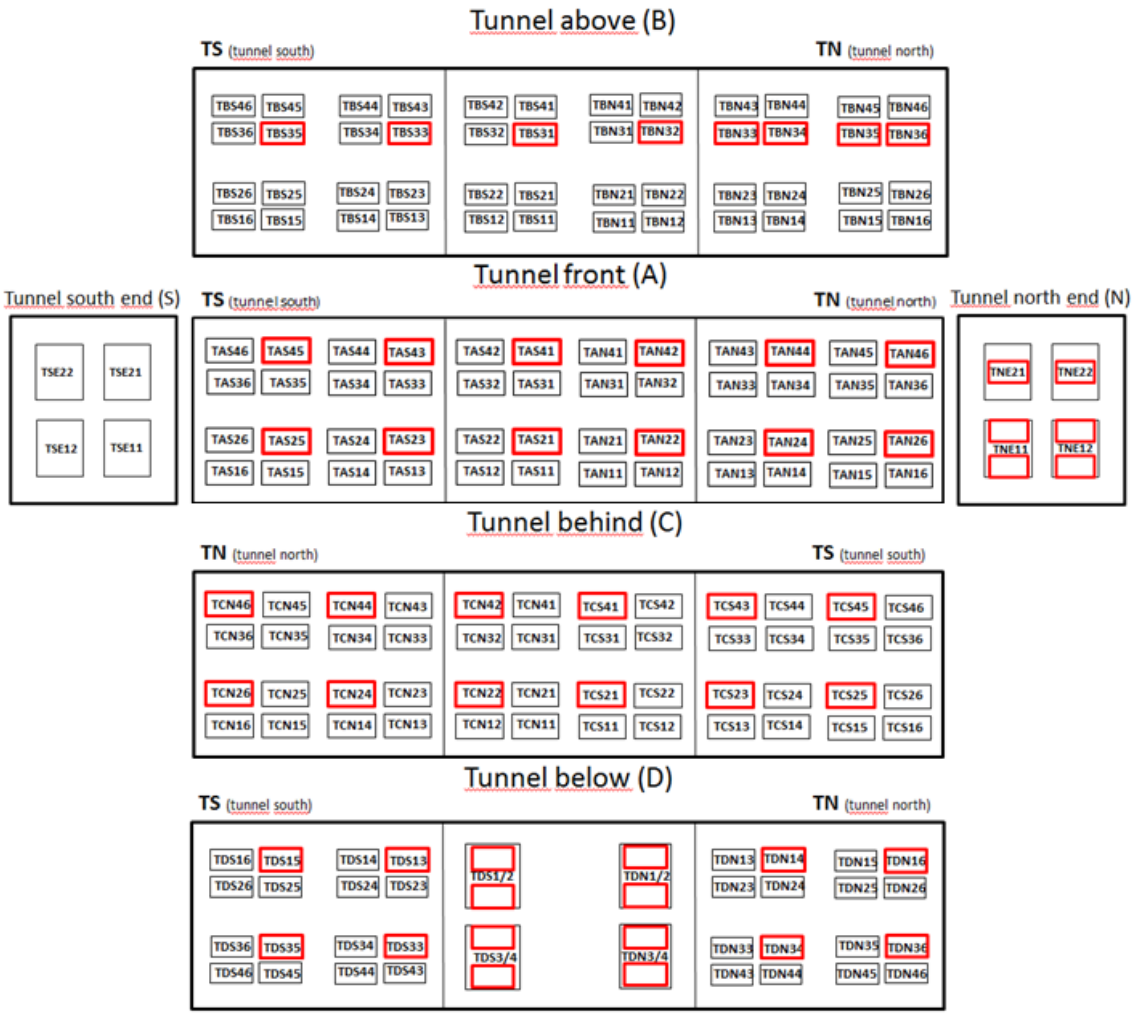

Figure A4-1. *Tunnel pellet sample locations marked with red bordered boxes.*

APPENDIX 5: TUNNEL BACKFILL BLOCK SAMPLE LOCATIONS

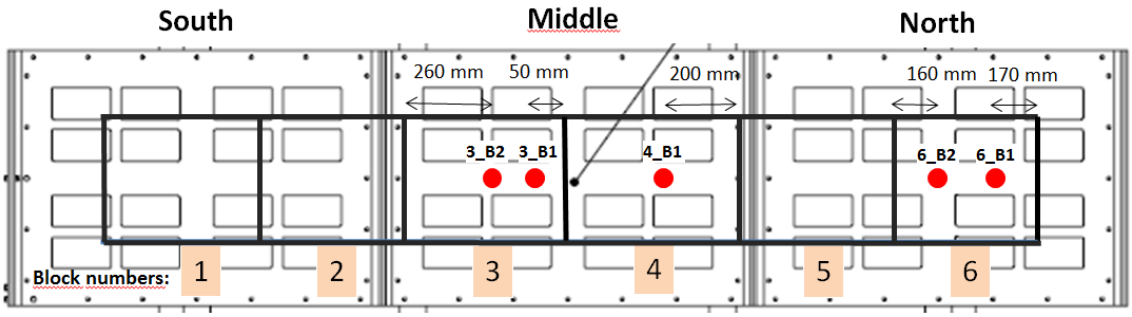

Figure A5-1. *Drilled sample locations shown from above the backfill blocks (B-side view), marked with red.*

APPENDIX 6: INTERFACE SAMPLE LOCATIONS

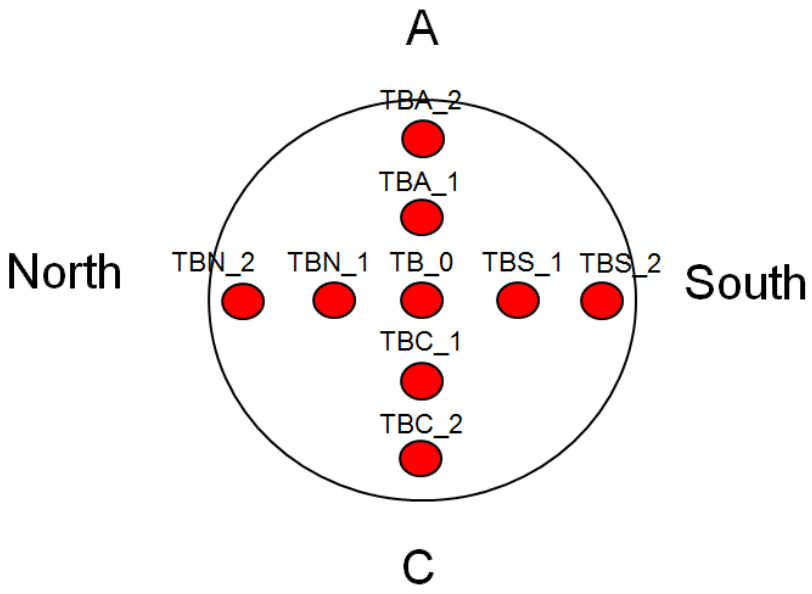

Figure A6-1. *Locations of the interface samples taken from above the buffer, containing the bottom pellet layer of the tunnel and a part from the uppermost buffer block or pellet.*

APPENDIX 7: BUFFER SAMPLE LOCATIONS

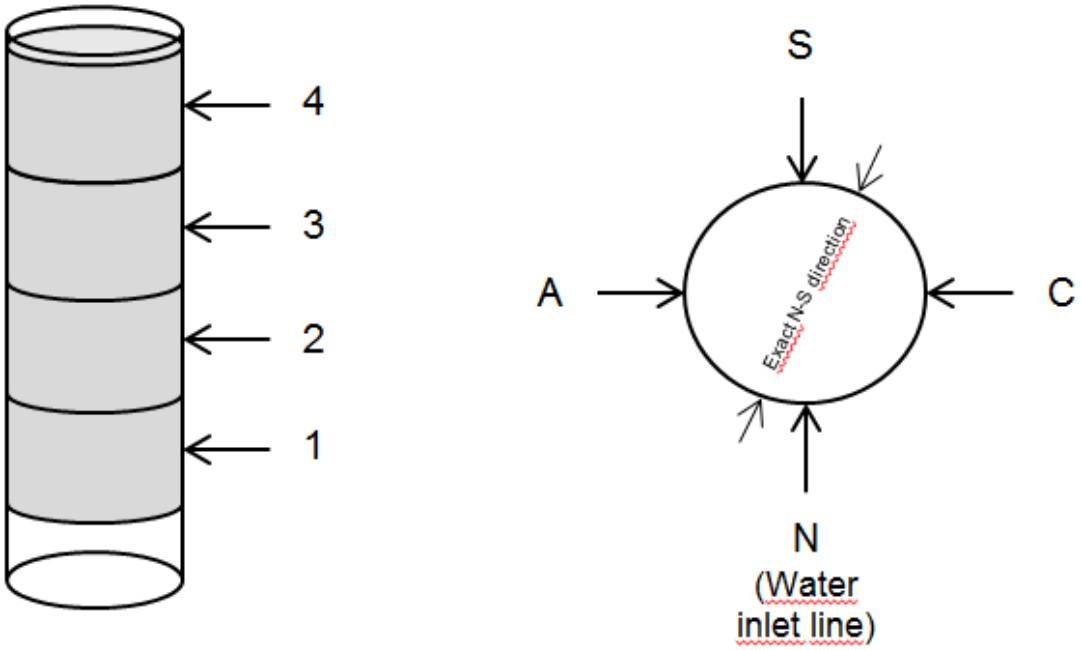

Figure A7-1. *Buffer samples were taken from four height levels, from the center of the buffer blocks. From each level, the samples were drilled through the buffer in two directions, N-S and A-C. Level 1 was right above the water inlet and N-S direction was in the line with the water inlet.*

APPENDIX 8: SAMPLE RESULTS

Table A10-1. *Tunnel pellet sample results (A in a label stands for a sample close to a window and B stands for a sample close to a backfill block).*

Label	Water content (%)	Bulk density (kg/m^3)	Dry density (kg/m^3)	Saturation degree (%)	Porosity
TAN46_A	59,8	1610	1007	94,7	0,64
TAN46_B	54,0	1633	1061	92,9	0,62
TAN26_A	57,7	1645	1043	96,6	0,62
TAN26_B	48,9	1646	1106	89,9	0,60
TAN44_A	58,3	1633	1031	95,8	0,63
TAN44_B	42,7	1572	1102	78,1	0,60
TAN24_A	60,8	1632	1015	97,3	0,63
TAN24_B	44,6	1535	1062	76,7	0,62
TAN22_A	47,3	1641	1114	88,1	0,60
TAN22_B	28,4	1331	1037	47,0	0,63
TAN42_A	49,5	1638	1096	89,7	0,61
TAN42_B	36,2	1408	1034	59,7	0,63
TAS41_A	59,7	1556	974	89,8	0,65
TAS41_B	48,4	1594	1074	84,9	0,61
TAS21_A	58,1	1639	1036	96,2	0,63
TAS21_B	58,8	1689	1064	101,5	0,62
TAS43_A	77,7	1617	910	105,3	0,67
TAS43_B	60,0	1627	1017	96,4	0,63
TAS23_A	60,8	1615	1005	95,8	0,64
TAS23_B	45,0	1558	1075	79,0	0,61
TAS45_A	63,3	1580	968	94,2	0,65
TAS45_B	57,0	1653	1053	96,8	0,62
TAS25_A	63,7	1625	993	98,5	0,64
TAS25_B	58,6	1603	1011	93,2	0,64
TBN36_A	59,5	1595	1000	93,2	0,64
TBN36_B	49,5	1610	1077	87,1	0,61
TBN35_A	57,7	1587	1006	91,2	0,64
TBN35_B	47,0	1597	1087	84,0	0,61
TBN34_A	53,3	1590	1038	88,4	0,63
TBN34_B	43,2	1541	1077	76,0	0,61
TBN33_A	54,1	1555	1009	85,9	0,64
TBN33_B	41,5	1579	1116	77,5	0,60
TBN32_A	56,1	1611	1032	92,3	0,63
TBN32_B	42,2	1603	1127	80,2	0,59
TBS31_A	54,5	1585	1026	88,8	0,63
TBS31_B	38,9	1546	1113	72,4	0,60
TBS33_A	31,5	1405	1069	54,7	0,62
TBS33_B	25,0				
TBS35_A	32,5	1396	1054	55,2	0,62
TBS35_B	32,6	1444	1089	58,5	0,61
TNE21_A	59,1	1637	1029	96,7	0,63
TNE21_B	49,8	1623	1083	88,7	0,61
TNE22_A	55,5	1653	1063	95,8	0,62
TNE22_B	52,7	1637	1072	92,1	0,61
TNE11_A_above	58,7	1612	1016	94,2	0,63
TNE11_B_above	50,0	1638	1092	90,1	0,61
TNE11_A_below	64,0	1552	946	92,0	0,66
TNE11_B_below	59,5	1636	1026	96,9	0,63
TNE12_A_above	63,2	1595	978	95,5	0,65
TNE12_B_above	60,9	1622	1008	96,6	0,64
TNE12_A_below	64,7	1592	967	96,0	0,65
TNE12_B_below	60,4	1651	1029	98,9	0,63

Label	Water content (%)	Bulk density (kg/m^3)	Dry density (kg/m^3)	Saturation degree (%)	Porosity
TCN46_A	61,8	1589	983	94,1	0,65
TCN46_B	55,7	1645	1056	95,2	0,62
TCN26_A	61,7	1610	995	96,0	0,64
TCN26_B	56,0	1641	1052	94,9	0,62
TCN44_A	64,1	1587	968	95,3	0,65
TCN44_B	55,1	1630	1051	93,3	0,62
TCN24_A	63,1				
TCN24_B	52,6	1657	1086	94,0	0,61
TCN42_A	58,4	1598	1009	92,6	0,64
TCN42_B	49,9	1655	1105	91,6	0,60
TCN22_A	60,8	1612	1002	95,5	0,64
TCN22_B	53,1	1607	1050	89,7	0,62
TCS41_A	52,5	1669	1094	94,9	0,61
TCS41_B	38,6	1499	1082	68,5	0,61
TCS21_A	65,1	1606	973	97,6	0,65
TCS21_B	57,1	1601	1019	92,0	0,63
TCS43_A	39,6	1543	1106	72,8	0,60
TCS43_B	30,7	1367	1046	51,5	0,62
TCS23_A	54,7	1642	1061	94,1	0,62
TCS23_B	49,7	1581	1057	84,8	0,62
TCS45_A	56,0	1633	1047	94,2	0,62
TCS45_B	43,7	1496	1041	72,9	0,63
TCS25_A	60,6	1605	999	94,7	0,64
TCS25_B	51,0	1617	1071	89,0	0,61
TDS15_A	61,4	1595	988	94,4	0,64
TDS15_B	55,0	1611	1039	91,5	0,63
TDS35_A	49,3	1633	1094	89,1	0,61
TDS35_B	35,0	1488	1103	64,1	0,60
TDS13_A	61,0	1628	1011	97,1	0,64
TDS13_B	55,8	1645	1056	95,2	0,62
TDS33_A	51,8	1652	1088	92,8	0,61
TDS33_B	41,8	1569	1107	77,0	0,60
TDS12_A	65,0	1575	955	94,7	0,66
TDS12_B	55,0	1624	1048	92,7	0,62
TDS22_A	63,1	1593	977	95,2	0,65
TDS22_B	49,2	1605	1076	86,5	0,61
TDS32_A	63,2	1592	975	95,2	0,65
TDS32_B	45,4	1685	1159	90,3	0,58
TDS42_A	69,2	1551	917	94,9	0,67
TDS42_B	58,7	1614	1017	94,3	0,63
TDN12_A	96,5	1427	726	95,0	0,74
TDN12_B	55,9	1641	1052	95,0	0,62
TDN22_A	126,7	1362	601	97,3	0,78
TDN22_B	64,7	1590	965	95,9	0,65
TDN32_A	108,2	1440	692	99,9	0,75
TDN32_B	62,8	1597	981	95,4	0,65
TDN42_A	73,4	1541	889	96,1	0,68
TDN42_B	61,8	1606	992	95,6	0,64
TDN14_A	73,4	1449	836	87,9	0,70
TDN14_B	59,3	1640	1030	97,2	0,63
TDN34_A	65,9	1595	961	97,1	0,65
TDN34_B	51,7	1598	1054	87,8	0,62
TDN16_A	59,9	1615	1010	95,3	0,64
TDN16_B	53,8	1636	1063	92,9	0,62
TDN36_A	64,3	1610	980	97,6	0,65
TDN36_B	51,0				

Table A10-2. *Tunnel backfill block sample results.*

Label	Water content (%)	Bulk density (kg/m^3)	Dry density (kg/m^3)	Saturation degree (%)	Porosity
3_B1_1	17,1	1879	1604	65,0	0,42
_2	16,7	1882	1613	64,2	0,42
_3	17,7	1933	1642	71,1	0,41
_4	17,1	1906	1627	67,4	0,41
_5	16,4	1915	1645	66,2	0,41
_6					
_7	18,5	1793	1514	61,5	0,46
_8	18,8	1715	1444	56,5	0,48
_9	19,7	1839	1536	67,7	0,45
_10	23,6	1771	1433	70,0	0,48
3_B2_1	16,2	1844	1587	60,1	0,43
_2	15,8	1961	1694	68,6	0,39
_3	15,8	1969	1701	69,3	0,39
_4	15,5	1975	1709	69,1	0,39
_5	15,3	1984	1720	69,4	0,38
_6	15,8	1958	1691	68,2	0,39
_7	15,9	1962	1693	69,0	0,39
_8	16,0	1953	1683	68,6	0,39
_9	16,3	1942	1669	68,4	0,40
_10	21,5	1396	1149	42,2	0,59
4_B1_1	20,8	1862	1542	72,0	0,45
_2	20,1	1918	1597	75,6	0,43
_3	19,2	1925	1615	74,2	0,42
_4	18,7	1882	1586	69,0	0,43
_5	18,2	1912	1617	70,7	0,42
_6	19,1	1898	1594	71,5	0,43
_7	19,7	1862	1556	69,8	0,44
_8	20,7	1836	1521	69,7	0,45
_9	21,2	1874	1546	73,9	0,44
_10	22,5	1549	1265	52,3	0,54
6_B1_1	21,6	1888	1552	76,2	0,44
_2	20,6	1872	1552	72,6	0,44
_3	19,9	1891	1577	72,7	0,43
_4	19,2	1891	1587	71,1	0,43
_5	19,0	1887	1586	70,5	0,43
_6	22,3	1964	1606	85,1	0,42
_7	19,4	1857	1555	68,7	0,44
_8	20,0	1855	1545	69,9	0,44
_9	20,3	1815	1509	67,1	0,46
_10	20,8	1826	1512	69,0	0,46
6_B2_1	21,3	1933	1594	79,6	0,43
_2	20,7	1922	1592	77,3	0,43
_3	20,2	1863	1549	71,0	0,44
_4	19,5	1871	1566	70,2	0,44
_5	19,2	1877	1574	69,9	0,43
_6	20,4	1868	1551	71,9	0,44
_7	19,9	1821	1519	66,7	0,45
_8	20,2	1651	1373	55,0	0,51
_9	21,7	1756	1443	65,3	0,48
_10	22,2	1811	1481	70,7	0,47

Table A10-3. *Buffer sample results (Number 1 in the end of a label stands for a sample closest to the buffer edge).*

Label	Water content (%)	Bulk density (kg/m^3)	Dry density (kg/m^3)	Saturation degree (%)	Porosity
N1_1	49,1	1648	1106	90,3	0,60
N1_2	36,0	1752	1289	86,6	0,54
N1_3	33,4	1803	1351	88,0	0,51
N1_4	30,9	1757	1343	80,3	0,52
N1_5	29,8	1811	1395	83,6	0,50
S1_1	43,1	1557	1088	77,2	0,61
S1_2	40,4	1665	1186	83,8	0,57
S1_3	32,0	1788	1355	84,7	0,51
S1_4	27,4	1829	1436	81,5	0,48
S1_5	28,4	1813	1412	81,7	0,49
A1_1	41,2	1683	1192	86,2	0,57
A1_2	37,9	1636	1187	78,6	0,57
A1_3	29,6	1707	1317	74,3	0,53
A1_4	32,3	1781	1346	84,5	0,52
A1_5	31,7	1761	1337	81,8	0,52
C1_1	40,1	1512	1079	70,8	0,61
C1_2	39,1	1676	1205	83,3	0,57
C1_3	35,0	1687	1249	79,6	0,55
C1_4	33,0	1758	1322	83,3	0,52
C1_5	31,9	1787	1355	84,5	0,51
N2_1	55,9	1637	1050	94,6	0,62
N2_2	49,6	1673	1118	93,0	0,60
N2_3	37,8	1754	1273	88,9	0,54
N2_4	34,2	1742	1298	83,5	0,53
N2_5	31,8	1724	1308	78,8	0,53
N2_6	30,8	1805	1379	84,6	0,50
S2_1	39,4	1582	1135	75,7	0,59
S2_2	37,8	1665	1208	80,9	0,57
S2_3	32,5	1782	1345	84,8	0,52
S2_4	30,4	1815	1392	84,9	0,50
S2_5	29,1	1747	1353	76,9	0,51
A2_1	40,3	1527	1088	72,3	0,61
A2_2	40,1	1718	1227	88,2	0,56
A2_3	34,4	1737	1293	83,3	0,53
A2_4	33,0	1803	1355	87,5	0,51
A2_5	31,2	1766	1346	81,7	0,52
C2_1	38,8	1555	1120	73,0	0,60
C2_2	33,4	1679	1259	76,9	0,55
C2_3	32,1	1771	1341	83,3	0,52
C2_4	31,1	1793	1367	84,0	0,51

Label	Water content (%)	Bulk density (kg/m^3)	Dry density (kg/m^3)	Saturation degree (%)	Porosity
N3_1	54,9	1627	1050	92,9	0,62
N3_2	53,0	1643	1074	92,9	0,61
N3_3	43,8	1707	1187	90,9	0,57
N3_4	39,1	1734	1247	88,5	0,55
N3_5	37,9	1694	1229	83,6	0,56
S3_1	39,0	1641	1180	80,2	0,58
S3_2	33,7	1747	1307	83,2	0,53
S3_3	31,3	1814	1381	86,2	0,50
S3_4	29,1	1733	1343	75,7	0,52
S3_5	28,1	1814	1416	81,2	0,49
A3_1	43,9	1620	1126	83,3	0,60
A3_2	42,3	1707	1200	89,4	0,57
A3_3	35,8	1746	1286	85,8	0,54
A3_4	33,7	1757	1314	84,1	0,53
C3_1	43,1	1576	1101	78,8	0,60
C3_2	41,5	1666	1178	85,0	0,58
C3_3	36,8	1706	1248	83,4	0,55
C3_4	34,5	1701	1265	80,2	0,54
C3_5	33,2	1739	1305	81,9	0,53
N4_1	48,3	1639	1105	88,8	0,60
N4_2	43,8	1641	1141	85,0	0,59
N4_3	36,5	1761	1290	88,0	0,54
N4_4	34,2	1733	1291	82,6	0,54
N4_5	32,7	1745	1315	81,7	0,53
S4_1	38,5	1628	1176	78,6	0,58
S4_2	34,5	1718	1278	81,7	0,54
S4_3	33,0	1788	1345	86,1	0,52
S4_4	32,0	1744	1321	80,7	0,52
A4_1	47,9	1613	1091	86,1	0,61
A4_2	46,1	1618	1107	85,0	0,60
A4_3	40,2	1715	1224	88,0	0,56
A4_4	37,4	1714	1248	84,8	0,55
A4_5	36,2	1646	1209	77,6	0,57
C4_1	44,7	1549	1071	78,0	0,61
C4_2	43,4	1671	1165	87,2	0,58
C4_3	38,4	1703	1230	84,9	0,56
C4_4	35,7	1741	1283	85,3	0,54
C4_5	34,6	1768	1313	86,3	0,53

Table A10-4. *Results of the interface samples taken from above the buffer.*

Label	Water content (%)	Bulk density (kg/m^3)	Dry density (kg/m^3)	Saturation degree (%)	Porosity
TB_0_buffer	36,2	1517	1114	67,4	0,60
TB_0_tunnel	41,8	1627	1148	81,8	0,59
TBN_1_buffer	39,5	1558	1117	73,9	0,60
TBN_1_tunnel	47,0	1701	1157	93,3	0,58
TBN_2_buffer	45,5	1631	1121	85,7	0,60
TBN_2_tunnel	53,2	1611	1051	90,2	0,62
TBS_1_buffer	40,5	1685	1200	85,6	0,57
TBS_1_tunnel	48,1	1708	1153	95,1	0,59
TBS_2_buffer	44,3	1685	1168	89,4	0,58
TBS_2_tunnel	52,9	1675	1096	95,8	0,61
TBA_1_buffer	39,1	1706	1227	86,0	0,56
TBA_1_tunnel	45,8	1689	1158	91,1	0,58
TBA_2_buffer	42,0	1616	1138	81,1	0,59
TBA_2_tunnel	49,8	1682	1123	94,0	0,60
TBC_1_buffer	40,5	1542	1097	73,6	0,61
TBC_1_tunnel	47,7	1704	1154	94,3	0,58
TBC_2_buffer	43,6	1665	1160	87,0	0,58
TBC_2_tunnel	50,7	1659	1101	92,6	0,60